Validation of Fire Dynamics Simulator (FDS) for forced and natural convection flows

Author: Piotr Smardz

Supervisor: Prof. Vasily Novozhilov

Master of Science in Fire Safety Engineering

University of Ulster

October 2006   (Revised November 2006)

ABSTRACT

Design of a smoke control system is often an important element of the fire safety strategy for a building. Fire safety engineers often refer to simple empirical correlations, zone models or field models as tools for smoke control design.

One of the most commonly used field models is called Fire Dynamics Simulator (FDS). It is a Computational Fluid Dynamics (CFD) model developed specifically for fire applications. FDS is widely used by fire researchers, investigators and engineers.

The main objective of this study is to assess the accuracy of FDS predictions for a scenario in which smoke spreads from a small compartment into an adjacent larger space, from which it is then extracted using powered ventilation system. Such a fire scenario can be encountered, for example, in a hotel building where bedrooms face onto a feature atrium or in a shopping centre with small retail units opening onto a mall.

A review of the existing and ongoing validation work for FDS is presented, based on the information obtained from published papers and other sources.

The assessment of predictive capabilities of FDS is made in the context of the statement made by the authors of the program, that it can predict flow velocities and temperatures to an accuracy of 5 to 20% for simulations that involve simple mass and heat transfer.

In this study, the results of small-scale physical experiments are compared with the FDS predictions. The main parameters for which assessment is made include temperatures in the fire compartment and in the smoke reservoir and the height of the smoke layer in the reservoir. The influence of different mesh types is investigated.

The comparison is primarily made for simple problems, where the heat release rate of a fire is decided a priori and it is treated as a model input. A brief study is also included on more complex fire scenarios where the burning rate is not know and it must therefore be calculated by the program.

The comparison between the FDS predictions and the experimental values made in this study confirms the observations made earlier by other authors that the resolution of the numerical grid is critical for accurate results. Where a coarse mesh was used, FDS predictions were in certain cases found to differ from the experimental results by more than 20%.

Where the burning rate is predicted by the program, prescribing proper thermal and combustion properties of the fuel was also found to be crucial.

ACKNOWLEDGEMENTS

PERMISSION STATEMENT

I hereby declare that with effect from the date on which the dissertation is deposited in the Library of the University of Ulster I permit the Librarian of the University to allow the dissertation to be copied in whole or in part without reference to me on the understanding that such authority applies to the provision of single copies made for study purposes or for inclusion within the stock of another library. This restriction does not apply to the copying or publication of the title and abstract of the dissertation.

IT IS A CONDITION OF USE OF THIS DISSERTATION THAT ANYONE WHO CONSULTS IT MUST RECOGNISE THAT THE COPYRIGHT RESTS WITH THE AUTHOR AND THAT NO QUOTATION FROM THE DISSERTATION AND NO INFORMATION DERIVED FROM IT MAY BE PUBLISHED UNLESS THE SOURCE IS PROPERLY ACKNOWLEDGED

Signed: _____   Date: _____

TABLE OF CONTENTS

1. INTRODUCTION

1.1 Smoke control design as part of the overall fire safety strategy

Predictions of smoke flow patterns in buildings and in particular the design of smoke control systems are important elements of devising a fire safety strategy for a building.

The need to control the flow of smoke within a building may be dictated by one or more of the following objectives:

- Ensuring safe means of escape for the occupants of the building
- Facilitating the fire service operations
- Protecting property

In order to be able to select a suitable smoke control strategy, a fire safety practitioner needs to establish several parameters describing the dynamics of smoke flow in the compartment(s) and the impact that smoke may have on the occupants of the building. These parameters typically include the temperature of the hot layer in the space of fire origin, the temperature of smoke in areas remote from the fire (e.g. in a smoke reservoir), velocities of smoke at selected locations, concentrations of combustion products, visibility, mass / volumetric flow rates of smoke etc.

Examples of buildings where smoke control plays a significant role include:

- Shopping centres
- Atrium buildings
- Large warehouse and industrial buildings
- Underground structures (including underground car parks and tunnels)

In predicting the smoke flow pattern in a building, fire safety engineers often refer to fire modelling tools such as simple empirical correlations, zone models or CFD models (also called field models). Therefore, there is a need in the fire engineering community for reliable fire modelling tools that can be confidently used to predict phenomena associated with smoke spread in buildings.

1.2   Application of CFD models in fire safety engineering

CFD models (also called field models) are one of the most sophisticated tools available to fire safety engineers. These models are based on fundamental laws of physics rather than empirical correlation. For this reason, CFD models offer the most versatile approach to solving problems of fire dynamics. However, due to their complex nature, they require expert knowledge from the user.

This section provides a brief history of CFD, its theoretical basis and also describes selected CFD models used in fire safety engineering.

1.2.1   Brief history of CFD

A concise description of the history of CFD can be found in [1] and it is summarised below.

The efforts to understand the behaviour of fluids are nearly as old as science itself. However, it was not until the eighteen century, that significant progress was made in mathematically describing the motion of fluids, thanks to the work of Bernoulli, Euler, Reynolds, Poisson, Lagrange and others. The Euler equations describe the conservation of momentum for an inviscid fluid, and conservation of mass.

In the nineteenth century, the Frenchman, Claude Louis Marie Henry Navier and the Irishman, George Gabriel Stokes introduced viscous transport into the Euler equations, which resulted in what is now called the Navier-Stokes equations. These differential equations describe the conservation of mass, momentum, pressure, species and turbulence and they form the basis of computational fluid dynamics.

At the beginning of the twentieth century significant progress was made in refining theories of boundary layers and turbulence in fluid flows, which are also fundamental elements of modern CFD.

1. Introduction

The Navier-Stokes equations are closely coupled and difficult to solve. Although attempts were made to solve these equations numerically in the early twentieth century, it was not until 1960s and 1970s when computers emerged, that they could be resolved for real flow problems.

In the early 1980s commercial CFD software became available to a wider market. Sine then, CFD modelling is used in nearly all disciplines of science and engineering which consider problems involving flow of fluids (i.e. liquids or gases).
The areas where CFD is commonly applied include among others:

- Aerospace industry
- Automotive industry
- Marine industry
- Chemical process engineering
- Medical sciences
- HVAC / Environmental design

The first attempts to apply CFD modelling in fire safety science were made in early the 1980s. One of the earliest examples of successfully applying CFD modelling to understand behaviour is the work carried out by BRE in 1988 as part of the investigation into the King's Cross underground station fire in London [2,3].

Also in the early 1980s, the development of CFD models for various fire applications started at The National Bureau of Standards (now known as NIST) in the US. These models were eventually consolidated into what eventually became Fire Dynamics Simulator (FDS) [4].
This work is concerned with validation of FDS for selected fire problems involving the flow of smoke.

1.2.2 Theoretical basis of CFD

A detailed review of current trends in CFD modeling of compartment fires can by found in the papers by Novozhilov [5] and also in the work by Cox and Kumar [2]. Only a brief summary is presented below.

The motion of fluid can be described by a set of partial differential equations called the Navier-Stokes equations. These equations describe the conservation of mass, momentum and energy for a flowing fluid.

Conservation of mass:

$$\frac{\partial \rho}{\partial t} + \nabla \cdot (\rho \mathbf{u}) = 0$$

Conservation of momentum:

$$\frac{\partial \mathbf{u}}{\partial t} + (\mathbf{u} \cdot \nabla)\mathbf{u} = -\frac{1}{\rho}\nabla p - \nabla \phi + \frac{\mu}{\rho}\nabla^2 \mathbf{u},$$

Conservation of energy:

$$\rho \left(\frac{\partial \varepsilon}{\partial t} + \mathbf{u} \cdot \nabla \varepsilon \right) - \nabla \cdot (K_H \nabla T) + p \nabla \cdot \mathbf{u} = 0.$$

The above equations are coupled differential equations. Although in theory it is possible to solve them analytically, in practice it is extremely difficult to find analytical solution to the NS equations for most practical problems.

In order to find a solution, approximations of these equations have to be solved numerically using techniques such as finite element method, finite volume method and finite difference method.

Computational Fluid Dynamics (CFD) can be summarized is a discipline that is concerned with solving the NS equations numerically.

1. Introduction

One of the most important aspects of CFD modelling is the method of treating the turbulence. CFD models can be divided into two major groups: Reynolds-Averaged Navier-Stokes (RANS) models and Large Eddy Simulation (LES) models.

Another approach available in some CFD codes is to resolve all the relevant scales occurring in the flow by Direct Numerical Simulation (DNS). However, this approach is not yet of practical use in modeling of building fires due to the requirement for extremely well resolved mesh and will not be discusses here.

Most of the CFD models used in fire modelling are based on the RANS approach, where the Navier-Stokes equations are time-averaged for all length scales considered. In this group the k-ε model is the most commonly used.

In the LES approach, turbulences in the flow are only averaged at scales smaller than the mesh size. The large scale eddies (larger than the mesh size) are resolved directly. While LES approach can potentially provide more information about the fluctuations in the flow, it is also more demanding computationally, as a finer mesh is required to obtain an accurate solution, compared to RANS models.

In addition to the problems described above, CFD models used in fire safety engineering have to include sub-models for thermal radiation and combustion.

The most commonly methods used for modelling radiative heat transfer include the flux models (e.g. six-flux model) and the Discrete Transfer method

Dealing with combustion is one of the most challenging problems in CFD modelling of fires. The most simplistic approach is to avoid modelling the combustion process as such by simply representing the fire source as a volumetric heat source.
The next level of sophistication in modelling combustion is to assume that the combustion process can be represented by a single, one-step reaction. In this approach fuel and oxygen react in an infinitely fast reaction to create combustion products. The Mixture Fraction model commonly used in CFD modeling of fires is based on this approach.
A more detailed treatment of combustion is provided by an Eddy Break-up model, in which the influence turbulence on chemical reaction is also included.

1.2.3   Examples of CFD models used in fire safety engineering

Thanks to continued improvement of CFD models, they are now an increasingly popular tool in fire safety engineering and research. This trend is also helped by continued increase in the computational power of computers, which makes relatively complicated CFD simulations available to a typical fire engineering practice. CFD models used in fire safety engineering can be broadly divided into the following two categories:

1. General purpose CFD codes:
    - CFX
    - Fluent
    - Phoenix
2. Codes developed specifically for fire engineering applications:
    - FDS (LES / DNS)
    - Jasmine (RANS)
    - KOBRA-3D
    - Smartfire (RANS)
    - Sofie (RANS)

The multi-purpose CFD codes are more versatile and they usually offer a selection of sub-models for the treatment of turbulence (RANS, LES, DNS), combustion, thermal radiation etc. However, the user may often be required to write sub-routines to deal with specific problems related to fire (e.g. visibility through smoke).

On the other hand, most of the CFD models that were developed specifically for fire science applications typically offer a fire-engineer-friendly approach, but they are more limited in terms of problems they can be applied to.

It is worth noting that most of the "fire specific" CFD codes listed in item 2 above use the RANS turbulence model. In this group FDS is the only model that uses the LES model. The LES technique is still considered to be relatively new in fire applications.

1.3   General problems of validation of CFD fire models

This section briefly discusses issues relevant to validation of CFD fire models such as the need for reliable experimental data and also the need for a uniform system of fire model assessment.

1.3.1   Definition of model validation

In order to discuss the relevant problems, we first need to define what a validation of a fire model is.

ASTM E1355 [6] defines model validation as *"the process of determining the degree to which a calculation method is an accurate representation of the real world from the perspective of the intended uses of the calculation method"*.

Another useful definition can be found in FDS Technical Reference Guide [4]: *"Validation is a process to determine the appropriateness of the governing equations as a mathematical model of the physical phenomena of interest. Typically, validation involves comparing model results with experimental measurement"*

1.3.2   Availability of experimental data

One of the problems immediately relevant to fire model validation is the availability of reliable experimental data suitable for comparison with model predictions.
While there is a significant amount of experimental data available from large-scale fire tests, many of those tests were performed for reasons other than validation of fire models.

The need for reliable experimental data is common to validation of all fire models be it simple empirical correlations, two-zone models of field (CFD) models.
However, as CFD models are highly sophisticated, they typically require a larger amount of input data than, for example, two-zone models.

Similarly, CFD models are usually capable of providing more detailed results in terms of spatial variation of temperature, flow velocities, concentration of species etc.

As a consequence of this increased sophistication of CFD models, their validation requires a large number of parameters to be recorded in the validation experiments. An 'ideal' experiment for CFD model validation should provide accurate information in relation to all model inputs (initial conditions, boundary conditions) and outputs (quantities predicted).

In terms of the description of the model inputs the following information is required:
- An accurate description of the geometry
- Information on physical properties of materials involved (particularly thermal properties)
- Information on the fire size, heat release rate, soot yield etc.
- Information on the external boundary conditions (temperature, flow velocities etc.)
- Information on active elements of the system such as sprinklers (if present)

In terms of experimental results at least some of the following measurement should be taken at locations relevant to the particular problem being investigated:
- Temperatures (gas and solids)
- Flow velocities
- Heat flux measurements
- Concentrations of selected species (e.g. O_2, CO_2, CO)
- Visibilities
- Visual records of fire and smoke behaviour

It should be noted that in more complex simulations parameters relevant to combustion (e.g. the burning rate) are not provided as inputs, but are predicted by the model, based on the properties of the fuel.

1.3.3   Development of standards for CFD fire models

CFD models are now widely use by the fire engineering community in solving practical problems in fire safety design of buildings
It is therefore crucial that the accuracy of the predictions and also the appropriateness of a CFD model for a particular fire engineering problem can be reliably assessed.

Efforts to develop a uniform system of standards for fire field models are already under way. In Europe, one such program was initiated by the Fire Research Division of the Office of Deputy Prime Minister in the UK [7]

In the United States, an ASTM standard for evaluating fire models was developed [6]. This standard provides guidance on methodology for evaluation the predictive capabilities of fire models (including CFD models) for a specific use.

1.4 Objective and approach of this work

The main objective of this study is to assess the accuracy of FDS predictions for a fire scenario often encountered by fire engineers when designing smoke control system for buildings. This scenario includes a fire in a small compartment (e.g. a hotel bedroom, an apartment, a prison cell or a small retail unit in a shopping centre) adjacent to a larger and higher space (e.g. an atrium or a shopping mall).

In this study, the results of small-scale physical experiments are compared with the FDS predictions. The main parameters for which assessment is made include temperatures in the fire compartment and in the smoke reservoir and the height of the smoke layer in the reservoir. Some limited investigation of flow velocities is also made.

The assessment of predictive capabilities of FDS is made in the context of the statement made by the authors of the program, that it can predict flow velocities and temperatures to an accuracy of 5 to 20% for simulations that involve simple mass and heat transfer.

One of the aims of this study is to investigate how using different mesh types (e.g. coarse, fine, stretched and multi-meshes) can influence the accuracy of predictions made by FDS.

This study mainly focuses on simple problems, where heat release rate of a fire is decided a priori and it is treated as a model input.

However, it also briefly investigates the accuracy of FDS predictions for more complex fire simulations where the burning rate is not know a priori and it must therefore be calculated by the program.

It can be argued that accuracy of most computer models can by improved if significant resources are committed to a simulation in terms of time, computational power, detailed investigation of material properties etc.

The main assumption made at the beginning of study is that it should look at the accuracy of FDS when "engineer's approach" is adopted and the resources are limited to what would typically be available to medium size fire engineering consultancy.

For this reason, highly sophisticated techniques such as multi-processor calculations or investigation of certain FDS model parameters are not included in this study.

2. BRIEF DESCRIPTION OF FDS

This chapter provides brief description of FDS based on the information contained in the User's Guide [8] and the Technical Reference Guide [4] accompanying the program.

2.1 Main Features of FDS

FDS is a computational fluid dynamics (CFD) model of fire-driven fluid flow. The main computer program is written in Fortran 90. The first version of the program was publicly released in February 2000. Since then several major improvements and new features were implemented in the program. This study was carried out using FDS version 4.07 which was released in March 2006.

FDS was developed primarily as a tool for solving practical problems in fire protection engineering, and also as a tool to tool to study fundamental fire dynamics and combustion.

FDS can be used to model the following phenomena:

- Low speed transport of heat and combustion products (mainly smoke) from fire
- Heat transfer between the gas and solid surfaces
- Pyrolysis
- Fire growth
- Flame spread
- Activation of sprinklers and heat detectors
- Fire suppression by sprinklers

FDS is widely used by fire safety professionals. One of the major applications of the program is for design of smoke control systems and sprinkler activation studies. FDS was also used in numerous fire reconstructions including the investigation into the World Trade Centre disaster.

Results of an FDS simulation can by displayed using a companion program called Smokeview.

2.1.1   Hydrodynamic Model

FDS solves numerically a form of the Navier-Stokes equations appropriate for low-speed, thermally-driven flow with an emphasis on smoke and heat transport from fires. The basic set of the conservation equations for mass, momentum and energy solved by FDS is presented below:

Conservation of mass:

$$\frac{\partial \rho}{\partial t} + \nabla \cdot \rho \mathbf{u} = 0$$

Conservation of momentum:

$$\frac{\partial}{\partial t}(\rho \mathbf{u}) + \nabla \cdot \rho \mathbf{u}\mathbf{u} + \nabla p = \rho \mathbf{f} + \nabla \cdot \tau_{ij}$$

Conservation of energy:

$$\frac{\partial}{\partial t}(\rho h) + \nabla \cdot \rho h \mathbf{u} = \frac{Dp}{Dt} + \dot{q}''' - \nabla \cdot \mathbf{q} + \Phi$$

Equation of state for a perfect gas:

$$p = \frac{\rho \mathcal{R} T}{M}$$

In terms of the mass fractions of the individual gaseous species the mass conservation equation can be written as follows:

$$\frac{\partial}{\partial t}(\rho Y_i) + \nabla \cdot \rho Y_i \mathbf{u} = \nabla \cdot \rho D_i \nabla Y_i + \dot{m}_i'''$$

Since there is no analytical solution for the fully-turbulent Navier-Stokes equations, the solution requires the use of numerical methods where the compartment is divided into a three-dimensional grid of small cubes (grid cells). The model calculates the physical conditions in each cell as a function of time.

The core algorithm is an explicit predictor-corrector scheme, second order accurate in space and time. Turbulence is treated by means of the Smagorinsky form of Large Eddy Simulation (LES). LES is the default mode of operation and it was used in the study described in this report.

It is also possible to perform a Direct Numerical Simulation (DNS) in FDS. However, DNS simulations require very fine numerical grids. Due to the current limits of computational power available to most engineers and researchers DNS can not be used to solve practical large-scale problems such as building fires.

It is noted that currently the most common method of treating turbulence in other CFD codes is to solve so the called Reynolds-averaged Navier-Stokes equations (RANS). However, this method is not used in FDS.

2.1.2   Combustion Model

FDS uses the mixture fraction model as the default combustion model. The mixture fraction is a conserved scalar quantity. It is defined as the fraction of gas at a given point in the flow field that originated as fuel, as follows:

$$Z = \frac{s\,Y_F - (Y_O - Y_O^\infty)}{s\,Y_F^I + Y_O^\infty} \quad ; \quad s = \frac{\nu_O M_O}{\nu_F M_F}$$

By design, mixture fraction varies from Z=1 in a region containing only fuel to Z=0 in regions (typically far away from the fire) where only ambient air with undepleted oxygen is present.

The model assumes that combustion is mixing-controlled, and that the reaction of fuel and oxygen is infinitely fast. The mass fractions of all of the major reactants and products can be derived from the mixture fraction by means of "state relations," empirical expressions arrived at by a combination of simplified analysis and measurement.

2.1.3 Radiation transport

Radiative heat transfer is included in the model via the solution of the radiation transport equation for a non-scattering grey gas, and in some limited cases using a wide band model. The equation is solved using a technique similar to finite volume methods for convective transport, thus the name given to it is the Finite Volume Method (FVM).

2.1.4 Geometry and use of multiple meshes

FDS approximates the governing equations on a rectilinear grid. The user prescribes rectangular obstructions that are forced to conform to the underlying grid.
This can be a limitation where certain geometric features do not conform to the rectangular grid, and they have to be approximated by rectangular obstructions. An example of such element is the middle part of the extraction hood modelled in this study, which is inclined (i.e. neither vertical nor horizontal)
FDS incorporates techniques to lessen the effect of "sawtooth" obstructions used to represent non-rectangular objects, but they can not be relayed on where boundary layer effects are of importance.

The grid cells can either be uniform in size (default mode) or they can be stretched in one or two of the three coordinate directions.

It is possible to use more than one rectangular mesh in a calculation. This allows creation of an efficient computational domain for geometries which can not be easily fitted into a single rectangular grid. It also allows using regions with different grid resolutions within one computational domain.

Both the grid stretching and the use of multiple meshes allow the user to apply better grid resolutions in critical areas (e.g. near the fire) without unnecessarily increasing the demand for computational power by applying fine mesh to the entire computational domain.

The use of multiple meshes is also required when an FDS simulation is to be run in parallel processing on more than one computer. However, such technique is outside the scope of this study.

2.1.5   Boundary conditions

All solid surfaces are assigned thermal boundary conditions, plus information about the burning behaviour of the material. Heat and mass transfer to and from solid surfaces is handled with empirical correlations (except when performing DNS analysis, which is not relevant in the subject study).

Material properties of solids can be prescribed as a function of temperature. This feature was used in this study when prescribing the thermal properties of the walls enclosing the fire compartment.

2.2   Input data required to run the model

All of the input parameters required by FDS to describe a particular scenario are conveyed via one or two text files created by the user.

These files contain information about the numerical grid, ambient environment, geometry of the problem modelled, material properties, boundary conditions and the fire itself. The input file should also contain information about the desired output quantities.

3.   EXISTING VALIDATION OF FDS AND OTHER CFD CODES

The first section of this chapter presents a review of literature describing validation efforts for FDS, including information on some FDS validation work currently under way where such work is known to the author.

The second section of this chapter briefly discusses selected examples of validation for other CFD codes.

3.1   Validation of FDS

Validation of FDS was undertaken by the developers of the program and also by other researchers and bodies using it.

FDS Technical Reference Guide [4] provides a concise summary of the validation work carried out for the program. However, this summary by its nature does not provide detailed information on each of the validation efforts mentioned. Also, some new validation work for FDS was carried out since the Technical Reference Guide was published.

The validation work described by the developers of FDS [4] can be divided into the following categories:

- Comparison with full-scale tests conducted specifically for the code evaluation
- Comparison with engineering correlations
- Comparison with previously published full-scale test data
- Comparison with standard test
- Comparison with documented fire experience

In general, the examples presented in this section include projects undertaken for validation of FDS specifically, and also projects where several fire models (including FDS) were validated and compared against one another.

3.1.1   Validation of FDS undertaken by NIST

3.1.1.1 Validation of pre-release versions of FDS

The work to develop a purpose-built CFD model for fire related phenomena started at NIST long before the first version of FDS was publicly released in February 2000. Originally, there was a suite of problem specific CFD codes such as LES, NIST-LES, LES3D, IFS and ALOFT which were then integrated into what eventually became FDS. Validation work for these early models concentrated mainly on the hydrodynamic model and it pointed out the need to improve it by introducing the Smagorinsky form of large eddy simulation. Only selected examples are discussed below.

Large scale experiments in an aircraft hangar

The predictive capabilities of NIST-LES (the predecessor of modern FDS) were assessed as part of a larger validation program for selected fire models. This study was undertaken by NIST in the mid 1990s and was described in detail in a report by Davis, Notarianni and McGrattan [9].

Large-scale experiments were conducted in a 15 m high Navy hangar at Barbers Point, Hawaii. The experiments involved JP-5 pan fires of varying sizes under a smoke reservoir 24.4 m long, 18.3 m wide and 3.7 m deep.

The experimental results were compared with the predictions of selected fire models (including NIST-LEST). The work focused primarily on temperatures in the plume and in the ceiling jet. Some limited velocity measurements were also taken.

Of the eleven tests conducted, two were selected as providing reliable heat release rate information. These two tests (with maximum heat release rate of 500kW and 2700kW respectively) were used for comparison with model predictions.

The NIST-LES simulations were performed using a computational domain of 30 m by 22 m by 14.9 m. A uniform grid was used, 144 by 64 by 96 cells, resulting in approximately 885,000 control volumes and mesh resolution of 0.15 m – 0.30 m. The above simulations required a computational power well in excess of what was available to fire safety practitioners at the time.

The study concluded that NIST-LES predicted the plume centreline temperatures with 38% accuracy and the ceiling jet temperatures with 62% accuracy. Ceiling jet velocities were predicted with 40% accuracy. Draft curtain filling time was predicted with 45% accuracy. All NIST-LES predictions described above were less accurate than those made by CFX, which was another CFD model tested in the study.

<u>Salt water experiments</u>

An interesting method used by NIST to validate the hydrodynamic model in the early versions of FDS was based on salt water experiments. Salt water flows can resemble the smoke flow in the early stages of a fire.

A similar approach has been used by other researchers to validate the hydrodynamic model of the first version of FDS released publicly – see section 3.1.3 for details.

3.1.1.2 Validation of FDS for the Howard Street Tunnel Fire Study

Following the fire caused by the derailment of a freight train in the Howard Street Tunnel in Baltimore on the 18th of July 2001, a study was undertaken by McGrattan and Hamins (NIST) to assess the thermal environment in the tunnel during the fire [10]. FDS was used in this study to simulate the fire's growth and spread in the tunnel.

In order to validate FDS ver. 2 for this particular application, the model predictions were compared with the results of two types of large scale fire tests:

- experiments in a large building conducted as part of the International Collaborative Project to Evaluate Fire Models for Nuclear Power Plant Applications (Benchmark Exercise #2)
- experiments conducted as part of the Memorial Tunnel Fire Tests Programme

Details of the former are discussed in section 3.1.1.4. In this section only the comparison with the results of the tunnel fire experiments will be discussed.

The Memorial Tunnel Fire Tests were conducted in a decommissioned, 853 m long highway tunnel in West Virginia from 1993 to 1995.

The principal parameters such as the cross-sectional area of the tunnel and the fire sizes used in the Memorial Tunnel Fire tests were similar to those in the Howard Street Tunnel incident.

Two tests were selected for the comparison with FDS predictions: a 20 MW fire and a 50 MW fire. The fuel in both experiments was No. 2 fuel oil poured on top of water in large pans. In both tests only natural ventilation was used.

The FDS simulations were conducted with numerical mesh in the order of 0.30 m for the 130 m long section of the tunnel nearest to the fire. The resolution of the mesh was varied along the length of the computational domain, with coarser grids used at the ends of the tunnel.

In both cases the peak near-ceiling temperatures calculated by FDS were within 50 $^{\circ}$C of the values measured in the experiments, which were 600°C for the 20 MW fire and 800 $^{\circ}$C for the 50 MW fire.
In terms of accuracy in predicting gas temperature rise, the above values correspond to 9% and 6% respectively.

For both fire sizes FDS under-predicted the extent of lower-temperature contours at the uphill end of the tunnel. This was attributed by the authors to the coarser grid used at the ends of the tunnel.

3.1.1.3 Validation of FDS for the World Trade Center Investigation

As part of the investigation into the WTC disaster, efforts were made to reconstruct the thermal and tenability environment in the effected buildings. FDS was selected as the model to be used for these reconstructions.

In order to assess the accuracy with which FDS can predict the thermal environment in a burning compartment, a series of large-scale experiments were conducted by NIST in 2003. A detailed description can be found in NIST NCSTAR 1-5E report [11].

The experiments were designed to recreate selected aspects of the WTC fires. Three computer workstations were placed in a 3 m by 7 m by 4 m high compartment lined with calcium silicate boards.

A 2 MW hydrocarbon fire (burning for up to 10 minutes depending on the fire scenario) was used to ignite the compartment furnishings

Six fire experiments were conducted and a large amount of measurement was taken in each experiment. The overall fire behaviour was documented using video cameras located in several positions.

The heat release rate and the thermal environment in the compartment were simulated using FDS version 4. Model predictions were then compared with the experimental results.

The findings of this validation study were summarized by its authors as follows:

- FDS was able to accurately predict the general shape and magnitude of the time dependant heat release rate.

- FDS predicted the time at which half of the energy was released to within 22% of the measurements.

- FDS predicted the value of the heat release rate when half of the energy was released to (on average) within 9% of the measurements. This was considered to be a good agreement in the context of the measurement uncertainty.

- FDS predicted the duration of significant heating of the fires to within 15% of the measurements (on average). However, the long tail in the heat release rate was under-predicted.

- FDS predicted the peak upper gas layer temperatures to within approximately 10% of the experimental measurements. This again was considered accurate in the context of model sensitivity to input parameters such as the heat release rate and the uncertainties associated with the measurements.

The results of the comparison of the FDS predictions with experimental measurements were considered sufficiently good to warrant the use of FDS to predict the thermal environment in compartments analysed as part of the WTC investigation.

3.1.1.4 Validation of FDS as part of the NRC / EPRI program

The U.S. Nuclear Regulatory Commission and The Electric Power Research Institute have jointly undertaken an extensive verification & validation program of selected fire models for Nuclear Power Plant (NPP) applications.
The study was undertaken recently, and a draft version of the report was issued for public comment in April 2006 [12, 13].

FDS was one of the five fire models assessed. It was also the only CFD model in the group. Other models reviewed included two libraries of engineering calculations and two different Two-Zone models.
The study was conducted using a consistent methodology described in ASTM E1355.

As the aim of the study was to assess the predictive capabilities of the selected fire models for NPP application, the first stage of the project was to define a set of fire scenarios that are typical for NPP. In total twelve scenarios were specified as typical for nuclear power plants. They included, for example, a fire in a switchgear room, a fire in a main control room and a fire in a turbine building. For each scenario a "range of conditions" was then defined.

The experimental data used to validate the fire models were selected as representative of the twelve NPP fire scenarios described above.
The experimental results were selected from the following three full-scale test series:

- Factory Mutual & Sandia National Laboratories test series conducted in the mid-1980s. Three tests were selected for the study. All three tests included a fire in an 18.3 m by 12.2 m by 6.1 m enclosure, with a propylene gas-fire burner used as the fire source.
- The National Bureau of Standard test series which involved 45 fire tests representing 9 different sets of experiments. These tests were conducted in the mid-1980s. The experimental set-up consisted of two rooms connecting to a relatively long corridor. Openings between the rooms and the corridors were modified for different experiments.

  Three experiments were selected to be used in the study, all involving a 100 kW fire but with different ventilation conditions between the rooms and the corridor.

- The International Collaborative Fire Model Project Benchmark Exercise test series. These tests were conducted as part of a large international verification and validation program for fire models. Experimental results from four different test series (further referred to as benchmark exercises) were selected for the study. These experiments were conducted by VTT in Finland, NIST in the U.S. and IBMB in Germany.

The experimental results selected from the above test series were compared with the model predictions. The relative differences between the experimental results and model predictions were compared in the context of combined uncertainty pre-determined for all attributes investigated in a given experiment.

Predictive capabilities of FDS were assessed with reference to the following fire modelling attributes:

- Hot layer temperature & height
- Ceiling jet temperature
- Plume temperature
- Flame Height
- Radiated heat flux to targets
- Total heat flux to targets / walls
- Wall / target temperature
- Smoke & Oxygen concentrations
- Room pressure

The predictive capability of FDS (and other models investigated) for each of the modelling attributes was characterized based on the following two criteria:

1. Are the physics of the model appropriate for the calculation being made?
2. Are the calculated relative differences outside the experimental and model uncertainty?

The predictive capability of the model for each modelling attribute was then graded:

- Green (Both criteria satisfied); or
- Yellow (First criterion satisfied but the calculated relative differences are outside the experimental uncertainty); or
- Red (The first criterion is not met)

FDS received a "green" rating for hot gas layer temperature (in the room of fire origin and in the adjacent room), hot layer height, oxygen concentration and room pressure. For all the other attributes it received a "yellow" rating.

The yellow rating means that the user must exercise caution when using the model (in this case FDS) to predict the particular quantity.

As a general remark, the study concluded that for cases where the heat release rate is known, FDS can reliably predict gas temperatures, major gas species and compartment pressures to within 15% accuracy and heat fluxes and surface temperatures to within about 25% accuracy.

3.1.2   Validation of FDS undertaken by VTT, Finland

VTT is the Technical Research Centre of Finland. The Fire Research group of VTT was actively involved in the development of FDS.

As a part of a larger project aimed at developing new tools for fire simulation, the group analysed several case studies in which predictions of pre-release version of FDS 4.0 were compared with the results of several experiments involving flame spread.

The objective of the project was to validate FDS for problems concerning flame spread and also to establish eligible material properties for engineering use of FDS and to provide directions for further development of FDS.

Details of the project can be found in the report by Hietaniemi, Hostikka and Vaari, which was published by VTT [14]

The fire experiments used in the study included the following:

- Cone calorimeter experiments
- SBI tests
- Room corner test
- Furniture calorimeter experiments
- ISO room test
- Full-scale experiments with a cavity arrangement

The following materials were investigated:

- Spruce timber (10 and 22 mm thick)
- MDF board (12 mm thick)
- PVC wall carpet on gypsum board
- Upholstered furniture
- Cables with plastic sheathing
- Heptane (pool fires)

One of the new features of FDS introduced in version 4 is the ability to model burning of charring fuels. This feature was also examined in the study and discussed by the authors in greater detail.

The principal findings of the study in relation to the various materials and experimental arrangements can be summarised as follows:

- For the cone calorimeter experiments involving spruce timber and MDF board FDS provided an accurate prediction of the first stage of the experiment, but was not able to reproduce the second rise in the HRR curve.

- For the SBI tests involving spruce timber and MDF board, FDS reproduced the initial reaction-to-fire performance of spruce timber with very good accuracy. However, after times corresponding to the thermal penetration time for the sample, the calculated HRR curves deviated from the measured ones. The authors concluded that the problem was caused by the fact that the back side boundary condition for the specimen could not be modelled accurately by either of the boundary condition options available in FDS.

- For the room corner tests involving spruce timber and MDF board, the HRR curve predictions made by FDS agreed well with the experimental results. Also, maximum compartment temperatures were reproduced well by FDS. For the room corner test involving PVC carpet on gypsum board, FDS incorrectly predicted flashover, which did not happen in the experiment. This was attributed to the differences in the way the sample backing was treated in the experiment and in the computer model.

- In the experiment involving flame spread in a timber-clad cavity FDS was not able to predict certain phenomena such as fire quenching. However overall, given the unstable nature of fire behaviour in this particular experimental set-up, the authors described the FDS results as "promising".

- For the ISO room and the furniture calorimeter tests involving upholstered furniture, FDS predicted faster ignition and HRR growth than was seen in the experimental data. This discrepancy was attributed to the fact that FDS model only included the fast igniting PU component of the furniture.

Overall, the agreement between the experimental data and the calculated results was considered to be good, although FDS was not able to predict certain phenomena as described above.

Below the findings in relation to heptane pool fires will be discussed in greater detail, as they are most relevant to the part of this project in which the burning rate of liquid fuels in a compartment fire was predicted in FDS and compared with the experimental results.

In the study conducted by VTT, the FDS predictions of the burning rate per unit area were compared with the experimental results obtained by numerous researchers and presented by Hamins, Yang and Kashiwagi [15].
Heptane pool fires with diameters in the range of 0.1 to 1.6 m were investigated. Different grid resolutions (in the range of 0.001 to 0.05 m) were used for each modelled fire diameter.

The authors concluded that the prerequisite for obtaining a good agreement for the burning rate prediction is that there must be at least 20 computational grid cells within the diameter of the pool.

3.1.3   Validation of FDS outside NIST / VTT

3.1.3.1 Work by Clement and Fleischmann

A similar approach to the one described earlier in section 3.1.1.1 was also used by Clement and Fleischmann [16] to validate the hydrodynamic model of the first version of FDS released publicly.

Experimental measurements of the fluid density of the salt water flow field were made using the Laser Induced dye Fluorescence technique. These measurements were then compared with the FDS predictions.
Both DNS and LES techniques available in FDS were investigated.

The study concluded that for coarse grids the LES model is more appropriate and that it is capable of resolving the flow field features that were evident in the experimental density measurements.

3.1.3.2 Work by Harrison

Harrison performed some validation of FDS for smoke flows as part of his research on spill plumes [17].
In this work both physical scale modelling and CFD modelling (using FDS ver. 3) were used to investigate factors effecting entrainment of air into spill plumes. Subsequently, empirical correlations were developed to predict the mass flow rate of gases produced by a free spill plume.

The experimental part was conducted using a $1/10^{th}$ physical scale model of a compartment with a balcony and channelling screens, with smoke discharged into an adjacent smoke reservoir (exhaust hood). The dimensions of the fire compartment in the physical model were 1 m by 1 m by 0.5 m high. The fire source was an ethanol pool fire. Flow of the hot gases produced by the fire was visualised by injecting smoke from a commercial smoke generator into the fire compartment.
The heat output from the fire was calculated from the measured flow rate of fuel through a flow meter into the tray, the heat of combustion and the density of fuel.

In order to gain confidence in FDS for this particular application, the model predictions were compared with the experimental results. The following quantities were compared:
- Temperature profiles at the compartment opening
- Temperature profiles at the spill edge
- Velocity profiles at the compartment opening
- Velocity profiles at the spill edge

The agreement between FDS predictions and the experimental results for temperature profiles depended on the width of the opening, but overall was described as 'good to excellent'. An 'excellent' agreement was also achieved for temperature profiles at the spill edge. In general, FDS accurately predicted the depth of the hot gas layer at the compartment opening and at the spill edge.

As regards velocity profiles, FDS predictions for the compartment opening could not be reliably validated due to suspected over-prediction in experimental measurements.
FDS predictions for flow velocities at the spill edge were described as 'good'.

3.1.3.3 Work by Zou and Chow

Zou and Chow compared the predictions of FDS ver. 3.01 with results of full-scale fire tests [18]. Experiments were carried out using a compartment similar to an ISO room. Gasoline pool fires of different diameters were used to give different heat release rates up to approximately 2.6 MW. The ventilation factors of the compartment were adjusted to produce flashover.

Fire-induced flow, temperature, and pressure fields in these different physical scenarios were calculated using FDS software. The simulations were carried out using a computational domain of approximately 93,000 uniform cells.

The predictions for temperature and radiative heat flux of a post-flashover fire in the specific configuration tested were in reasonably good agreement with experimental results. However, the authors noted that FDS under predicted the compartment temperatures in the cooling (decay) stage by up to 40%.

3.1.3.4 Work by Pope and Bailey

Pope and Bailey compared the predictions of FDS ver. 4 and two empirical models with the results of large-scale post flashover fire tests carried out at the BRE test facility in Cardington as part of the Natural Fire Safety Concept (NFSC) programme [19].

The tests were conducted in a 3 m high compartment with a floor area of 12 m^2. Timber and a timber/plastic mixture were used as a fuel. These tests were not as such conducted to provide validation data for CFD models. However, their results provided reliably large-scale data for fire compartment temperatures that would otherwise be difficult and expensive to obtain.

The FDS simulations were carried out using two grid resolutions: 0.2 m^3 and 0.4 m^3, resulting in computational domains of 100,000 and 12,000 cells respectively. These relatively coarse mesh resolutions were forced by the length of the experiments (and hence the length of the simulations) which was 120 minutes.

FDS was used to model five test scenarios, out of eight carried out within the NFSC programme. The program was used to predict compartment gas temperatures. The HRR curve was established from mass loss measurements taken during the experiments and it was used as model input (i.e. the burning rate was not predicted by the program). The authors noted that the above method of establishing the HRR profile for each experiment relied on the value of heat of combustion for the fuel provided in the original test report and that the accuracy of this value was difficult to define.

The authors found that FDS consistently under-predicted the maximum gas temperatures in the compartment. This effect is particularly pronounced when readings of individual thermocouples are analysed, rather that average compartment temperatures. The simulations with finer mesh resolution generally produced better results. The maximum (averaged) gas temperature was under predicted by between 11 to 33 % for the coarse (0.4 m) mesh, and between 3 and 11 % for the finer (0.2 m) mesh.

3.1.3.5 Work by Moghaddam et al.

Moghaddam et al. compared the results of FDS simulations of corner fires in an ISO room with published experimental data [20].

Two types of fire scenarios were studied:
- Scenario 1 - an ethanol pool fire in a compartment without combustible linings
- Scenario 2 - a fire involving combustible wall linings in the compartment

Three different grid resolutions were investigated for each type of simulation. For simulations involving pool fire tests with prescribed heat release rate, grid resolutions of 0.2, 0.1 and 0.05 m were used.
For simulations involving fire spread on wall linings (where the burning rate was predicted by FDS) 0.1, 0.05 and 0.025 m grid resolutions were used.
The computational domain used in the simulations was 2.4m x 2.4m x 5m.

Scenario 1 was initially modelled in such a way that the model would predict the burning rate of the fuel.

In the first run the heat release rates were significantly under-predicted by FDS.
The authors found that this phenomenon was caused by the limitation on the maximum burning rate that incorporated in the fuel data in the program database. This limitation was introduced by FDS developers in order to deal with the problem of FDS over-predicting the burning rates, as described by Hostikka, Hamins and McGrattan [21], and also discussed in the FDS User's guide [8].

In the second run the limitation on the burning rate was removed, which resulted in FDS strongly over-predicting the heat release rate. This is consistent with the findings mentioned above (similar problems were encountered in the modelling conducted as part of this dissertation project – see sections 5.1.3 and 6.1 for details)
Subsequently, the FDS simulations for Scenario 1 were conducted using a prescribed HRR curve, based on the experimental measurements.
The authors concluded that where the heat release rate of the fire was prescribed, FDS could reproduce compartment temperatures well (provided that a fine grid was used).

In Scenario 2, where the program was required to predict the burning rate significant inconsistencies were found. Also, the choice of a finer computational grid did not necessarily result in a better model prediction.

3.1.3.6 Work by Kashef et al.

Kashef et al. undertook a study to compare predictive capabilities of selected models for smoke movement in large spaces [22]. A two-zone mode called FIERA and a CFD model (i.e. FDS version 1) were investigated. The study was conducted at the National Research Council Canada.
Two case studies were investigated: a pool fire in a paint workshop of an aircraft hangar and a fire in a mechanically ventilated atrium.
For the second case study, FDS predictions were compared with the experimental results of fire tests in a large compartment (9 m x 6 m x 5.5 m high).
Only this second case study will be descried here.

The fire source in the tests was a square propane sand burner, capable of simulating fires ranging from 15 kW to 1000 kW with three possible fire areas 0.145 m^2, 0.58 m^2 and 2.32 m^2.

Fresh air was supplied into the compartment through openings in the floor around the walls, using a supply fan.

Hot gases were extracted through 32 exhaust points in the ceiling of the compartment. All exhaust points were connected to a central plenum from which smoke was extracted.

The fire compartment was instrumented with thermocouples and pitot tubes. CO_2 concentrations were measured at selected locations. The heat release rate was determined using two methods: measuring volume flow rate of propane supplied to the burner and by measuring oxygen-depletion, temperature and the volumetric flow rate in the main exhaust duct.

FDS simulation was carried out for a quarter of the fire compartment using symmetry boundary conditions.

The computational domain was divided into a uniform grid of 96 x 60 x 72 cells (414,720 cells in total).

HRR values were obtained from the experiments and were used as an input into the FDS simulation. HRR was varied during the simulation and was set at 150 kW in the initial stage, 250 kW in the intermediate stage and 600 kW in the final stage. HRR was maintained steady for approximately 15 minutes in each stage.

FDS predictions of the temperature profile along the centreline of the room agreed well with the experimental values when readings were taken slightly off the centreline. When FDS predictions were taken for the room centre exactly, there were significant discrepancies between the experimental values and the FDS predictions. This was attributed by the authors to possible inaccuracies in placing the thermocouples at the room centreline in the experiments.

For temperature profiles at other locations within the compartment there was some disagreement between the experimental and numerical values. In the experiments, the temperatures within the hot layer were quite uniform and the interface between the hot and cold layers is clearly defined. Temperature profiles predicted by FDS show an increase with height (even within the hot layer) and the hot layer interface itself is not clearly defined. A similar phenomenon was observed for CO_2 concentration profiles.

3.1.3.6 Work by VFDB

VFDB is the German Fire Protection Association. As part of the development work on guidelines on methods in fire engineering, VFDB conducted (in conjunction with several other German research institutions) a round robin test where different methods of predicting smoke spread in enclosures were compared [23].

The project involved comparison of results of two large scale fire tests with the predictions of CFD models, zone models and physical models.

FDS was one of the four CFD models tested (the other CFD models were: Fluent, CFX and a simple model Kobra3d).

The full scale tests were conducted after the physical modelling and the numerical simulations were completed.
Two scenarios were considered: a fire in a large atrium space (8.2 x 6.2 x 10 m) and a fire in a smaller compartment (5.3 x 4 x 2.6 m) adjacent to the atrium.
Quantities such as smoke temperature, velocities, thickness of smoke layer and CO_2 concentrations were compared.

Due to a difference between the heat release rate assumed for the blind simulations and the heat release rates actually measured in the large scale tests, the experimental and modelled results could not be strictly compared. However, general observations on the quality of predictions were made.

The study concluded that for certain fire scenarios CFD models provide much better predictions of smoke layer height, compared to zone models. Such scenarios include a situation where the smoke flow field is dominated by the replacement air inflow rather than by the plume flow.

3.1.3.7 Work by Rein at al.

Rein et al. [24] applied FDS ver. 3 and two other fire models (i.e. an analytical model and a zone model CFAST) to study three accidental fires that occurred in single-family dwellings. They concluded that in spite of the differences in the sophistication of these three models, the results were in relatively good agreement, particularly when describing simple aspects of the fire such as ceiling layer growth and smoke concentration in the early stages of the fire. However, only a field model, in this case FDS, was found capable of providing detailed conditions after the initial stages of the fire.

3.1.4 Recent and on-going validation work for FDS

This section presents several examples of FDS validation work that is currently ongoing. Information on such recent validation projects was found by the author through internet mailing lists and personal communication with fire researchers and engineers.

3.1.4.1 Work at the Lund University.

A project to investigate the validity of performance based fire safety design is currently under way in Sweden. This project is carried out jointly by the Lund University and SP Swedish National Testing and Research Institute. As part of the project, validation work on a number of CFD codes is to be conducted.

In this validation project the following scenarios are to be simulated:
- An industrial building 16m x 10m x 5m room with a constant fire source (propane burner) at one end and passive smoke ventilation in the ceiling at the other end of the room.
- A corridor (dimensions 15m x 7.5m x 6m), with end walls removed. A fire source is located on the floor in the middle of the corridor. In this case the fuel input is varied with time giving an increase of fire energy release rate Q proportional to time squared. Two different ventilation conditions are investigated.
- A long Tunnel (about 800 m)
- An atrium about 30x30x30 m
- The last scenario has not been chosen yet.

The CFD-codes involved are FDS (LES), CFX (RANS), and two University codes, SOFIE (RANS) and SMAFS (RANS and LES). The simulations are done without access to the experimental results (blind simulations). The experiments used in the program has been chosen carefully (repeatability, error bars etc).
The programme will be completed in December 2007 [25].

3.1.4.2 Work at Kingston University.

A research project aimed at investigating the effects of venting on fires in basements is currently under way at Kingston University, London.
The research is carried out on behalf of the Fire Statistics and Research Division of the Department for Communities and Local Government, UK.
The project is aimed particularly at investigating ventilation factors that may lead to a backdraft during fire-fighting operations in basements.

As part of the research, FDS is used to model and investigate different ventilation scenarios for basement fires. In order to validate FDS for this particular application, model predictions are compared with the results of a full-scale experiment involving an under-ventilated wood-crib fire in a 6 m by 4.9 m by 2.6 m compartment. The vents in the compartment walls are arranged to resemble a typical basement with an entrance door and a "pavement light".
The project is still on-going and the results are not available at the time of writing this report. Publication of results is expected in November 2006 [26].

3.1.4.3 Work by MDE Inc.

MDE Engineering Inc. is a multi-disciplinary forensic engineering firm based in Seattle, Washington. The company is currently conducting FDS validation work for flame spread problems. The aim of the work is to reproduce ASTM E84 tunnel tests using FDS [27].

3.1.4.4 Work by Senez Reed Calder Engineers.

Senez Reed Calder Fire & Forensic Engineering Ltd. is a fire and forensic engineering company with offices in Vancouver and Delta, Canada.
In order to validate FDS for the scenarios of interest, the company conducted full and reduced scale testing, mainly concerned with flame spread. The tests included cone calorimeter tests, ISO room tests, three-storey wall tests, and real house burns.
All versions of FDS since version 3 were used for validation work.

The general approach adopted by the company is similar to that conducted by NIST as follows:

- Cone calorimeter testing of materials is conducted initially to obtain material properties.
- Full or reduced scale tests are then conducted to confirm the accuracy of the derived material properties and/or calibrate these properties.
- If good agreement is reached between the model and the experimental results a full-scale modelling exercise is carried out.

Most validation work has been conducted following the guidelines of ASTM E1355.

The FDS predictions were generally within 10-20% agreement with the experimental results [28].

3.2   Validation of other CFD models

3.2.1   Validation of Jasmine

Jasmine is a fire special-purpose CFD code developed by the Building Research Establishment (BRE) in the UK. Jasmine is a three-dimensional finite volume CFD code, which employs a k-ε turbulence model.

An example of Jasmine validation against full-scale fire tests is provided by Miles [29]. The results of four confined pool fire tests were compared with the model predictions. All tests were performed in a single-opening compartment, resulting in ventilation controlled burning and post-flashover conditions.
One test was performed in a 135 m^2 compartment, while the other three tests were performed in a larger 415 m^2 compartment (with three different vent sizes).
The fuel used was a mixture of pentane, hexane, heptane, octane, nonane and some higher hydrocarbons. Heat release rates in the experiments ranged from 10.6 MW to 78.9 MW. Compartment walls were made of Pyrolog insulating blocks with 1 mm steel liner internally.

CFD simulations were preformed with computational meshes of approximately 100,000 and 200,000 cells for the small and large compartment respectively. A vertical symmetry plane was imposed through the centre of the compartment and opening.
The quasi-steady state reached in the tests was approximated with steady state simulations for all cases except one, for which a transient state simulation was performed.

The quantities for which comparison was made included temperatures in the compartment and at the opening, flow velocities at the opening and concentrations of selected species (i.e. O_2 and CO_2) at the top of the compartment opening.
Good agreement was achieved for the mass flow rate and the O_2 concentration.
There was a discrepancy in the C02 concentration prediction, which was attributed to the fact that the combustion model did not predict CO (the combined CO_2+CO measurement agreed better with the predicted CO_2 concentration).
Agreement between the temperature measurements and predictions was described as reasonably good.

There was a discrepancy in wall temperatures and incident fluxes at the back of the compartment. However, this discrepancy was at least partially due to the way in which surface temperatures were measured on the steel lining, which was not rigidly attached to the insulating block. Also, due to a layer of soot on the heat flux meters, there was an increased uncertainty in the heat flux measurements.

3.2.2   Validation of Smartfire

Smartfire is a fire specific CFD code developed by the Fire Safety Engineering Group (FSEG) at the University of Greenwich. The code employs a k-ε turbulence model, and a six-flux radiation model. Smartfire uses unstructured meshes, which allows simulations involving irregular geometries.

An example of Smartfire validation against fire tests is provided by Gale et al. [30]. As part of validation exercise for Smartfire, temperature predictions of the model were compared with the experimental results of one of the CIB Round Robin test series (Scenario B). The fire compartment measured 14.4 m x 7.2 m x 3.53 m. There was a single door opening measuring 2.97 m x 2.13 m located in the front wall.
The test used a burning wood crib as the fire source. The maximum heat release rate reached in the test was approximately 11 MW.

Two CFD simulations were preformed, one with a coarse mesh and one with a fine mesh, utilizing 12,480 cells and 41,325 cells respectively. A simple volumetric heat release model was used in both simulations.

The model was found capable of reproducing the overall qualitative results.
In both simulations, the model over-predicted the temperatures. A better result was achieved in the simulation with a finer mesh, where the maximum recorded experimental temperature (1214 $^{\circ}$C after 39 min) was over-predicted by 12%.

4.   PHYSICAL MODELLING

4.1   Description of experimental set-up

The experiments were carried out at the FireSERT facility at the University of Ulster. The experimental set-up consisted of a 1/3rd scale ISO room model used as the fire compartment and a 3x3 m extraction hood used as the smoke reservoir. A construction imitating a balcony with two channelling screens was added for experiments 1-4. Thermocouples were placed within the fire compartment, the spill plume and in the smoke reservoir. Bi-directional probes were located at the compartment opening and in the spill plume. A computer data logging unit was used to collect the results. Heat release rate was measured by an oxygen consumption calorimeter integrated with the extraction hood. The general arrangement of the experimental stand is illustrated in figure 4.1 below.
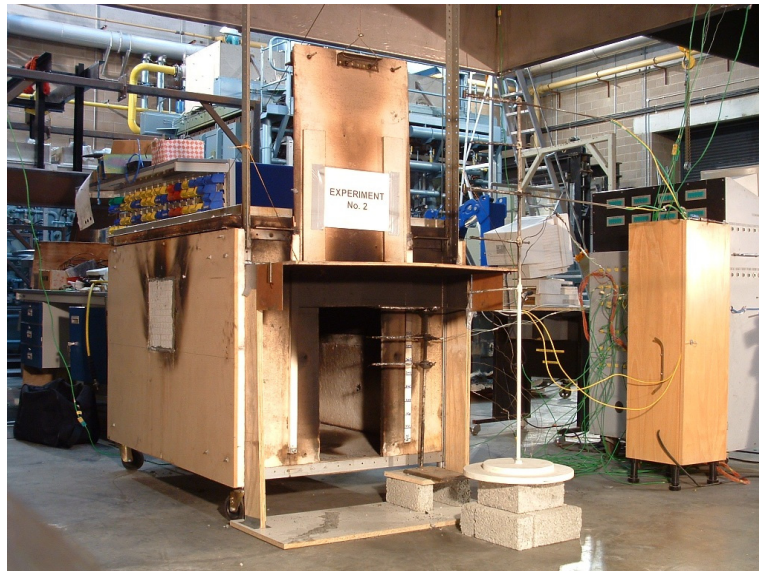

Fig. 4.1 Experimental stand

4.1.1 Experimental scenarios

Two main scenarios were considered in the experimental part of this work:

Scenario A – balcony spill plume, diesel oil used as a fuel (Experiments 1 to 4)

Scenario B – no balcony present, ethanol used as a fuel (Experiments 5 & 6)

Fig. 4.2 Experiment no. 2 – General view

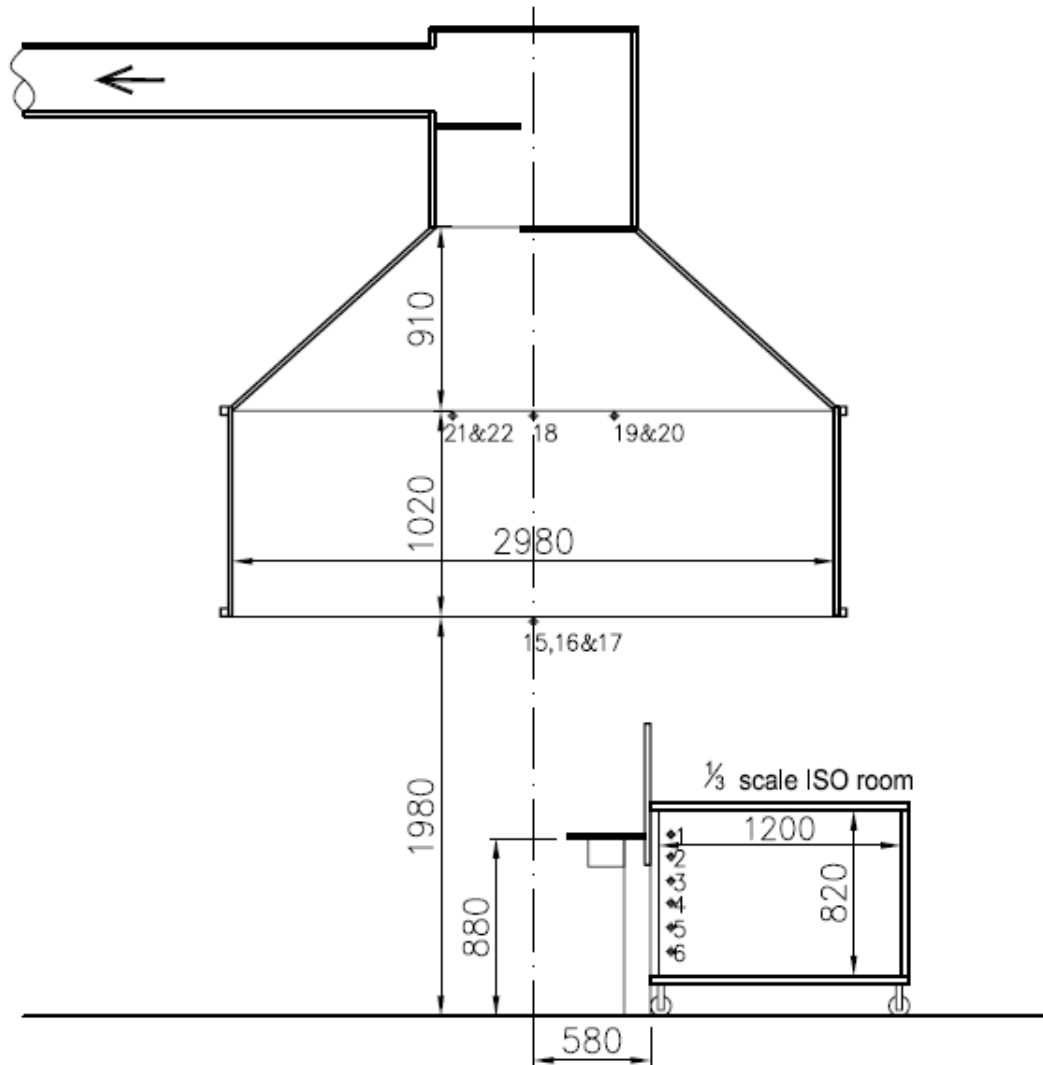**Fig. 4.3 Experiment no. 5 – General view**

A summary of the main parameters including the type of fuel, ventilation conditions, ambient air temperatures etc. for all experiments is provided in table 1.

Principal dimensions of the experimental stand are provided in figure 4.4 below. Balcony and channelling screens were not included in experiments no. 5 & 6.

Fig. 4.4 Longitudinal section of experimental set-up

Case	Date	Tray Size [mm]	Distance to edge [mm]	Fuel	Burning time	Extraction rate [m^3/s]	Opening Height [mm]	Width [mm]	Ambient temp	Description
Exp_1	25/04/06	200x200	400	Diesel oil 500 ml	515 s	0.74/ 0.85/ 0.98	550	270	14 ^{o}C	Balcony, no channelling screens
Exp_2	26/04/06	200x200	400	Diesel oil 500 ml	620 s	1.00 / 1.15	550	270	14 ^{o}C	Balcony + channelling screens
Exp_3	28/04/06	200x200	400	Diesel oil 500 ml	590 s	1.10	550	270	12 ^{o}C	Balcony + channelling screens
Exp_4	04/05/06	200x200	400	Diesel oil 500 ml	620 s	1.10	550	270	12 ^{o}C	Balcony + channelling screens
Exp_5	04/05/06	250x250	350	Ethanol 1000 ml	795 s	1.10	500	270	14 ^{o}C	Balcony removed, wall extended
Exp_6	04/05/06	250x250	350	Ethanol 1000 ml	830 s	1.10	500	270	14 ^{o}C	Balcony removed, wall extended

Table 4.1 Summary of parameters for experiments carried out

4.1.2   The fire compartment

A 1/3rd scale model of ISO-room was used as the fire compartment in all experiments. This ISO-room model was used in earlier experiments carried out at the university. External walls of the compartment were made of 25 mm LD Fiberfrax Duraboard temperature resisting slabs (internally) with an external layer of 10 mm MDF board. The front opening was 270 mm wide. The height of the opening was adjustable. A simple arrangement was added for the purpose of imitating a balcony in experiments no. 1 to 4. The balcony slab and side supports were made of 12.5 mm thick plywood. Channelling screens (180 x 140 mm high), made of 1 mm thick sheet steel were added in experiments no. 2-4.

4.1.3   Measuring equipment

Heat Release Rate was measured using the oxygen consumption calorimeter integrated with the extraction hood. The calorimeter was not calibrated specifically for the experiments and the possible error of its measurement was estimated by the laboratory staff to be 10%. It should be noted that the magnitudes of HRR measured in the experiments were close to the lower threshold of the measuring capability of the calorimeter used.

Compartment temperatures were measured using 6 no. insulated 1.5 mm type-K thermocouples. Other temperature measurements were taken using bare type-K thermocouples.

3 no bi-directional probes were used to measure flow velocities. It should be noted that calibration of the bi-directional probes was relatively crude and it was done using a hand-held anemometer. The accuracy of the flow velocity measurements is estimated to be +/- 20%.

All experiments were recorded using two digital camcorders.

4.2   Experimental results

A comprehensive set of measurements was taken in each experiment. However, the post experiment analysis of the results revealed that some of them are more reliable than others.

This is due the fact that some of the thermocouples and bi-directional probes were located in areas where even small difference in device location could results in significant difference in the values of measurement taken.

An example of this is thermocouple no. 12, which is located close to the boundary of the flowing smoke layer under the balcony. A small change in the positioning of this thermocouple could mean that it is either located within the flowing mass of hot smoke or in a much colder mass of fresh air.

Conversely, for thermocouples no. 18 to 22 which were located in the smoke reservoir (i.e. the extraction hood), small changes in device location would not have any significant impact on the temperature readings.

The uncertainty in establishing the positions of the thermocouples was relatively large, up to 30 mm in at least one direction.

For this reason, it was decided that only selected measurements should be used for comparison with the results of FDS modelling, namely:

- Compartment temperatures (thermocouples 1-6)
- Centreline spill plume temperatures at high level (thermocouples 8-11)
- Average reservoir temperature (thermocouples 18-22)
- Vertical velocity in the spill plume (bi-directional probe no. 24)

Experiments no. 2 and 5 were selected as the most representative for diesel and ethanol fires respectively, as explained below. Their results are discussed in detail in this section.

Detailed results for all the experiments undertaken can be found in Appendix D

4.2.1 Heat Release Rate (HRR)

Heat Release Rate was measured using the oxygen consumption calorimeter available at the FireSERT laboratory. HRR curves are presented in figure 4.2 below:
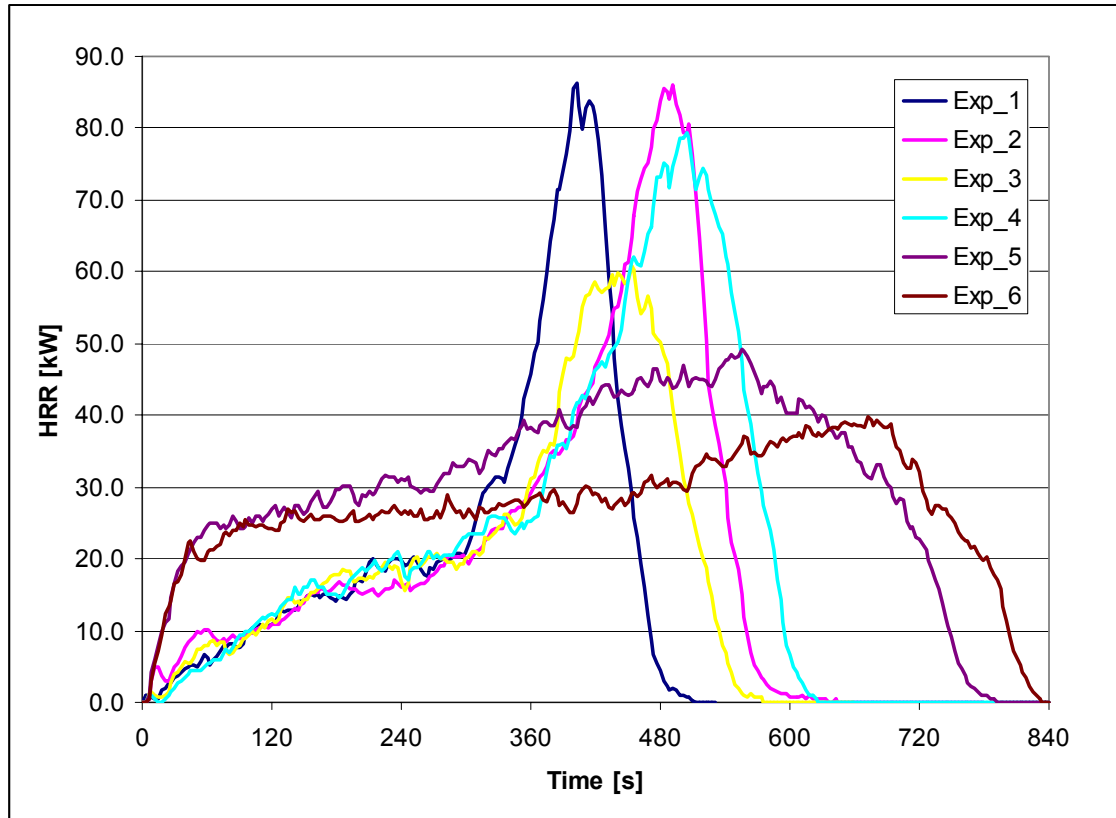
Fig. 4.5 HRR measured in the experiments

For the experiments involving diesel oil, similar HRR curves were obtained for experiments no. 1, 2 and 4. For experiment no. 3, the HRR profile differs substantially from the remaining three experiments, with the peak HRR approximately 30% lower. A simple analysis of the obtained HRR curves leads to the conclusion that the most reliable results in terms of HRR measurement were obtained in experiment no. 2 (Exp_2). The maximum HRR reached is consistent with experiment no. 1, while the overall shape of the HRR curve is in good agreement with experiment no. 4.

For this reason, Experiment 2 was selected for comparison with the FDS results as the most representative for the experiments involving diesel oil as fuel.

For experiments 5 and 6 (ethanol), it is not possible to assess which HRR measurement is the most accurate, as only two experiments were carried out.

Both HRR curves are reasonably similar, with the overall amount of heat released in each experiment not differing by more than 10%. However, the maximum recorded values of Heat Release Rate differ by approximately 20%.

Case	HRR$_{max}$ [kW]	m''$_{max}$ [kg/m²s]	D [m]	Q$_{total}$ [kJ]	Q*	D* [m]
Exp_1	86.00	0.0524	0.20	12,150	4.37	0.36
Exp_2	**86.00**	**0.0524**	**0.20**	**15,740**	**4.37**	**0.36**
Exp_3	61.00	0.0372	0.20	13,090	3.10	0.31
Exp_4	79.00	0.0482	0.20	17,440	4.01	0.35
Exp_5	**49.00**	**0.0293**	**0.25**	**24,940**	**1.43**	**0.29**
Exp_6	40.00	0.0239	0.25	22,510	1.16	0.27

Table 4.2 Total heat released, dimensionless HRR and characteristic fire diameter

In order to provide an additional assessment of the heat release rates measured in the experiments, it is proposed to compare the overall energy released in each experiment with the theoretical values.

$$Q_{theoretical} = m * \rho * \Delta h \qquad (1)$$

For Scenario A (500 ml of diesel oil burnt):

$$Q_{theoretical} = 0.5 \times 10^{-3} * 850 * 41,000 = 17,425 \text{ kJ}$$

The calculated theoretical amount of energy released by burning 500 ml of diesel oil is higher than the recorded value in experiments 1-3. This can be explained by the fact that there was some spillage of smoke from the reservoir at the peak burning period, which might have caused under-estimation of the peak heat release rate and hence also a slight underestimation of the total amount of energy released.

In experiment no. 4 the measured value of total energy released agrees very well with the theoretical value.

For Scenario B (1000 ml of ethanol burnt)

$Q_{theoretical} = 1.0^{x}10^{-3} * 789 * 26,800 = 21,145$ kJ

The calculated theoretical amount of energy released by burning 1000 ml of ethanol is very close to the value recorded in experiment no. 6. (over-estimated by 6%, which is well within the uncertainty of the measurement).

There is a bigger discrepancy in experiment no. 5, with the amount of energy released over predicted by 18%.

4.2.2 Compartment temperatures

Compartment temperatures were measured using a thermocouple tree located in one of the front corners of the compartment (T1 is the thermocouple located nearest to the ceiling of the compartment).

In experiment no. 2, the maximum recorded compartment temperature was 552 ^{o}C (recorded by thermocouple no. 3 between 482s and 492 s)
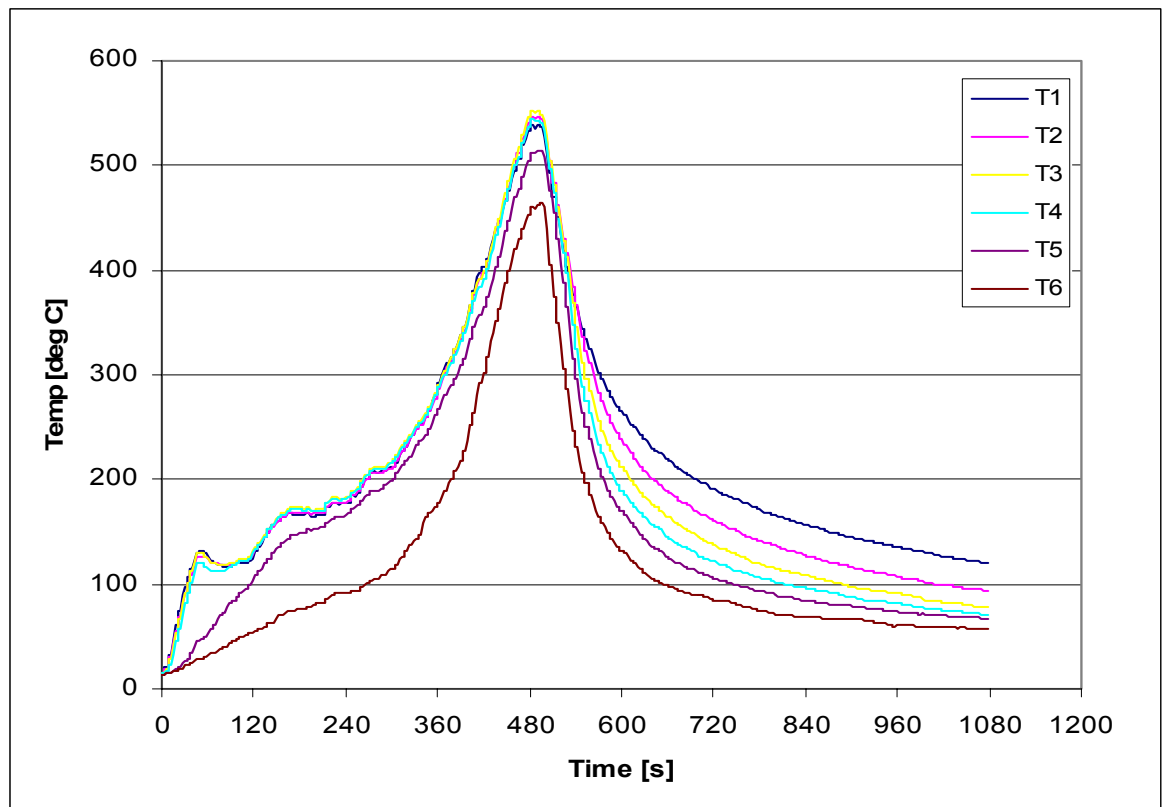
Fig. 4.6 Compartment temperatures – Experiment 2

In experiment no. 5, the maximum recorded compartment temperature was 437 $^{\circ}$C (recorded by thermocouple no. 1 at 565 s)
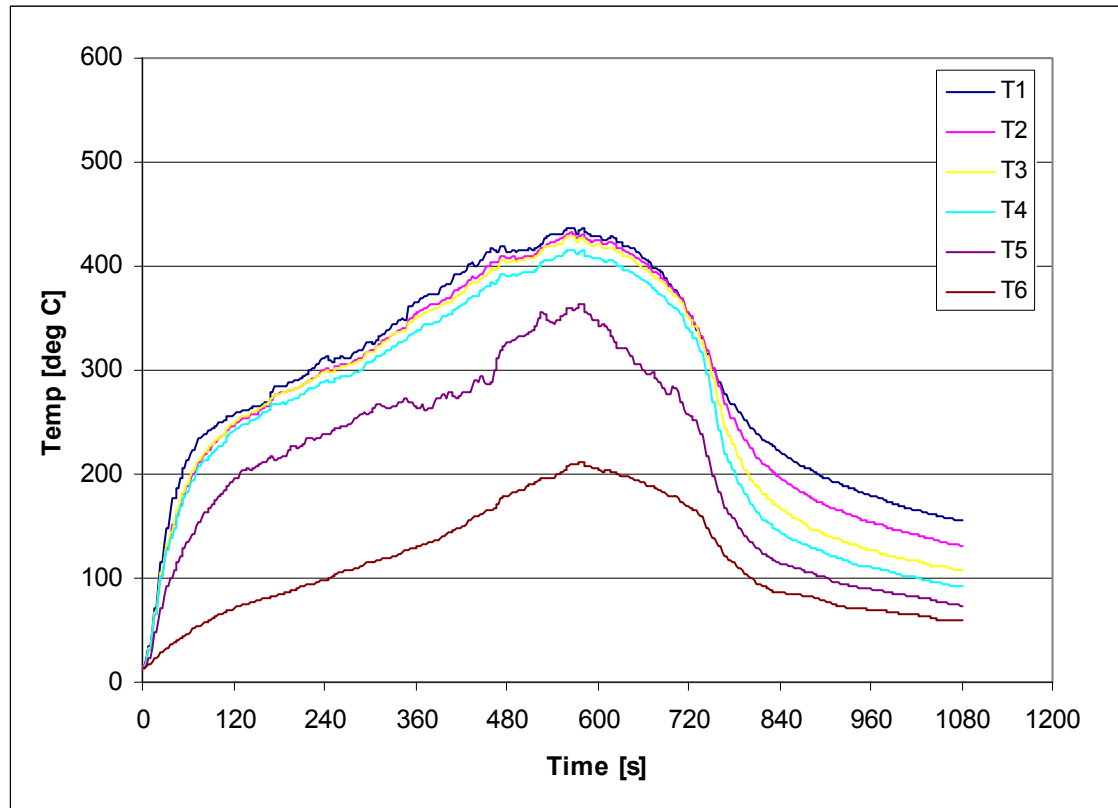
Fig. 4.7 Compartment temperatures – Experiment 5

It is difficult to assess the accuracy of the temperature measurements for the experiments undertaken.

The recorded heat release rates for experiments 1 to 4 differ between one another and also a quasi-steady state was not reach in any of the experiments. Therefore it is not possible to judge the accuracy of temperature measurements statistically.

As a qualitative observation it is noted that the thermocouples inside the compartment were covered with soot. The thermocouples were not cleaned after each experiment as this only became apparent after the experiments were finished and the compartment ceiling was removed. A thick layer of soot on the thermocouples inside the compartment might have decreased their sensitivity and also might have slightly decreased the maximum temperatures recorded.

4.2.3 Spill plume temperatures

Spill plume temperatures were measured using a thermocouple tree located at the centreline of the spill plume.

In experiment no. 2, the bottom of the thermocouple tree was positioned approximately at the level of the spill edge (i.e. the edge of the balcony). The axis of the thermocouple tree was approximately 120 mm form the spill edge.
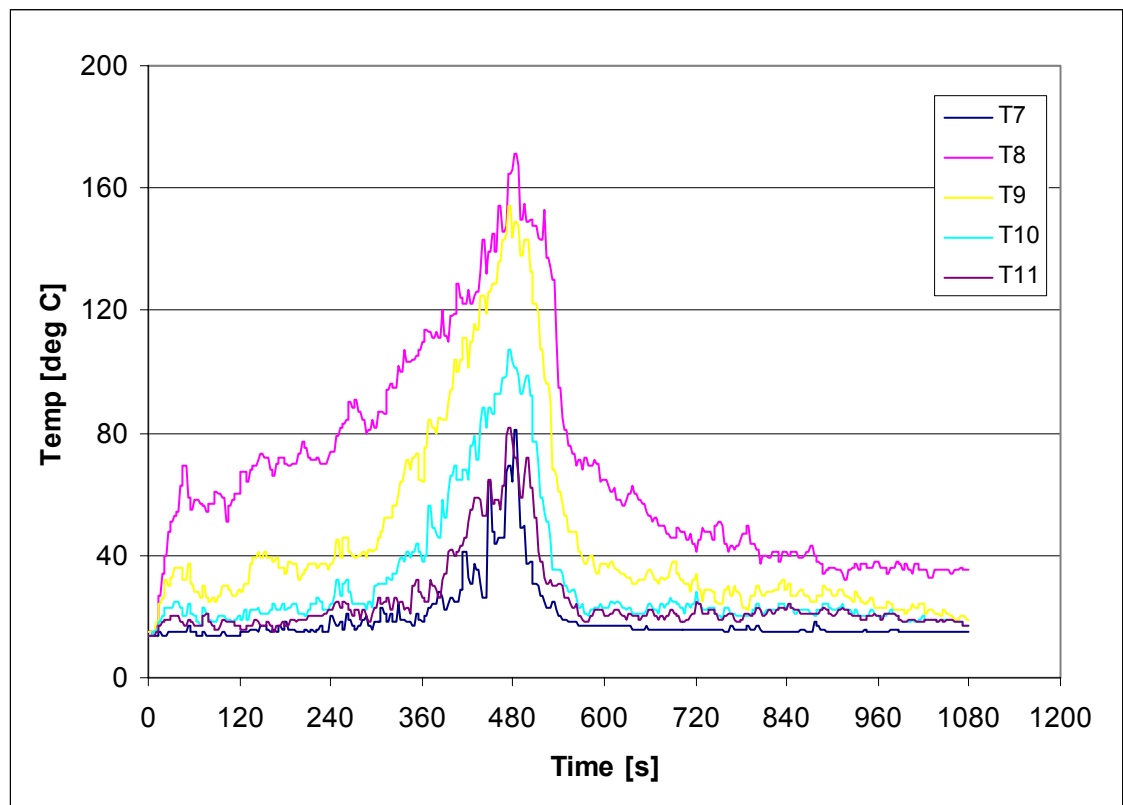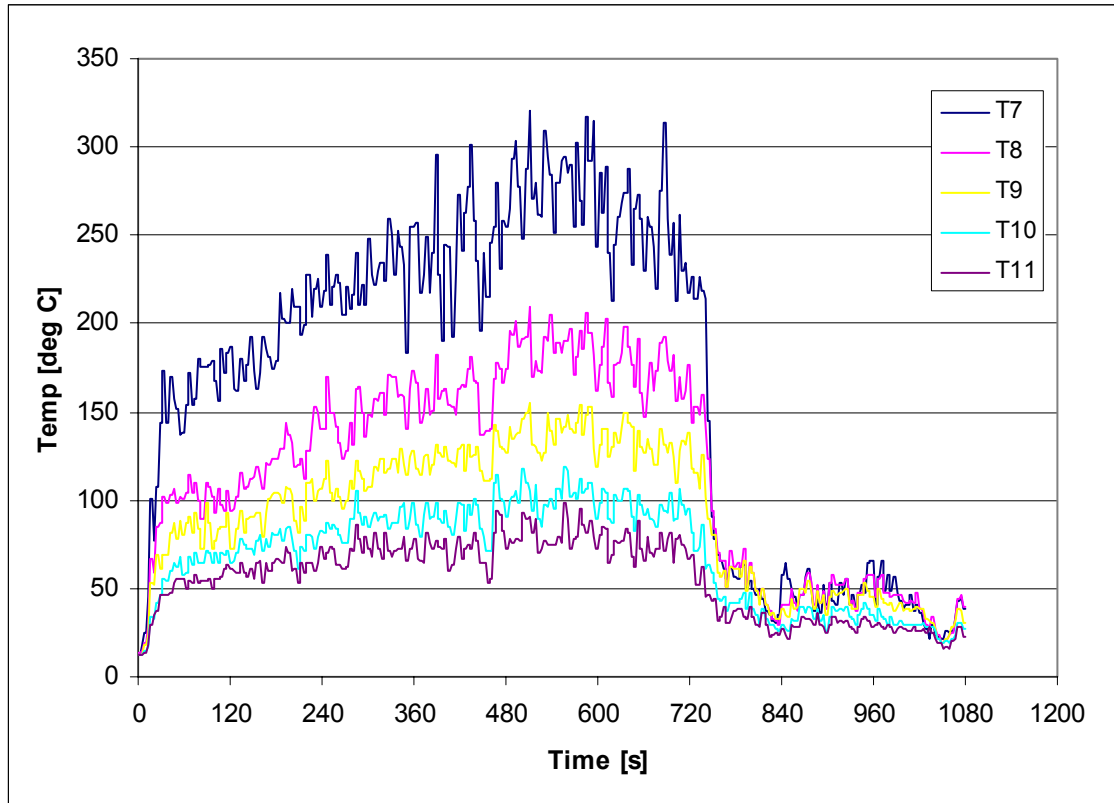

Fig. 4.8 Spill plume temperatures – Experiment 2

From analysing the spill plume temperatures recorded in experiment no. 2 it appears that the lowest thermocouple (T7) was located below the stream of hot gases leaving the compartment, as it recorded the lowest temperatures.

In experiment no. 5, the bottom of the spill plume thermocouple tree was positioned 120 mm above the top of the compartment opening. The axis of the tree was approximately 250 mm away from the front of the compartment.
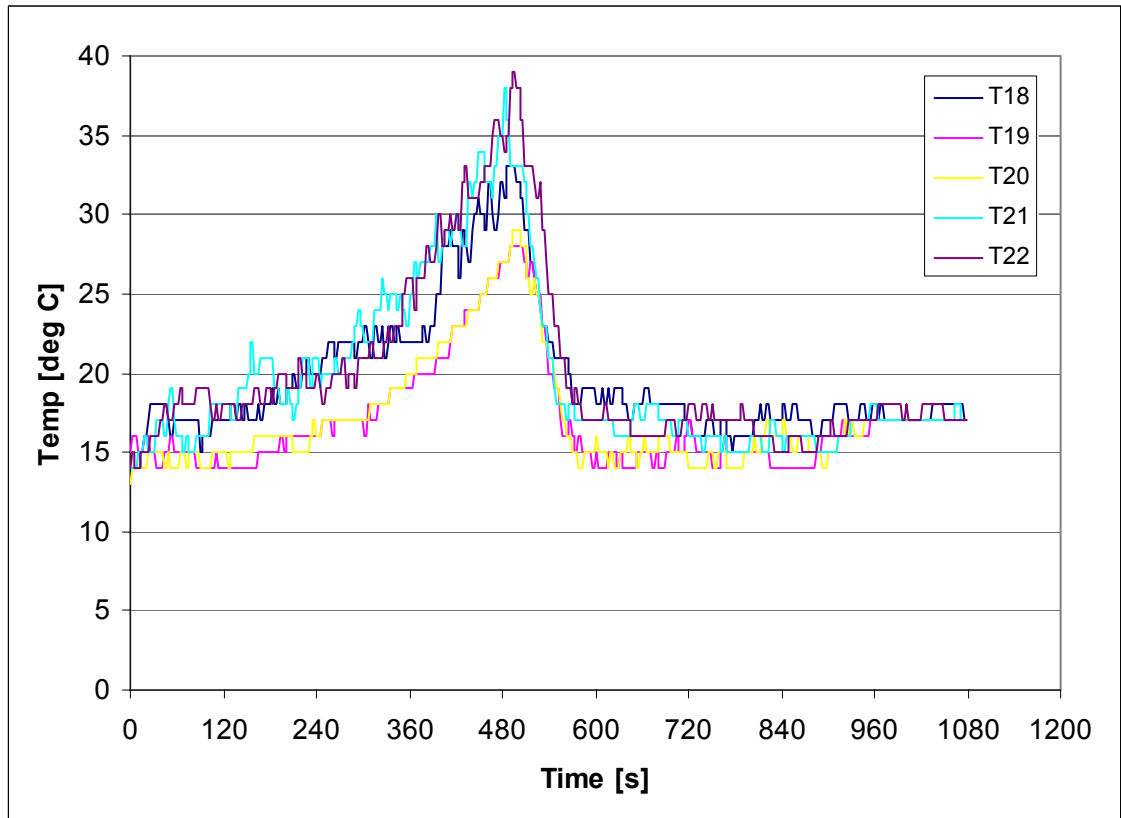

Fig. 4.9 Spill plume temperatures – Experiment 5

The smoke plume temperatures recorded in experiment no. 5 gradually decrease with the increasing height.
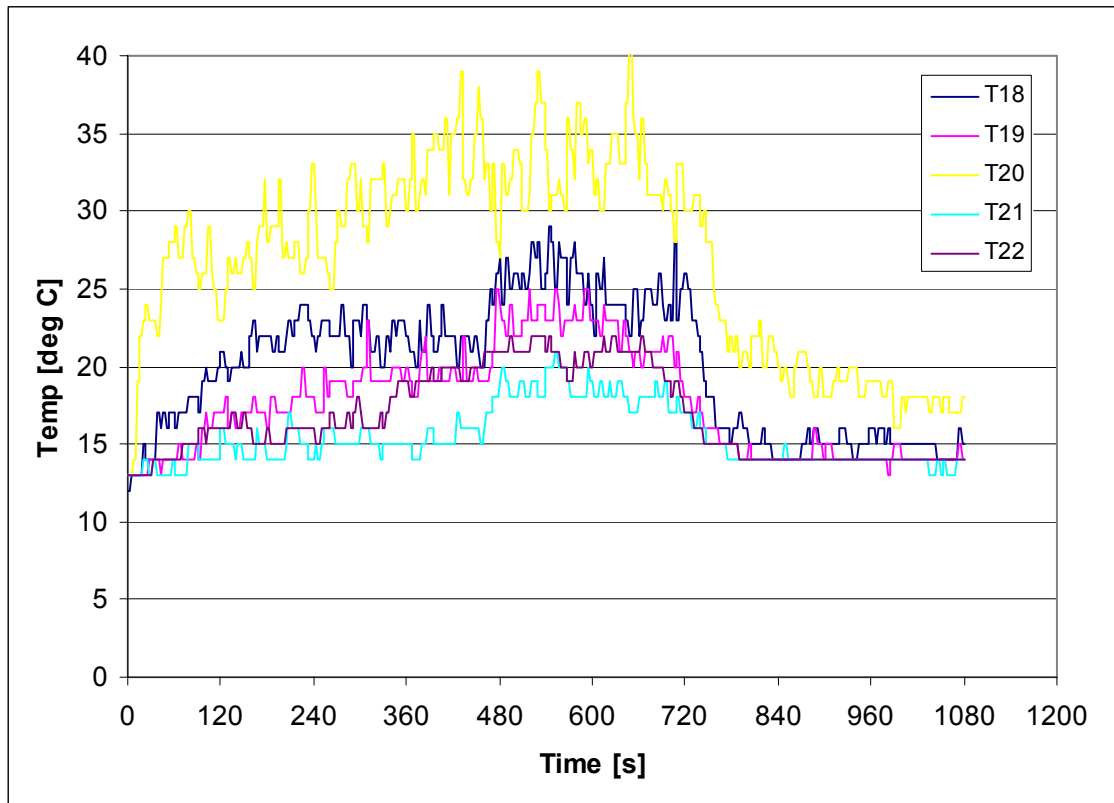
4.2.4   Smoke reservoir temperatures

The temperature of smoke in the reservoir was measured using an array of 5 thermocouples located symmetrically at high level within the extraction hood.

Fig. 4.11 Smoke reservoir temperatures – Experiment 2

The analysis of the above graph (experiment no. 2) indicates that the flow of the hot smoke in the spill plume was directed towards the front of the reservoir (the highest temperatures are recorded by thermocouples T21 and T22, while the temperatures recorded by thermocouples T19 and T20 are significantly lower. This agrees well with the visual observations of the smoke flow made during the experiments.

Fig. 4.11 Smoke reservoir temperatures – Experiment 5

In experiment no. 5 an unexpected results is recorded for reservoir temperatures. One of the thermocouples (T20) recorded significantly higher temperatures than the remaining four, with the recorded temperature rise above ambient nearly twice as high as for the other devices.

A similar phenomenon was observed in experiment no. 6 where T20 was again recording the highest temperature, although the difference was not as significant.

The above suggests that the smoke plume might have not been symmetrical, possibly due to a draft or prevailing air flow in the laboratory at the time.
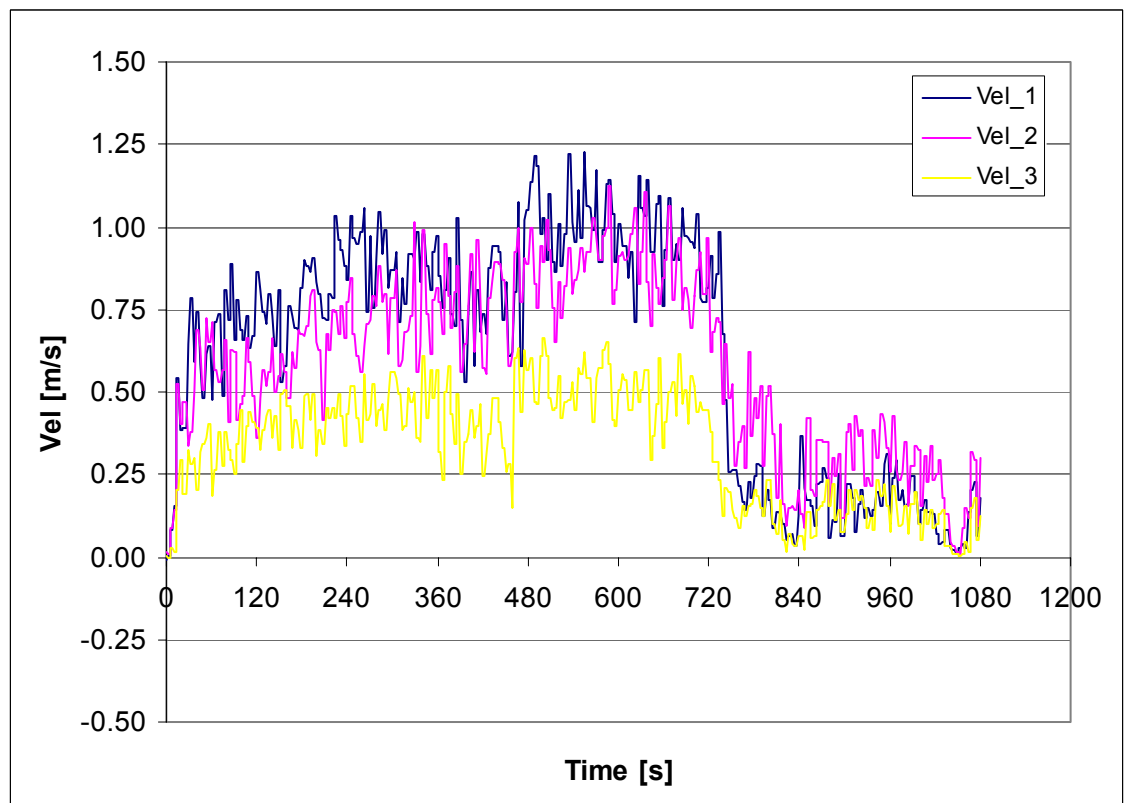
4.2.5   Flow velocities

Flow velocities were measured using three bi-directional probes.

In experiment no. 2, the first bi-directional probe measured the horizontal velocity of smoke below the balcony, and the remaining two bi-directional probes measured the vertical velocity in the spill plume. In experiment no. 5 all three bi-directional probes were used to measure the vertical flow velocity of the smoke plume.
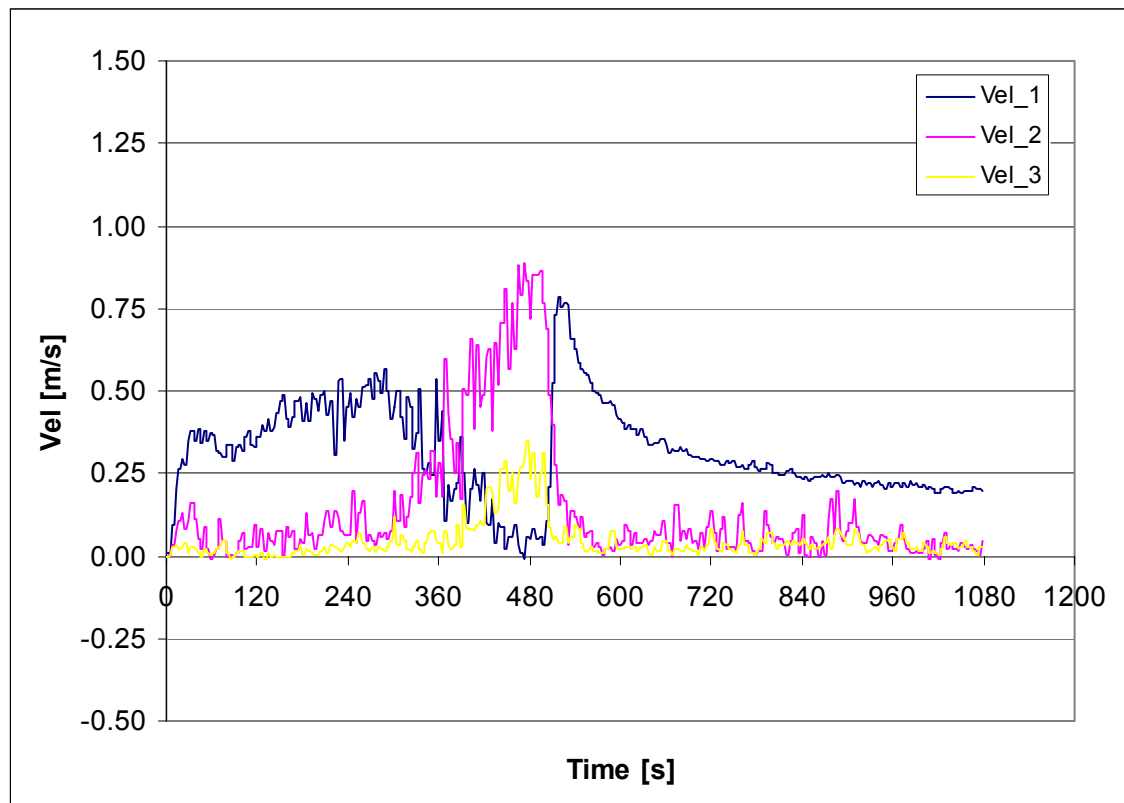
Fig. 4.12 Flow velocities – Experiment 2

Fig. 4.13 Flow velocities – Experiment 5

4.2.6   Visual observations of fire and smoke behaviour

During all experiments the behaviour of fire and smoke was observed and recorded using two digital camcorders. In particular, the time at which the smoke layer descended to the bottom of the extraction hood was noted in experiments 1 to 4. In experiments no. 5 and 6 it was not possible to determine it visually, due to low soot yield of the fuel and resulting low visibility of smoke.

Fig. 4.14 Spill plume – Experiment 1   **Fig. 4.15 Spill plume – Experiment 3**

During experiment no. 2 it was noted that the smoke layer descended to the bottom edge of the extraction hood at approximately 710 s. Some minor spillage of smoke was then observed for approximately 80 s.

It is important to note that during all the experiment conducted the fire was confined to the compartment i.e. flames were not observed outside the compartment.

Fig. 4.14 Spill plume – Experiment 4

5.   FDS SIMULATIONS

## 5.1   Assumptions made in FDS simulations

This section describes the principal assumptions made when the FDS input file was created for each simulation. FDS version 4.07 was used in all the simulations.

5.1.1   Geometry

All blockages in the FDS model have to conform to the computational mesh. For this reason, it is usually not possible for the FDS model geometry to be exactly the same as that of the physical model (unless a very fine mesh is used).

In all the cases modelled the main geometrical features were represented with 5% accuracy, with the exception of the smoke channelling screens which were 20% smaller in the FDS model compared to the physical model.
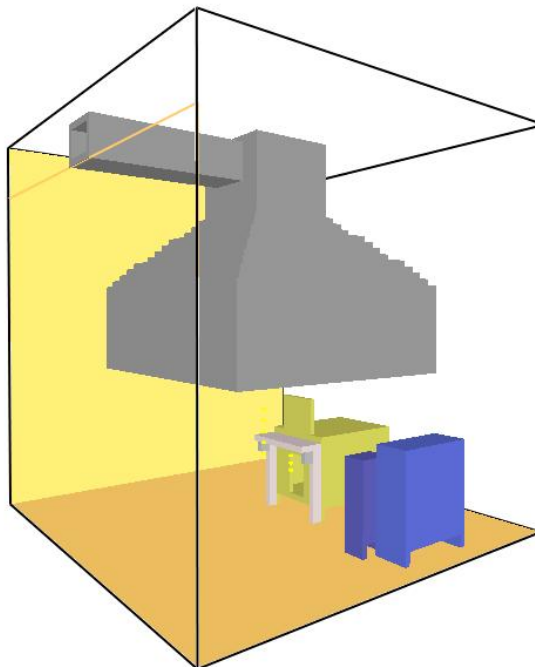
Fig. 5.1 Simulation Exp_2_CW – general view of the geometry

5.1.2 Numerical grid

In order to investigate the influence of the extent and resolution of the numerical grid, several simulations were run for each experiment.

For experiment no. 2 the following numerical grids were used:

- A narrow domain with a standard (coarse) single mesh (CN)
- A wider domain extended to the nearest wall, with a standard single mesh (CW)
- A narrow domain with a single mesh stretched in two directions to provide finer resolution within the fire compartment (SN)
- A narrow domain with a fine single mesh (FN) – due to limited computational resources available only the first 240 s of the experiment were simulated.
- A narrow domain with two meshes used (MM)

For experiment no. 5 the set of simulations was limited to the following:

- A narrow domain with a standard (coarse) single mesh (CN)
- A wide domain with a standard single mesh (CW)
- A narrow domain with two meshes used (MM)

It should be noted that the terms "coarse mesh" and "narrow domain" used above may be somehow misleading and they are the consequence of the naming convention adopted at the beginning of study. Narrow domain with a coarse mesh is in fact the baseline numerical grid adopted in this study.

The summary of mesh sizes and resolutions for all the numerical grids investigated is provided in table 5.1

Grid	Code	Domain co-ordinates / dimensions [m]			Number of cells			Cell size [m]			Total no. of cells
		X	Y	Z	IBAR	JBAR	KBAR	Δx	Δy	Δz	
Single mesh											
Coarse / narrow	CN	-2.24 / 2.24 = 4.48	-2.24 / 2.24 = 4.48	0.00 / 5.12	64	64	64	0.07	0.07	0.08	262,144
Coarse / wide	CW	-2.52 / 2.52 = 5.04	-2.38 / 2.66 = 5.04	0.00 / 5.12	72	72	64	0.07	0.07	0.08	331,776
Stretched / narrow	SN	-2.24 / 2.24 = 4.48	-2.24 / 2.24 = 4.48	0.00 / 5.12	64	80	80	0.07	0.07/0.035	0.08/0.04	409,600
Fine / narrow	FN	-2.10 / 2.10 = 4.2	-2.10 / 2.10 = 4.2	0.00 / 5.00	120	120	125	0.035	0.035	0.040	1,800,000
Multi-mesh											
Mesh #1 (narrow)	MM	-2.24 / 2.24 = 4.48	-2.24 / 2.24 = 4.48	0.00 / 1.92= 1.92	128	128	48	0.035	0.035	0.040	786,432
Mesh #2 (narrow)	MM	-2.24 / 2.24 = 4.48	-2.24 / 2.24 = 4.48	1.92 / 5.12= 3.20	64	64	40	0.070	0.070	0.080	163,840
Total		4.48	4.48	5.12	-	-	-	-	-	-	950,272

**Table 5.1 Summary mesh sizes / grid resolutions for FDS simulations**
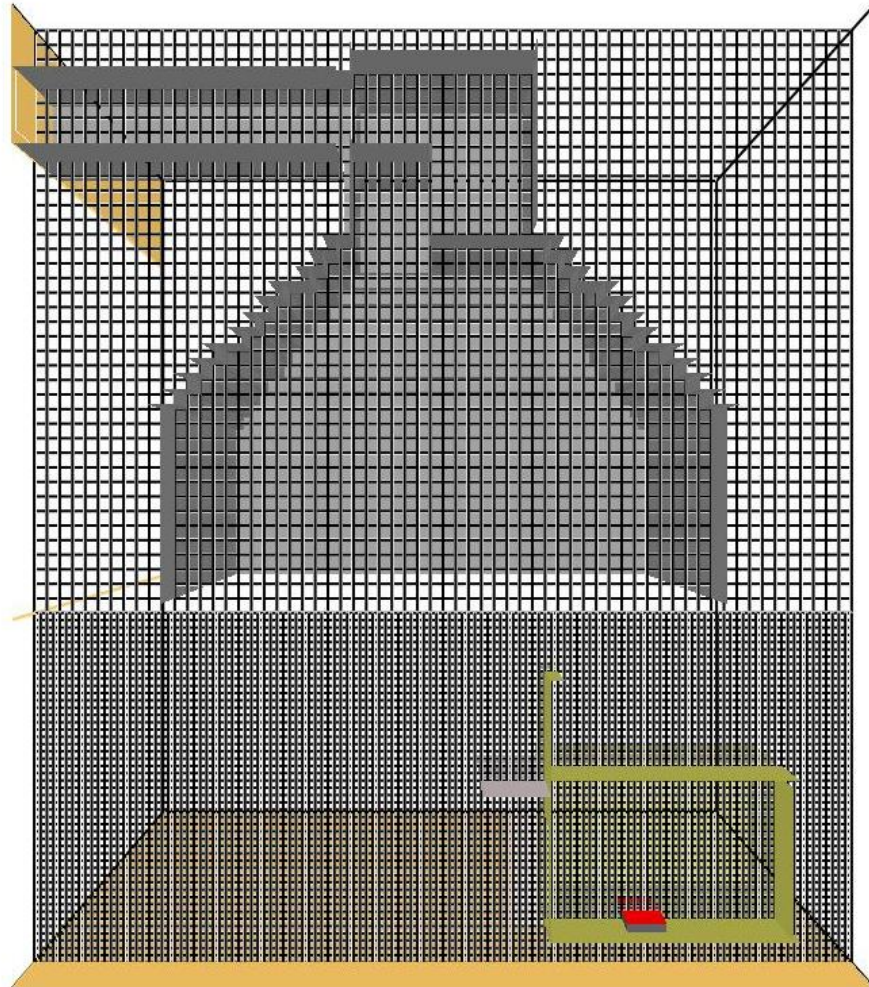
Fig. 5.2 Simulation Exp_2_MM - two meshes visible
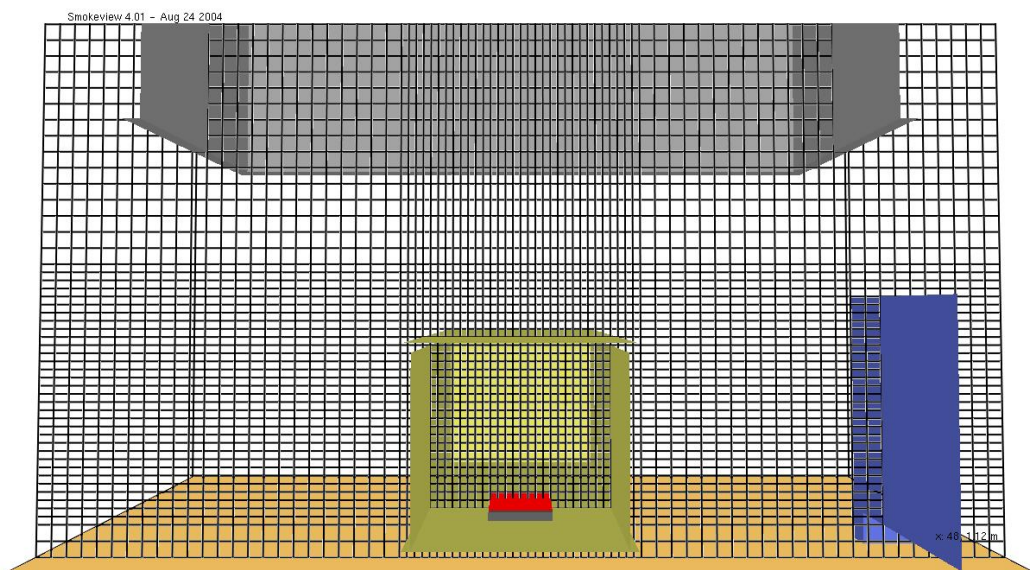
Fig. 5.3 Simulation Exp_2_SN – stretched mesh

5.1.3   Fire description

In the first part of the study the FDS simulations were performed with the HRR curve provided as a model input. The HRR curves recorded during each experiment were approximated with a simplified curve which was than used as in input into the relevant FDS simulation. In this case, the heat release rate history of the fire (and hence the burning rate) was not predicted by FDS.
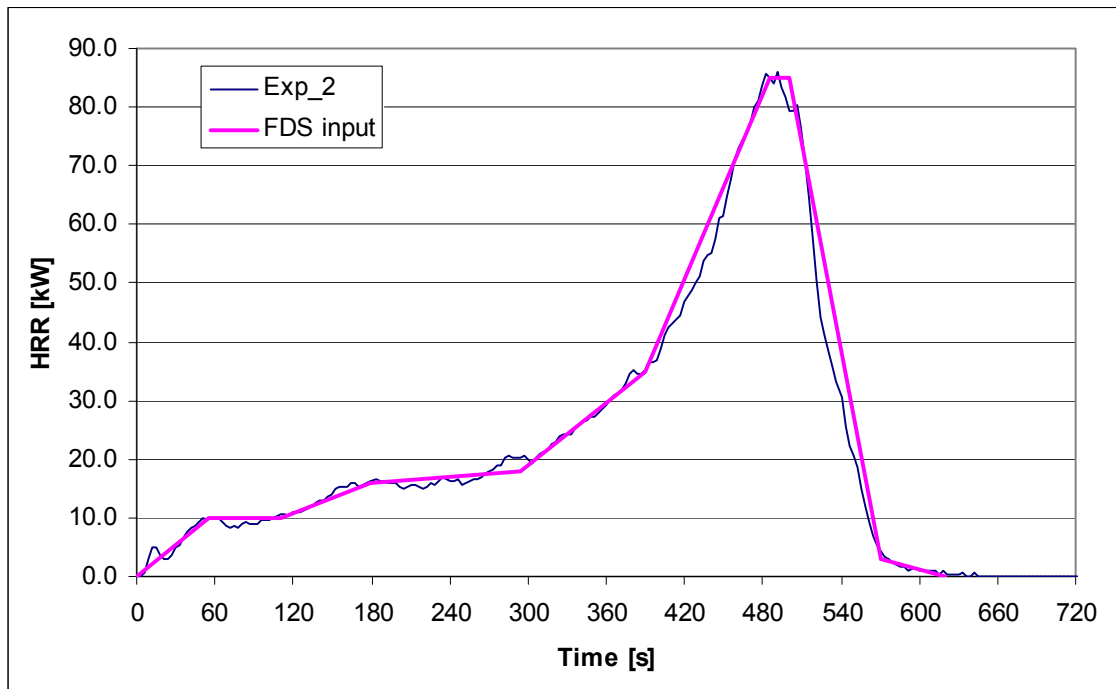
Fig. 5.4 Exp_2 – simplified HRR curve for FDS simulations

In the second part of the study, the simulations were modified so that the fire was defined by the properties of the fuel such as heat of vaporization and heat of combustion. The burning rate in this case was predicted by FDS.
A small heat source (i.e. pilot flame) was simulated adjacent to the fuel tray, in order to cause the ignition of the fuel, and it was removed shortly afterwards.
FDS simulations where the burning rate was predicted by the program are distinguished with suffix BR.

The predicted burning rate of a fuel is strongly dependant on the energy fed back from the fire and hot surrounding objects such as walls of the fire compartment.

Based on the literature review, it was established that FDS may over-predict burning rates due to inaccuracy in calculating the radiative heat flux from the fire to the fuel. A study of this problem is provided by Hostikka et. al [21]. In this study the accuracy of FDS predictions of heat fluxes and burning rate was investigated for pool fires. The authors found that the burning rates for ethanol pool fires were over-predicted.

As a solution to the problem a variable limiting the maximum burning rate was introduced in FDS (i.e. BURNING_RATE_MAX).
The information on maximum burning rate is included for most of the fuels described in the FDS database file, with the values in the range of 0.015 to 0.065 kg/m^2/s. Where the value is not prescribed explicitly, the default value of 0.1 kg/m^2/s is adopted by FDS. However, the values provided in the FDS database file appear to be based on pool fire experiments. For compartment fires, where a high heat feed-back from the enclosure may be expected, these values may not be appropriate.
A discussion of this problem can also be found in the paper by Moghaddam et al. [20].

Based on the preliminary considerations described above, it was decided that the influence of changing the value of the maximum allowed burning rate should be investigated.

The maximum burning rates for the two fuels included in this study were chosen based on the default values from the FDS database file and the values measured in the experiments as follows:

Diesel oil:
1)   0.10 kg/m^2/s – i.e. default maximum burning rate in FDS
2)   0.06 kg/m^2/s - burning rate approximately 10% above of the maximum
            burning rate recorded in the experiment no. 2 (see table 4.2)

Ethanol:
1)   0.015 kg/m^2/s – default value for ethanol in database4.data
2)   0.030 kg/m^2/s - burning rate approximately equal to the maximum burning rate
            recorded in the experiment no. 5 (see table 4.2)

5.1.4   External boundary conditions

The 'OPEN' boundary condition was assigned to all the external boundaries of the domain except for the floor. In the simulation with extended (wide) domain one side of the domain was also defined as a solid obstacle in order to model the wall nearest to the experimental stand.

Given the substantial size of the laboratory hall, the 'OPEN' boundary condition is considered to be realistic.

The extraction fan was defined as a velocity boundary condition (within the extraction duct). The velocity was calculated to achieve the extraction rate used in each particular experiment.

5.1.5   Properties of materials

Thermal properties for the inner layer of the compartment walls were obtained from the company supplying Duraboard LD Fiberfrax boards.
Although in reality the compartment walls consisted of two layers (see section 4.1.2), in the FDS model they were approximated as uniform walls 40 mm thick, made entirely of Fiberfrax boards.

In the preliminary simulations, the balcony was defined as a plywood obstacle (as it was in the physical experiment). However, this resulted in the balcony surface igniting in the simulation, when no such behaviour was observed in the experiments. For this reason the balcony surface was subsequently changed to a non-combustible material in al the relevant FDS simulations.

5.2 Results of FDS simulations

Selected results of FDS simulations for experiments no. 2 and 5 (coarse grid / narrow domain) are presented in this section.

Detailed results for all the FDS simulations performed can be found in Appendix E.

5.2.1 Heat Release Rate (HRR)

<u>Simulations with the burning rate prescribed by the user</u>

In simulations were the heat release rate is prescribed by the user, it is not considered to be a model output as such. However, the actual heat release rate calculated by the program may in fact differ from the prescribed curve (for example due to insufficient amount of oxygen available). It is therefore a good practice to compare the HRR curve calculated by the program with the prescribed HRR curve.

Indeed, the calculated values of heat release rate fluctuate around the intended values when ventilation conditions become vitiated (see figures 5.5 and 5.6.).
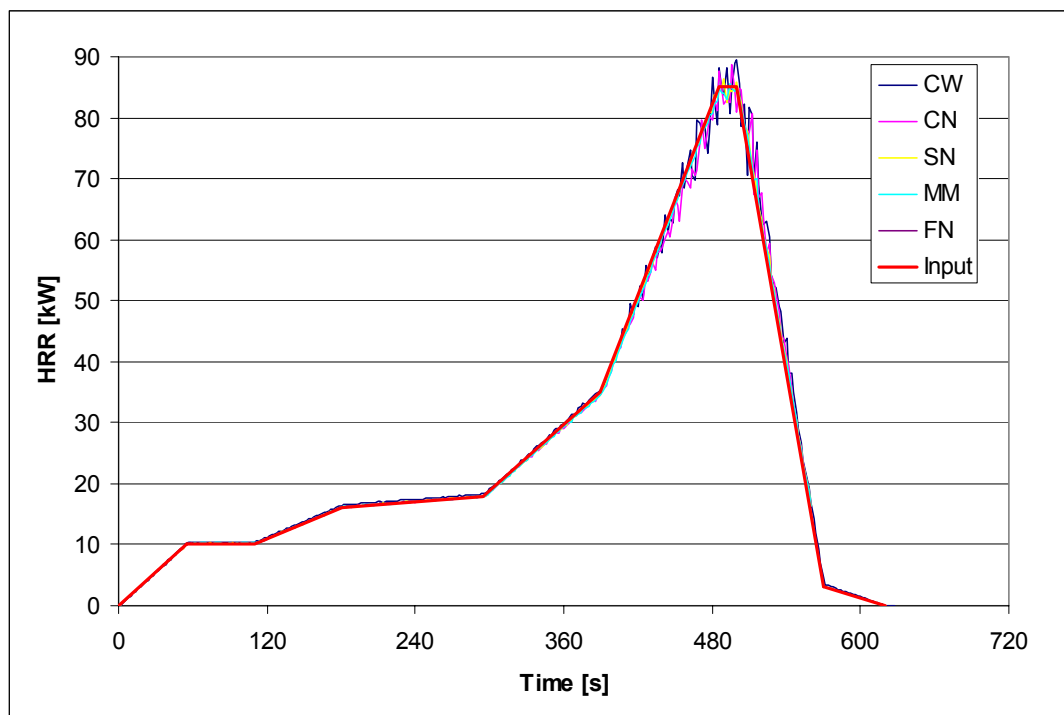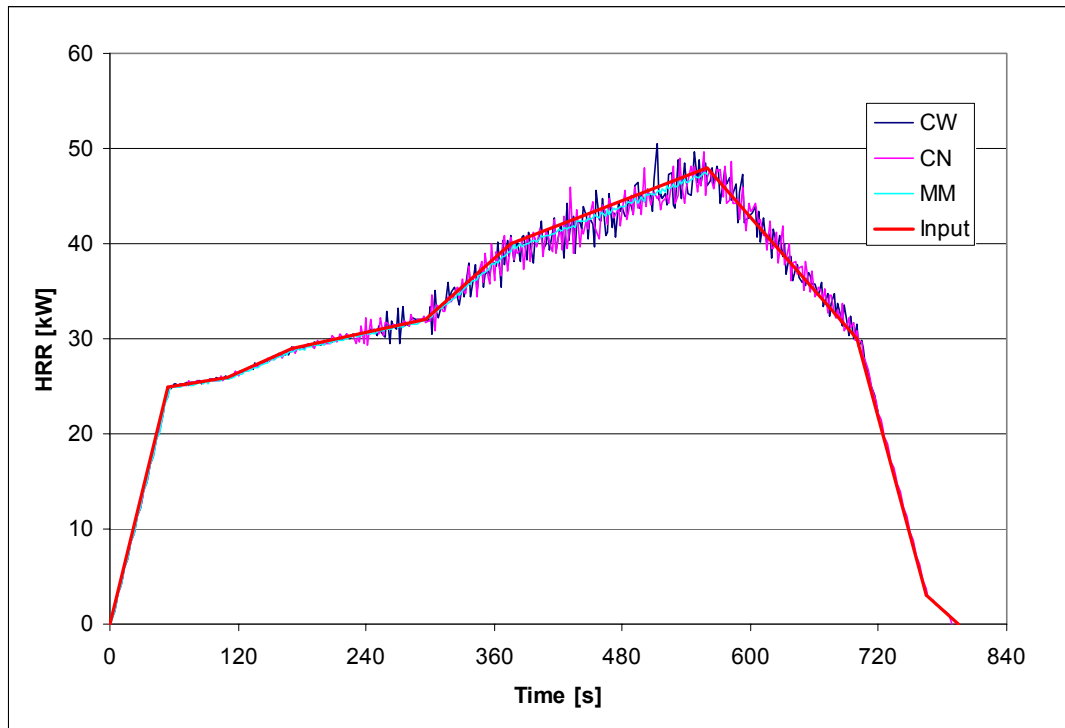

Fig. 5.5 Experiment 2 – actual heat release rate calculated by FDS

It should be noted that in both cases the fluctuations in the heat release rate were smaller in the simulation involving a finer mesh around the fire.

Fig. 5.6 Experiment 5 – actual heat release rate calculated by FDS

Simulations with the burning rate predicted by FDS

FDS predictions of the burning rate are influenced strongly be several factors including the thermal properties of the fuel and also the predicted feed-back of heat to the fuel surface.

For both fuels investigated, the maximum allowed burning rate was varied and it was found to have a profound impact on the FDS predictions. A detailed discussion of this problem is provided in chapter 6.
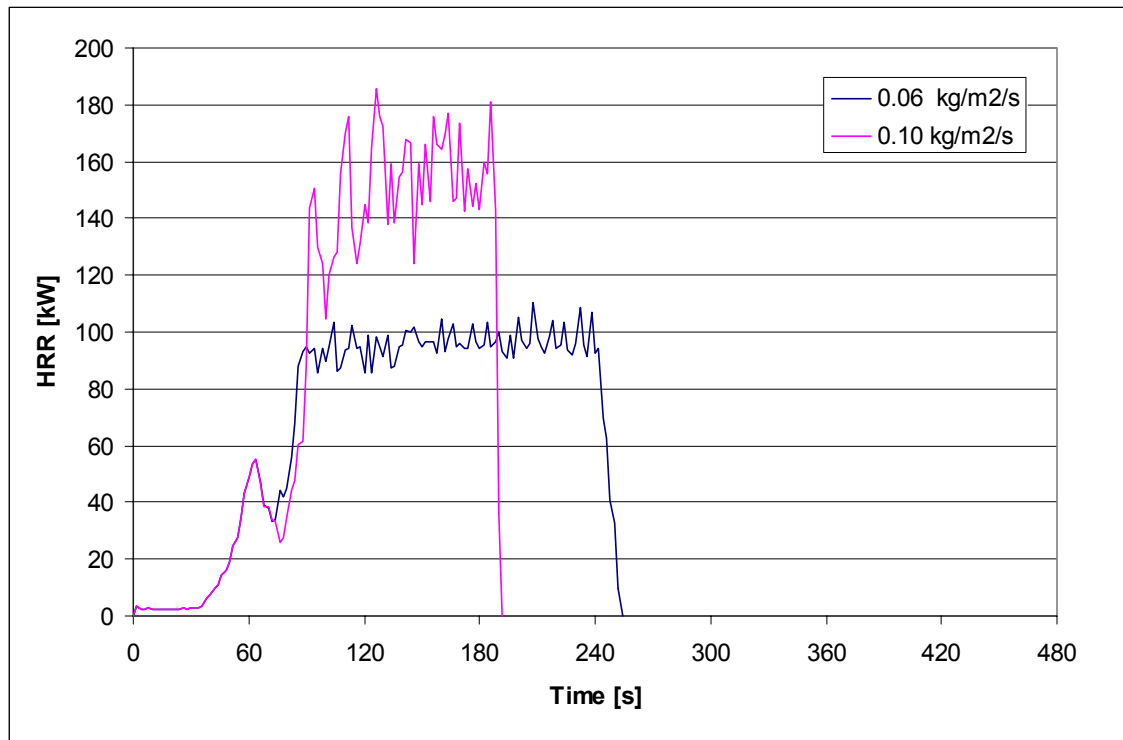
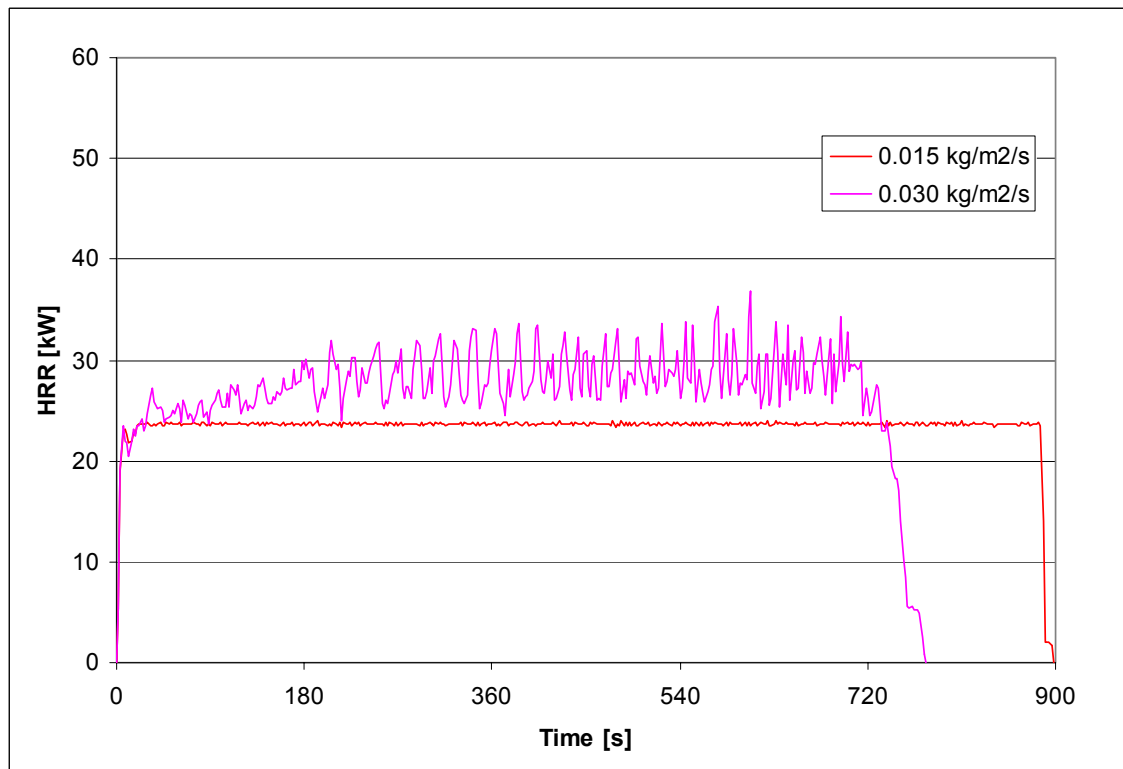**Fig. 5.7 Exp_2_CN_BR - heat release rates predicted by FDS**

Fig. 5.8 Exp_5_CN_BR - heat release rates predicted by FDS

5.2.2 Compartment temperatures

Compartment temperatures predicted by FDS were higher than the experimental measurements for all the simulations performed. Temperatures predicted by FDS in the baseline simulations (coarse grid / narrow domain) are presented below.
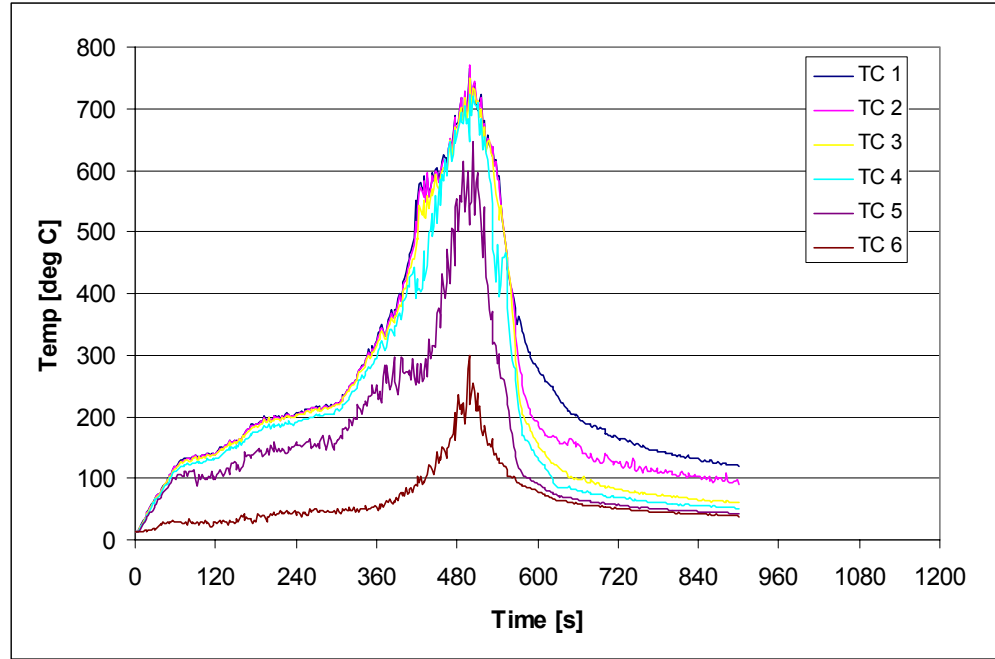

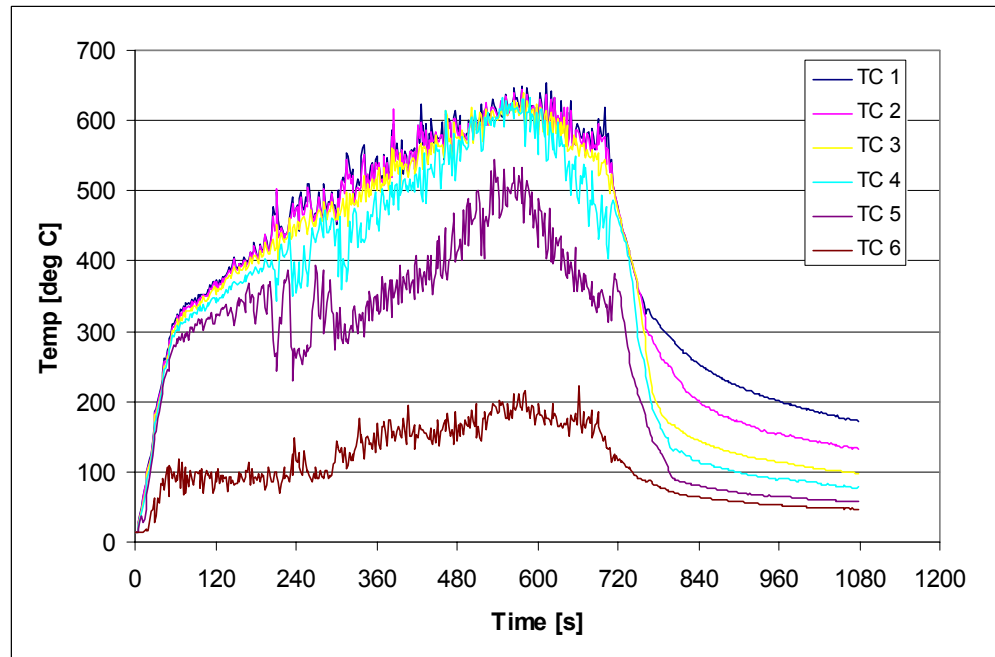**Fig. 5.9 Exp_2_CN – compartment temperatures predicted by FDS**

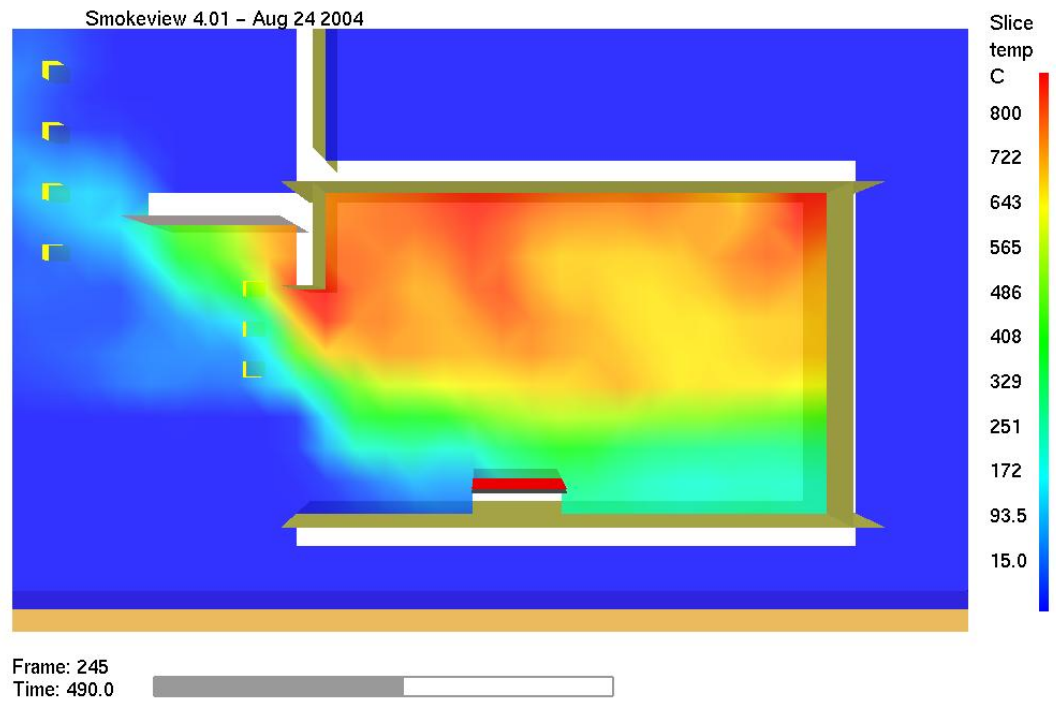**Fig. 5.10 Exp_5_CN – compartment temperatures predicted by FDS**

66

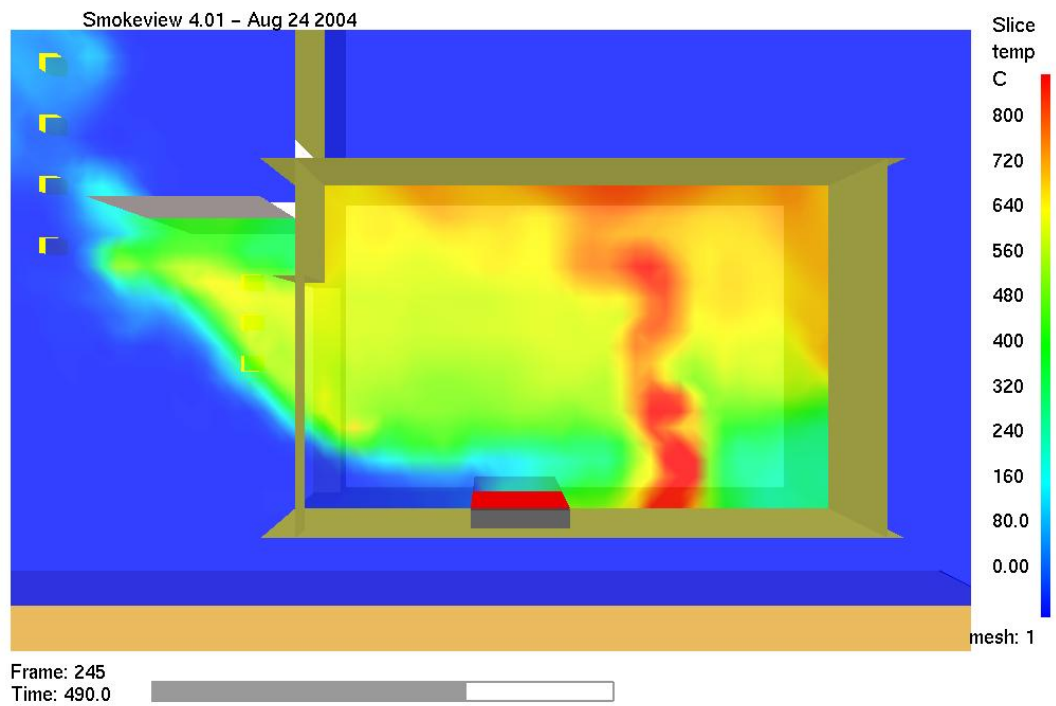**Fig. 5.11 Exp_2_CN – FDS temperature slice at 490 s**

Fig. 5.12 Exp_2_MM – FDS temperature slice at t=490 s

It was noted that the qualitative description of the thermal environment within the fire compartment provided by FDS changed dramatically depending on the resolution of the computational mesh.

Figures 5.11 and 5.12 on the previous page illustrate a snapshot of gas temperatures in the compartment taken at the time step t=490 s for simulations involving a coarse mesh (0.07 m x 0.07m x 0.08 m cell size) and a fine mesh (0.035 m x 0.035 m x 0.04 m cell size for mesh no. 1) respectively.

The differences in the predicted temperature field within the compartment can more than likely be linked to the differences in the predicted shape of the flame region. Very significant differences are seen in the shape of the mixture fraction iso-surfaces predicted by FDS for the peak burning period, when using different grid resolutions. With the coarse mesh, the flame seems to be stretching throughout the upper portion of the compartment and reaching out of the front opening.

With the fine mesh, the flame seems to be pushed towards the rear of the compartment, possibly due to higher velocities of inflowing fresh air at low level.

Exp_2_CN   Exp_2_MM
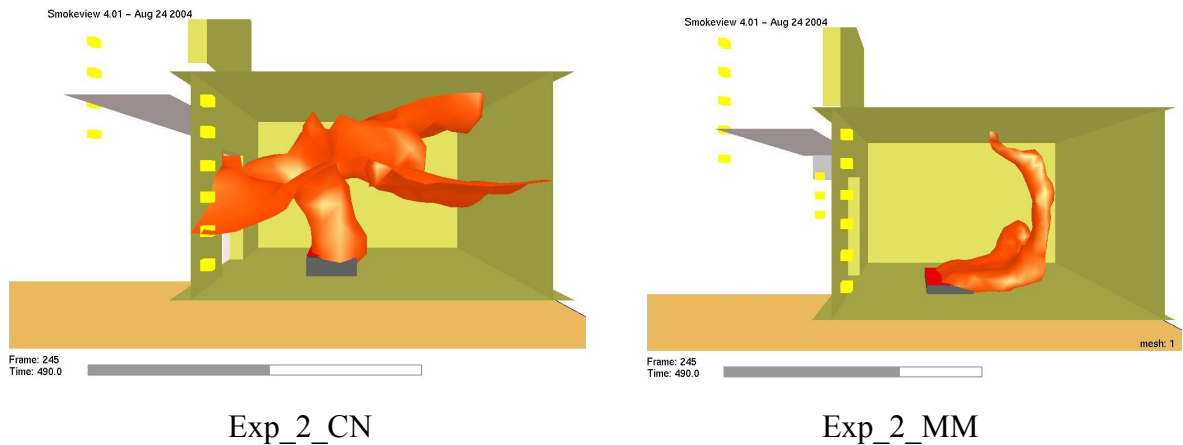
Fig. 5.13 Exp 2 - Comparison of mixture fraction iso-surfaces for different grid resolutions

5.2.3 Spill plume temperatures

Spill plume temperatures predicted by FDS were higher than the experimental measurements for all the simulations performed. Temperatures predicted by FDS in the baseline simulations (coarse grid / narrow domain) are presented below.
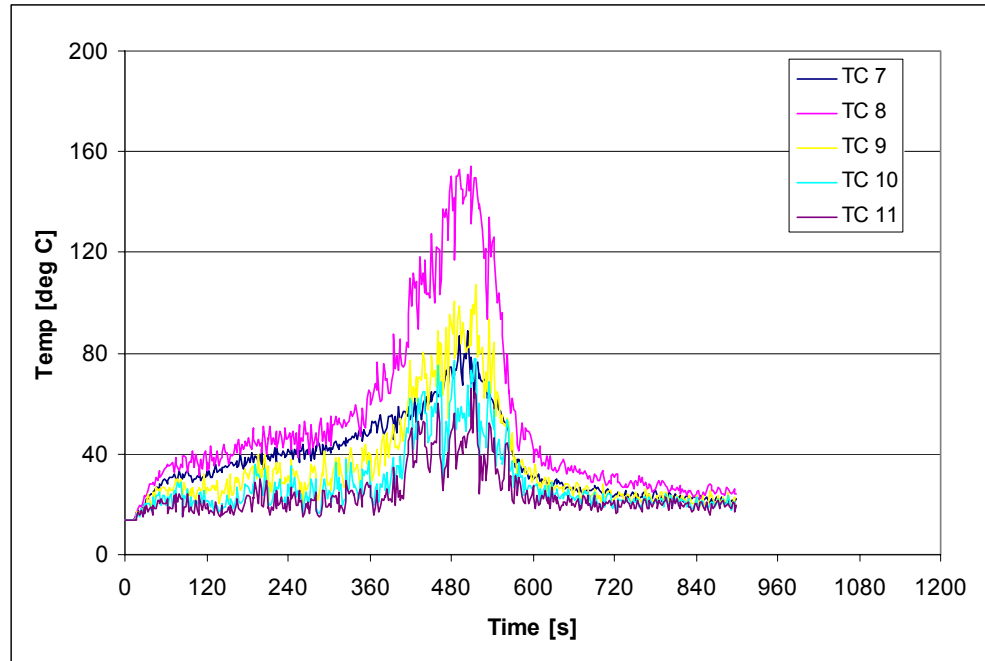
Fig. 5.14 Exp_2_CN – spill plume temperatures predicted by FDS
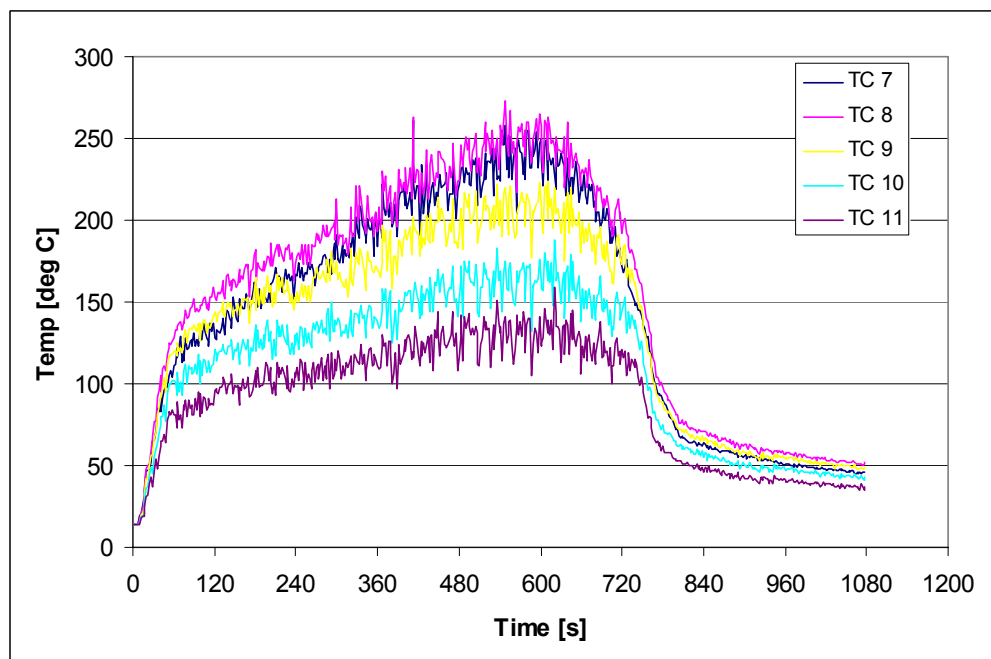
Fig. 5.15 Exp_5_CN – spill plume temperatures predicted by FDS

5.2.4 Smoke reservoir temperatures

Smoke reservoir temperatures predicted by FDS for experiment no. 2 generally follow the behaviour observed in the experiments, with thermocouples T19 and T20 recording slightly lower temperatures than the other three devices.
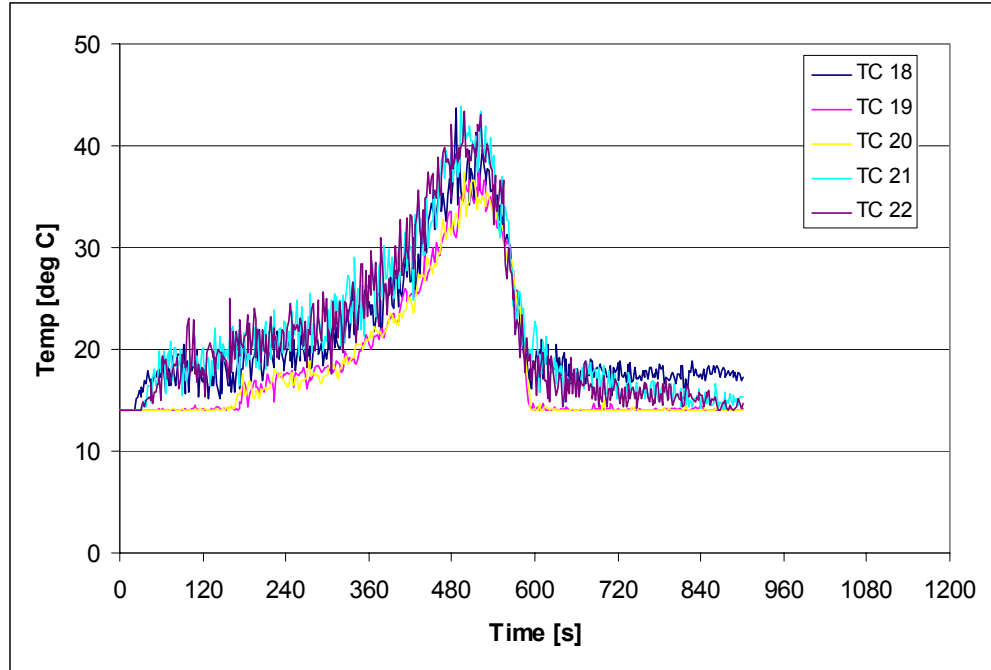
Fig. 5.16 Exp_2_CN – smoke reservoir temperatures predicted by FDS
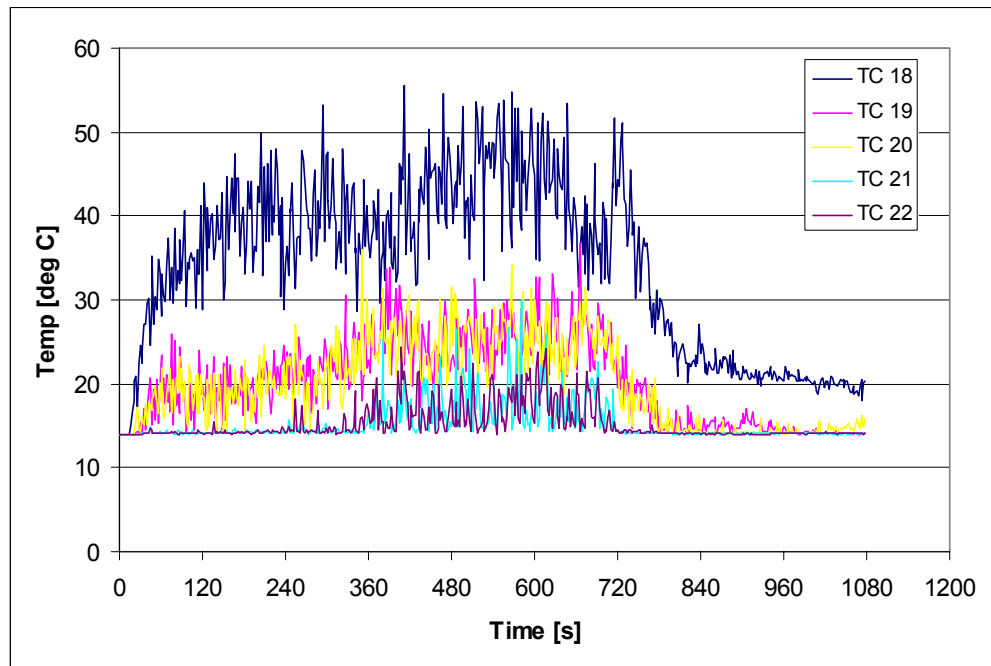
Fig. 5.17 Exp_5_CN – smoke reservoir temperatures predicted by FDS

For experiment no. 5, the highest temperatures within the smoke reservoir were predicted for the central thermocouple (T18).
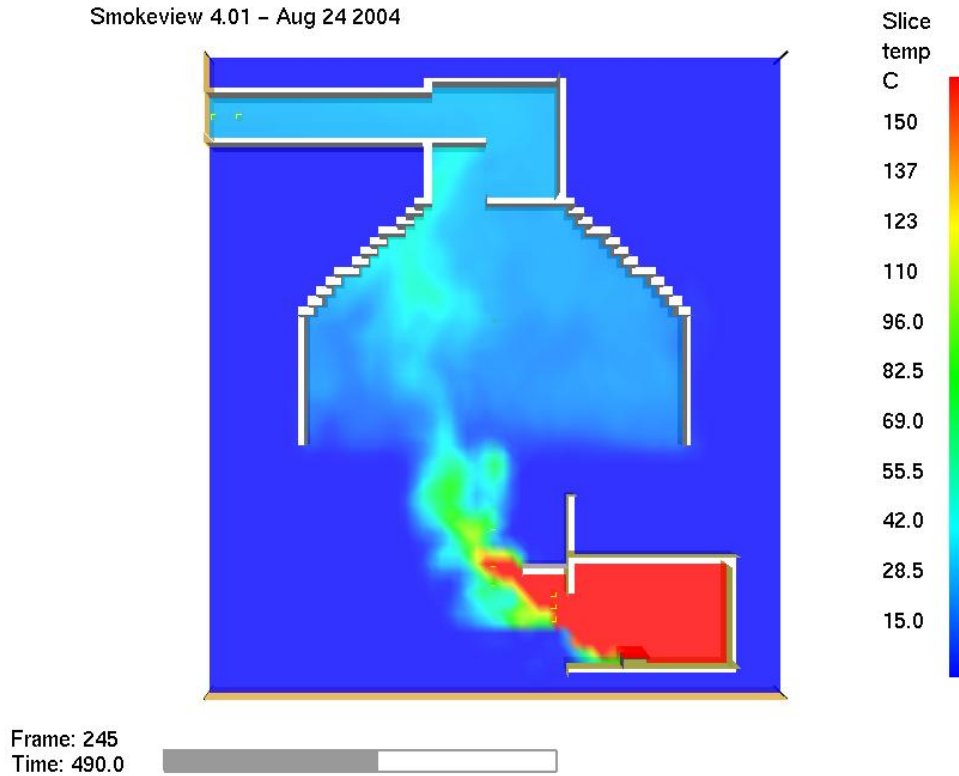
Fig. 5.18 Exp_2_CN – FDS temperature slice at t=490s
(temperatures adjusted for the reservoir)

FDS correctly predicted the descending of the smoke layer to the bottom of the extraction hood during the peak burning period.

5.2.5   Flow velocities

Flow velocities predicted by FDS are presented here only for general information. As explained in chapter 4, the velocities measured in the experiments are not considered to be very accurate. Also, the readings of some of the bi-directional probes could have been influenced by even relatively small change in the positioning of the probe.
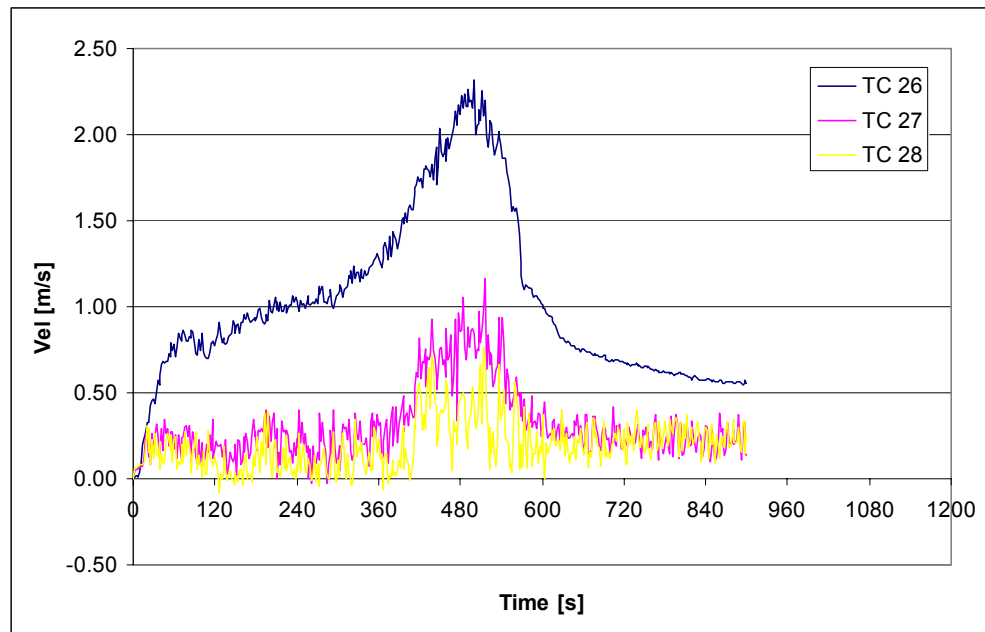
Fig. 5.19 Exp_2_CN – flow velocities predicted by FDS
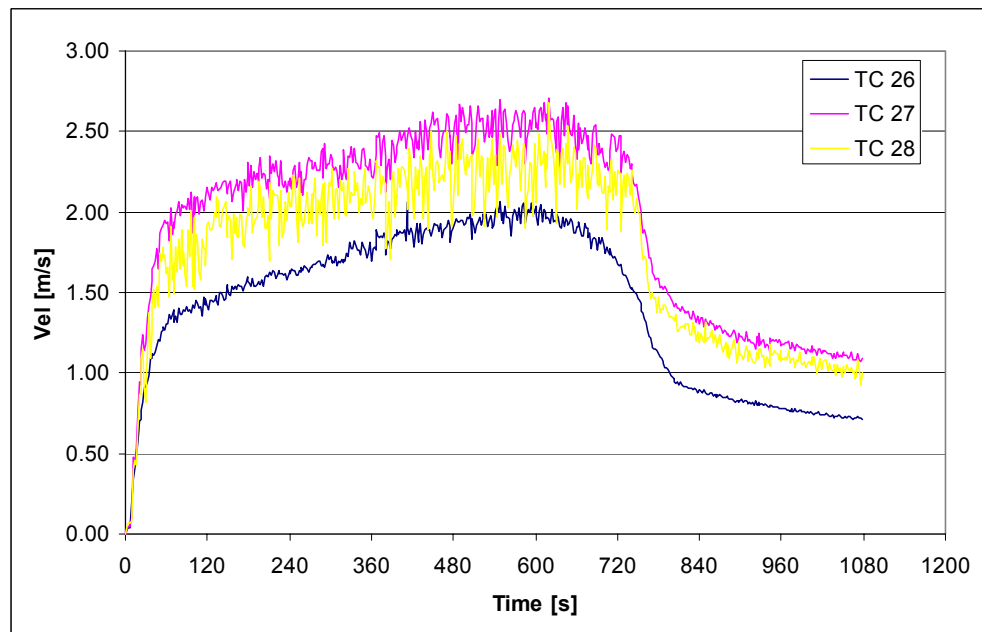
Fig. 5.20 Exp_5_CN – flow velocities predicted by FDS

6.   COMPARISON OF RESULTS

This chapter presents the comparison of FDS predictions with the experimental results. Experiments no. 2 and no. 5 are selected as the most representative for scenario A and scenario B respectively (see chapter 5 for details).

For single-point comparisons such as, for example, maximum temperatures reached, the results of the comparison are expressed as a relative difference.
Accuracy of a prediction is expressed in terms of prediction error, defined as percentage difference between the FDS prediction and the experimental value (when referenced to the experimental value):

$$\text{Prediction error} = \frac{\text{FDS value} - \text{Experimental value}}{\text{Experimental value}} * 100 \%$$

For temperature predictions, the assessment is made by comparing the value of temperature rise (and not the temperature itself).

Where predictive capability of FDS for a given quantity is described qualitatively, the following grading convention is used:

- Excellent   Error in prediction   < 10%
- Good   Error in prediction   10% - 20%
- Satisfactory   Error in prediction   20 % - 30%
- Poor   Error in prediction   30% - 55%
- Very poor   Error in prediction   > 55%

It should be noted that the grading convention presented above was proposed by the author and by its nature is subjective. It is likely that for certain research problems a prediction error of say 18% will not be acceptable. At the same time, there may be an engineering problem for which a CFD model with a prediction error of say 50% will still be the best available tool and such an error will be accepted.
 A decision whether a particular prediction error is acceptable for a particular problem must always be made by the person responsible for the simulation.

The accuracy of FDS predictions which are presented in this chapter should be considered in the context of the experimental error, which was very significant for some of the quantities measured.

It is particularly important to remember that the measurement error for heat release rate is estimated as approximately 10%. The rate of heat release is either used as an important input (where it needs to be prescribed by the user) or is directly compared with the FDS prediction (where it is predicted by the program). Therefore, it can be argued that all estimations of prediction error made in this chapter are to some extent effected by experimental uncertainty in measuring the heat release rate.

In order to limit the influence of poor experimental data, the comparison presented in this chapter only includes the quantities measured for which the experimental results are judged as relatively reliable. These include the heat release rate (only considered for simulations where the burning rate was predicted by the program), the compartment temperatures and the smoke reservoir temperatures.

Some assessment is provided for the flow velocities as well as general qualitative predictions of the fire and smoke behaviour.

Other measurements were found to be highly sensitive to the location of the measuring device and are deemed unsuitable to provide meaningful comparison.

6.1 Burning Rate

Simulations where the burning rate is predicted by the program, pose a much higher challenge compared to simple cases where the HRR curve is prescribed by the user.

Firstly, detailed information about the thermal and burning properties of the fuel is required. For many fuels, especially non-homogeneous, such information may be difficult to obtain and indeed it may be necessary to carry out small-scale tests such as the cone-calorimeter test to establish some of these properties.
Also, certain numerical parameters of the simulation such as resolution of the grid or the parameters for the radiation model used may have a more significant influence on the results.

Diesel oil (Experiment no. 2)

For the diesel oil fire, two simulations were performed to predict the burning rate. For these simulations, different values of the BURNING_RATE_MAX variable were prescribed. One was the default value used by FDS, and the other was related to the maximum burning rate recorded in the experiment (see section 5.1.3 for details)
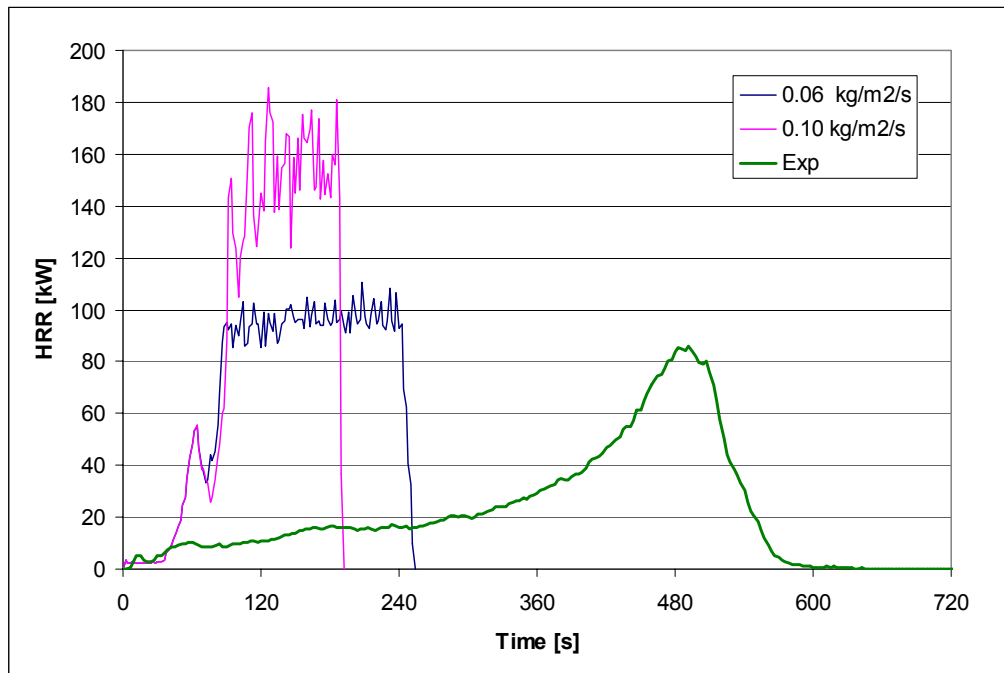
Fig. 6.1 Exp_2_CN_BR – comparison of HRR curves

As can be observed in figure 6.1, the difference in value of the maximum allowed burning rate had a dramatic impact on the shape of the predicted HRR curve.

Nevertheless, both HRR curves predicted by FDS differ very significantly from the one recorded in experiment no. 2. For both simulations there is a very rapid increase in the heat release rate. In both cases, the fire grows very close to its maximum heat release rate within the first 90 seconds of the simulation. After this initial period of rapid growth the heat release rate remains relatively constant (at the level which is controlled by the BURNING_RATE_MAX variable) until all fuel is consumed.

In contrast to the simulations, fire growth in the experiment was much slower, and the maximum heat release rate was reached approximately 480 seconds after the experiment was started.

After analysing the data it is seems likely that the accuracy of prediction might have improved if finer mesh had been used (see also section 6.2.1).
It is noted that in the basic simulations (with HRR prescribed) the temperatures were over-predicted for the coarse mesh. Over-predicted compartment temperatures might have caused unrealistically high heat feed-back to the fuel surface which in turn increased the burning rate (and hence the temperatures within the compartment) even further.
Unfortunately, due to limited computational resources and the time constraints of this work, it was not possible to verify this hypothesis.

Another factor that might have influenced the results is the appropriateness of the fuel properties assumed in the simulations. It is acknowledged that some of those properties may not be accurate, as they were not obtained from a peer-reviewed source.

Overall, the accuracy of FDS predictions of the burning rate for the diesel fire was very poor when a coarse mesh was used.

Ethanol (Experiments no. 5 & 6)

For the ethanol fire, two scenarios with two different values of the maximum burning rate were investigated, similarly to the process described for experiment no. 2. One was the default value provided for ethanol in the FDS database fire (i.e. 0.015 $kg/m^2/s$), and the other was related to the maximum burning rate recorded during the experiment.
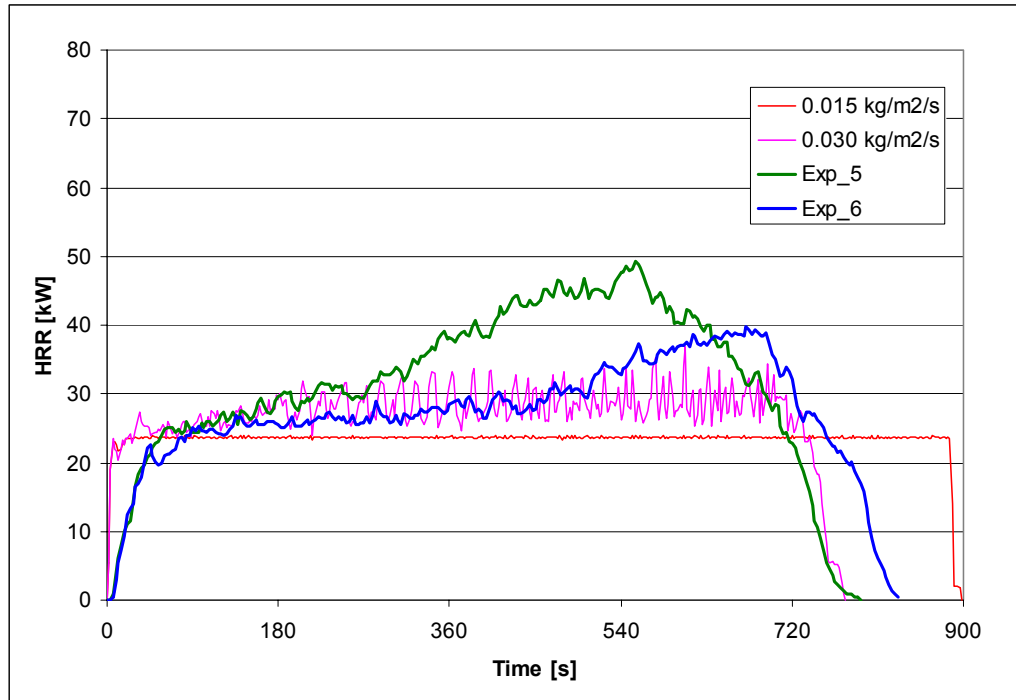
Fig. 6.2 Exp_5_CN_BR – comparison of HRR curves

For ethanol fire, the impact of the value of the maximum allowed burning rate does not seem to be as significant as it was for the diesel oil fire. It is important to note that the default value of maximum burning rate provided in the FDS database file does not seem appropriate for compartment fires, as it is significantly lower than the burning rates recorded in the experiment.

The increase in the heat release rate is again more rapid in the simulations than it was in the experiment. However, it may be argued that the HRR curve obtained in the simulation with the higher maximum burning rate allowed is relatively similar to the HRR curve recorded in experiment no. 6.

Insufficient resolution of the computational mesh used in the simulations may have had significant impact on the accuracy of the FDS predictions of the burning rate.

6.2   Temperatures

6.2.1   Compartment temperatures

In order to simplify the comparison of the compartment temperatures, the average temperature value for the top three thermocouples (i.e. T1 to T3) will be used. Such an average temperature of the hot layer in the fire compartment is often established using simple engineering correlations or two-zone models.

Generally, the readings of thermocouples T1 to T3 were similar, except for the decay / cooling phase when variation of gas temperature with respect to height was clearly apparent. This applies to both the experiments and FDS simulations.

Experiment no. 2
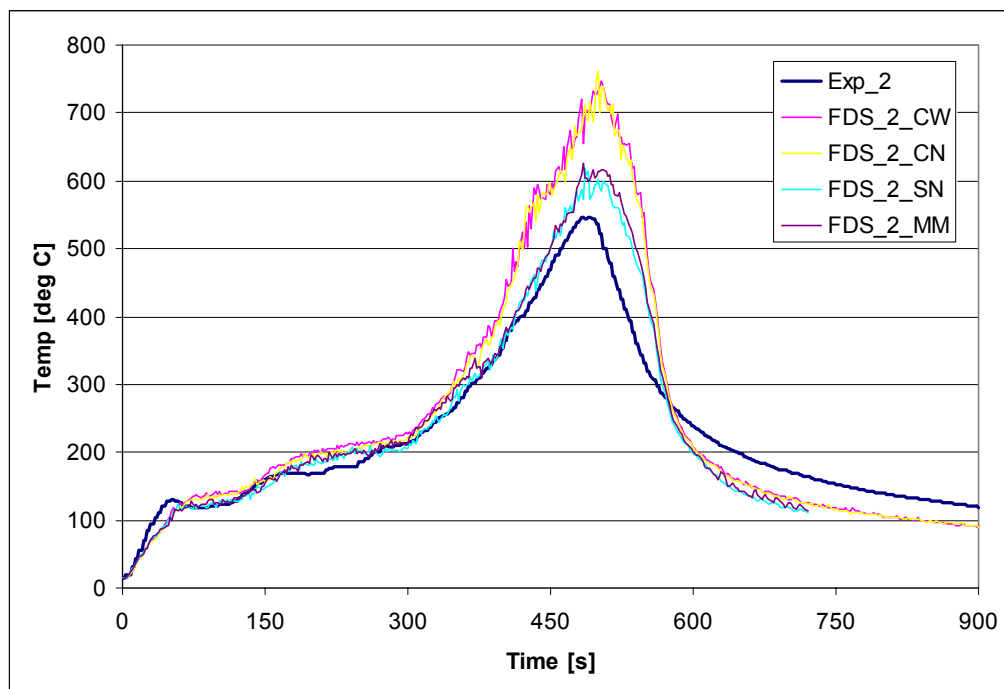
Fig. 6.3 Exp_2 - Comparison of calculated compartment temperatures (hot layer)

The accuracy of compartment temperature predictions for experiment no. 2 is much improved for simulations with finer mesh within the fire compartment (SN and MM).

	Exp 2	**FDS_2_CW**	**FDS_2_CN**	**FDS_2_SN**	**FDS_2_MM**
Max temp	546 ^{o}C	747 ^{o}C	762 ^{o}C	619 ^{o}C	626 ^{o}C
Temp rise	531 ^{o}C	733 ^{o}C	748 ^{o}C	605 ^{o}C	612 ^{o}C
Accuracy	n/a	38 %	41 %	14 %	15 %

Table 6.1   Exp_2 - Comparison of maximum reached compartment temperatures

Overall, the agreement for compartment temperature predictions is good if sufficiently well resolved computational grid is used. For coarse mesh the compartment temperature predictions are poor.

As a general observation, FDS seemed to under-predict the compartment temperatures in the cooling phase (i.e. further to fuel consumption).

Experiment no. 5
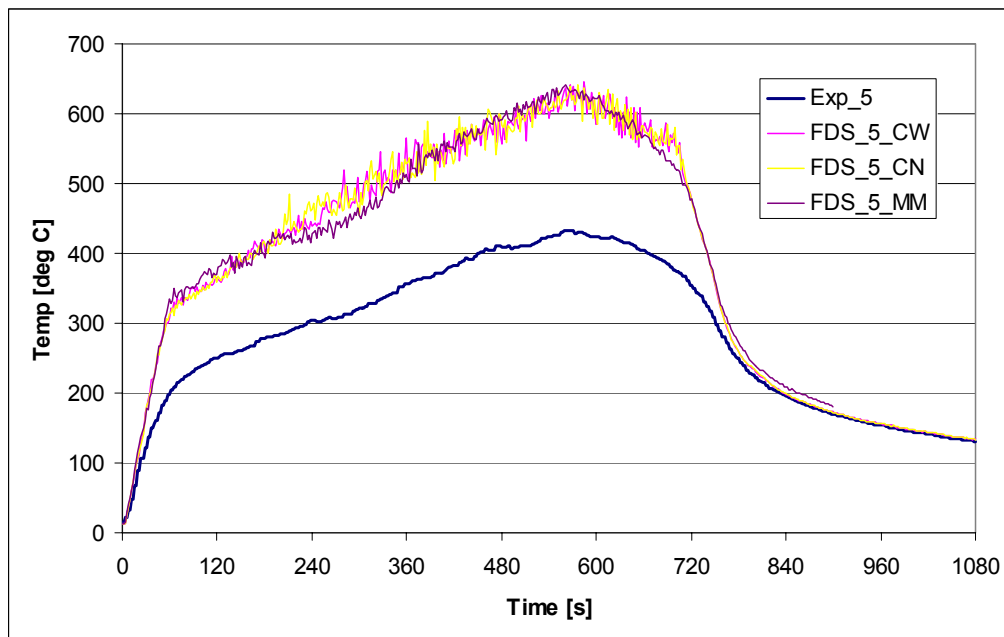
Fig. 6.4 Exp_5 - Comparison of calculated compartment temperatures (hot layer)

The accuracy of compartment temperature predictions for experiment no. 5 is poor and does not seem to improve with finer mesh.

	Experiment 5	FDS_5_CW	FDS_5_CN	FDS_5_MM
Max temp	433 ^{o}C	645 ^{o}C	640 ^{o}C	641 ^{o}C
Temp rise	418 ^{o}C	631 ^{o}C	626 ^{o}C	627 ^{o}C
Accuracy	n/a	51 %	50 %	50 %

Table 6.2 Exp_5 - Comparison of maximum reached compartment temperatures

This poor performance may be caused by insufficient mesh resolution (even in the simulation with finer mesh).

This is further explained when we take into account the fact that the dimensionless diameter of the fire in experiment no. 5 is only 0.29 m, compared to 0.36 m for experiment no. 2.

Therefore, if the same D^*/δ ratio was to be maintained, an even finer grid mesh should have been used for simulations considering experiment no. 5 (say in the order of 0.025 m).

6.2.2 Smoke reservoir temperatures

In order to simplify the comparison of reservoir temperatures, the average value for all the 5 thermocouples located in the smoke reservoir was calculated.

It is noted that in simple engineering correlations and in two-zone models, the temperature of the smoke layer is also described by a single averaged value, without any information on spatial variation of the smoke temperature within the reservoir.

Experiment no. 2
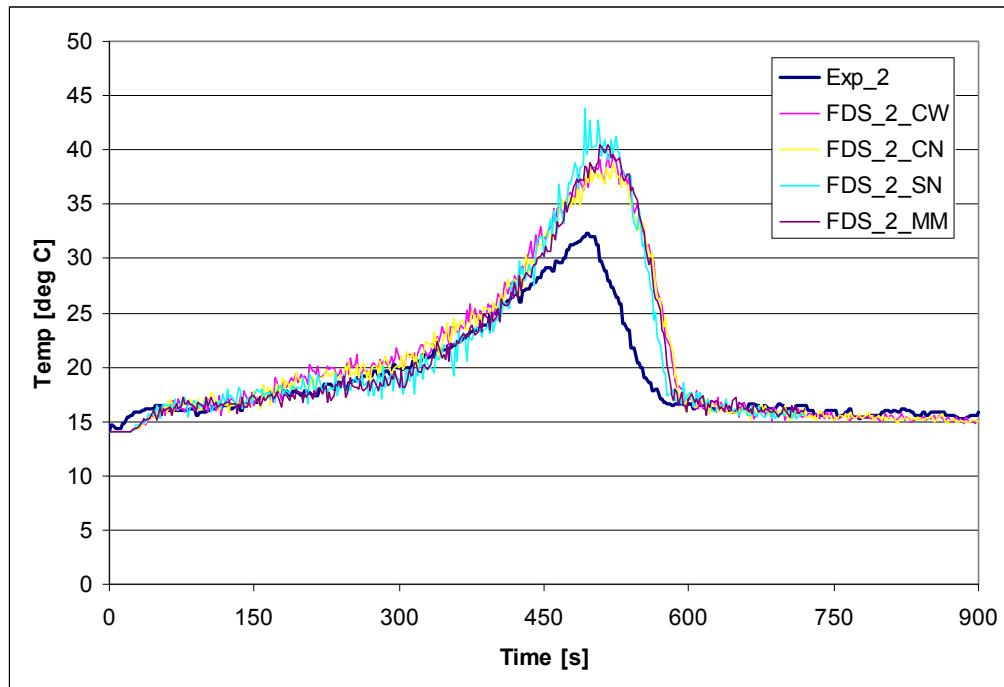
Fig. 6.5 Exp_2 - Comparison of calculated average reservoir temperatures

	Exp 2	**FDS_2_CW**	**FDS_2_CN**	**FDS_2_SN**	**FDS_2_MM**
Max temp	32 °C	40 °C	39 °C	44 °C	41 °C
Temp rise	18 °C	26 °C	25 °C	30 °C	27 °C
Accuracy	n/a	44 %	39 %	67 %	50 %

Table 6.3 Exp_2 - Comparison of maximum reached average reservoir temperatures

For experiment no. 2, the average smoke temperature in the reservoir predicted by FDS agrees well with the experimental results for the first 7 minutes of the simulation (i.e. during the growing phase of the fire).

During the fully developed stage, with the fire close to its maximum heat release rate, FDS significantly over-predicted the reservoir temperatures. This is particularly visible for the simulation where a stretched mesh is employed (domain type SN).

Experiment no. 5

For experiment no. 5, the average reservoir temperatures predicted by FDS agree well with the experimental values. The overall shape of the temperature vs. time curve obtained in all thee simulations is similar to one recorded in the experiment.

Generally, FDS predictions exhibit larger fluctuations than the experimental results. This is particularly visible when coarse mesh is used (domain types CN and CW). When FDS predictions are averaged over longer time intervals (say 6 seconds), the resulting curve better resembles the experimental result – see figure 6.7
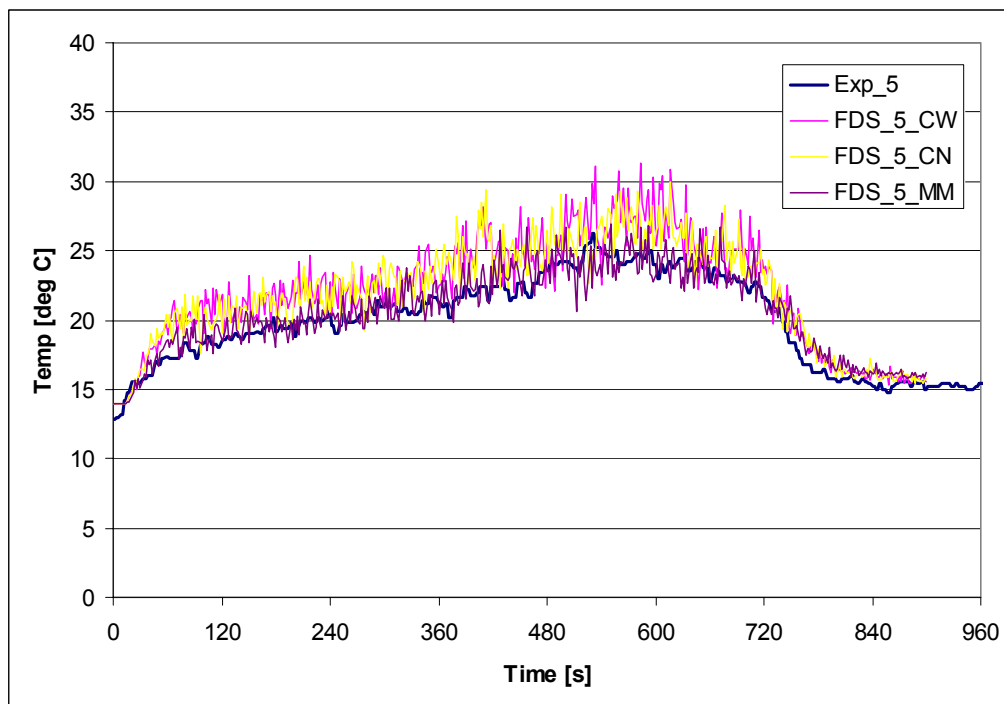
Fig. 6.6 Exp_5 - Comparison of calculated average reservoir temperatures

Overall it may be said that FDS predictions of reservoir temperatures for experiment no. 5 are good when a coarse mesh is used and excellent when a multi-mesh (with fine grid close to the fire) is used.
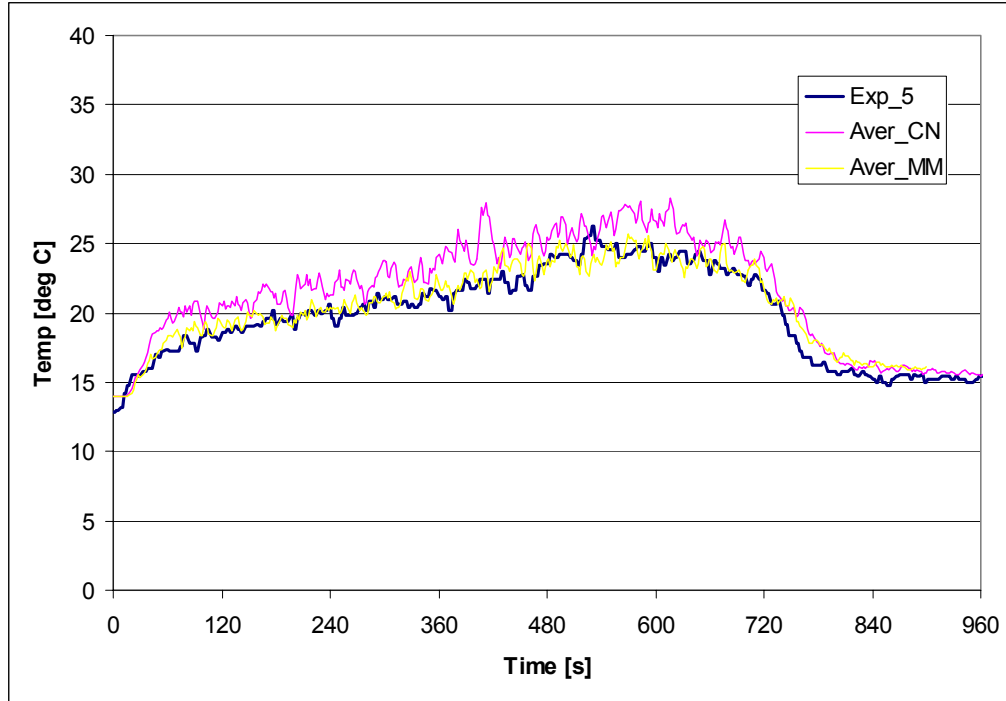
Fig. 6.7 Exp_5 - Comparison of time-averaged (6 s) reservoir temperatures

For experiment no. 5 the peak in heat release rate (and hence the temperatures) is not as well defined as for experiment no. 2, which makes it more difficult to compare the maximum average reservoir temperatures directly.

Instead, reservoir temperatures averaged for the 120 s long period of the most intense burning (i.e. between 540 and 660 s) will be compared. Temperature rise is calculated considering the ambient (starting) temperature for the experiment and the simulations, which were 13 ^{o}C and 14 ^{o}C respectively.

	Experiment 5	**FDS_5_CW**	**FDS_5_CN**	**FDS_5_MM**
Average temp	24 ^{o}C	27 ^{o}C	26 ^{o}C	24 ^{o}C
Temp rise	11 ^{o}C	13 ^{o}C	12 ^{o}C	10 ^{o}C
Accuracy	n/a	19 %	13 %	7 %

Table 6.4 Exp_5 - Comparison of time-averaged reservoir temperatures

6.3 Flow velocities

There appears to be little agreement between the flow velocities measured in the experiments and the values predicted by FDS. Generally, FDS consistently over-predicted flow velocities for all locations, sometimes by over 100%.

It is unclear to what extent this disagreement is caused by poor calibration of bi-directional probes and by the differences between the actual and the modelled positions of the probes.

Therefore, it is not possible to draw any meaningful conclusions on the actual accuracy of FDS predictions of flow velocities within the bounds of the work carried out

6.4 Qualitative prediction of smoke and fire behaviour

6.4.1 Smoke flow patterns

In general, FDS accurately predicted the behaviour of smoke with regard to its flow from the compartment and then rising in the form of a spill plume (Exp 2) into the smoke reservoir.
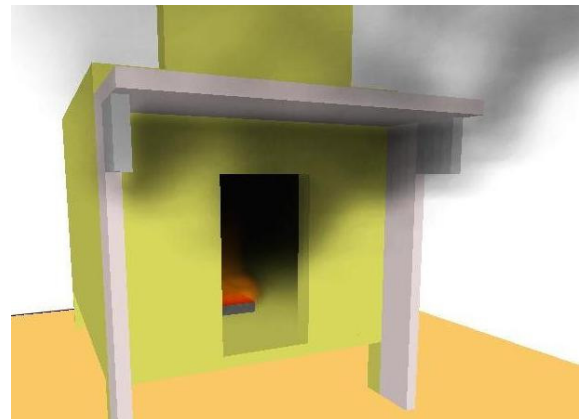
Experimental   FDS_2_MM

Fig. 6.8 Comparison of smoke flow visualisations (spill plume)

In experiment no. 2 it was noted that the smoke layer descended to the bottom edge of the extraction hood at approximately 430 s and some minor spillage of smoke was then observed for approximately 80 s.

This was very closely replicated by the behaviour of smoke predicted by FDS with smoke spillage starting at 460s and remaining for the same time i.e. 80 s.

Based on visual observations, it is noted that density of smoke was not accurately predicted for either of the two fuels used.

This assessment is made based on visual observations made during the experiments and the visualisations provided in Smokeview. Therefore, it is not as accurate as a comparison of measured smoke densities.

For diesel oil, the density of smoke predicted by FDS and visualized by Smokeview was lower than in the actual experiment. This suggests that the value of smoke yield prescribed in the input file was too low.

For ethanol, FDS predicted some visible smoke, where in fact none was observed in the experiments. This suggests that the value of smoke yield variable for ethanol may be set lower.

6.4.2 Flame behaviour

With reference to flame behaviour, it is noted that during all the experiments conducted flames were confined to the compartment i.e. flames were not observed outside the compartment.

However, in the FDS simulations flames (visualized by mixture fraction iso-surface) were observed just outside the compartment opening. This behaviour was observed especially for the diesel fire simulations when a coarse mesh was used.

7. CONCLUSIONS

7.1 Temperature predictions

Based on the comparison of the FDS temperature predictions with the experimental measurements, the following conclusions were reached:

- The accuracy of compartment temperature predictions depends strongly on the resolution of the computational mesh. Generally, good predictions were only achieved where the size of the computational cells within the fire compartment was less than $1/10^{th}$ of the characteristic fire diameter (i.e. for stretched mesh and multi-mesh used in FDS simulations of experiment no. 2).

  The only exception to the above was the initial growing phase of diesel fire (experiment 2) where good agreement was observed irrespective of mesh resolution used until the fire reached approximately 50% of its maximum heat release rate.

  Where coarse mesh was used, the accuracy of maximum compartment temperature predictions was found to be poor, with temperatures consistently over-predicted by FDS.

  However, it is acknowledge that the difference between the experimental results and the FDS predictions might have been caused (to some extent) by the fact that thermocouples inside the compartment were covered with a thick layer of soot produced by burning the diesel oil.

- The accuracy of FDS predictions of the average smoke reservoir temperatures was found to be different for the two scenarios investigated.

  For scenario A (diesel fire / balcony spill plume) predictions of the maximum average reservoir temperature were found to be poor to very poor, with temperatures generally over-predicted. The reasons for this poor performance could not be identified.

  For scenario B (ethanol fire/no balcony) predictions of the maximum reservoir temperature (time averaged) were found to be good to excellent.

It is noted that the above conclusion in relation to the importance of proper mesh resolution (particularly in the near field) is in line with the results published by other authors.

7.2   Predictions of burning rate

Before the conclusions are presented here on the accuracy of the burning rate predictions made by FDS it is important to note the following:

- The mesh resolution in all the simulations in this study were the burning rate was predicted by the program was relatively coarse (relative to the characteristic fire diameter). This was due to the time constraints (finer meshes require much longer computational times), and the potential influence of such coarse mesh was not realized until the experimental and the numerical results were compared. It is likely that the accuracy of FDS predictions would have been better if finer mesh was used.
- Some of the combustion and thermal properties of diesel oil used in the simulations might have not been very accurate.

For the burning rate predictions the following conclusions were reached:

- For diesel fire, the shape of the HRR curves predicted by FDS differs very significantly from the one recorded in the experiment. The initial phase of slow fire growth was not reproduced by FDS. Instead, in both simulations the fire quickly reached its maximum heat release rate (dictated by the value of the BURNING_RATE_MAX variable) which was maintained until the fuel was consumed.
- The value of the variable that controls the maximum burning rate is very important in FDS simulations where the burning rate is to be predicted by the program. It is crucial that this value is accurately assessed for the fuel of interest, bearing in mind that it should be assessed for burning conditions similar to those for which the simulation is to be performed (e.g. a compartment fire as opposed to an open pool fire).
- For ethanol fire, FDS predictions of the burning rate (and hence the HRR curve) were more similar to the HRR curves recorded in experiment no. 5 and 6.
- The maximum burning rate for ethanol prescribed in the FDS database file appears to be too low for compartment fires. The same observation was made by Moghaddam et. al in their earlier work [20].

8.   REFERENCES

[1]   A Brief History of CFD, Fluent Inc., www.fluent.com

[2]   G. Cox S. Kumar. Modeling Enclosure Fires Using CFD, The SFPE Handbook of Fire Protection Engineering, Section 3 / Chapter 8, SFPE, Maryland, Third Edition, 2002

[3]   D. Fennel. Investigation into the King's Cross Underground Fire, HMSO, London, 1988

[4]   K. McGrattan (editor). Fire Dynamics Simulator (Version 4), Technical Reference Guide. NIST Special Publication 1018, National Institute of Standards and Technology, Gaithersburg, Maryland, July 2004

[5]   V. Novozhilov. Computational fluid dynamics modeling of compartment fires, Progress in Energy and Combustion Science, Nanyang Technological University, Singapore, 2001

[5]   V. Novozhilov. Computational fluid dynamics modeling of compartment fires, Progress in Energy and Combustion Science, Nanyang Technological University, Singapore, 2001

[6]   American Society for Testing and Materials, ASTM E 1355-04, Standard Guide for Evaluating the Predictive Capabilities of Deterministic Fire Models, 2004

[7]   B. Hume, Development of Standards for Fire Field Models, Fire Research Report No. 85, ODPM, London, 2003

[8]   K. McGrattan G. Forney. Fire Dynamics Simulator (Version 4), User's Guide. NIST Special Publication 1019, National Institute of Standards and Technology, Gaithersburg, Maryland, July 2004

[9]   W. Davis K. Notarianni K. McGrattan. Comparison of fire model predictions with experiments conducted in a hangar with 15 meter ceiling. NISTIR 5927, National Institute of Standards and Technology, Gaithersburg, Maryland, December 1996

[10]   K. McGrattan A. Hamins. Numerical Simulation of the Howard Street Tunnel Fire, Baltimore, Maryland, July 2001, NISTIR 6902, National Institute of Standards and Technology, Gaithersburg, Maryland, August 2002

[11]   A. Hamins A. Maranghides K. McGrattan T. Ohlemiller R. Anleitner. Experiments and Modeling of Multiple Workstations Burning in a Compartment, NIST NCSTAR 1-5E, National Institute of Standards and Technology, Gaithersburg, Maryland, September 2005

[12]   Verification and Validation of Selected Fire Models for Nuclear Power Plant Applications, Volume 1: Main Report, U.S. Nuclear Regulatory Commission, Office of Nuclear Regulatory Research, Rockville and Electric Power Research Institute, Palo Alto, NUREG-1824 and EPRI 1011999 (Draft), July 2006

[13]   Verification and Validation of Selected Fire Models for Nuclear Power Plant Applications. Volume 7: Fire Dynamics Simulator, U.S. Nuclear Regulatory Commission, Office of Nuclear Regulatory Research, Rockville and Electric Power Research Institute, Palo Alto, NUREG-1824 and EPRI 1011999 (Draft), July 2006

[14]   J. Hietaniemi S. Hostikka J Vaari. FDS Simulation of fire spread – comparison of model results with experimental data. VTT Working Papers 4, Espoo, 2004

[15]   A. Hamins J. Yang T. Kashiwagi. Global model for Predicting the Burning Rates of Liquid Pool Fires, NISTIR 6381, National Institute of Standards and Technology, Gaithersburg, Maryland, 1999

[16]   J. Clement C Fleischmann. Experimental verification of the Fire Dynamics Simulator hydrodynamic model, Fire Safety Science - Proceedings of the 7th International Symposium, IAFSS, 2002

[17]   R. Harrison. Smoke Control in Atrium Buildings: A Study of the Thermal Spill Plume. Fire Engineering Research Report 04/1, University of Canterbury, 2004

[18]   G. Zou W. Chow. Evaluation of the field model, Fire Dynamics Simulator, for a specific experimental scenario, Journal of Fire Protection Engineering, 15 (2) 2005

[19]   N. Pope C. Bailey. Quantitative comparison of FDS and parametric fire curves with post-flashover compartment fire test data, Fire Safety Journal 41 (2006)

[20]   A. Moghaddam K. Moinuddin I. Thomas I. Bennetts M. Culton, Fire Behaviour Studies of Combustible Wall Linings Applying Fire Dynamics Simulator, 15th Australasian Fluid Mechanics Conference, The University of Sydney, December 2004.

[21]   S. Hostikka K. McGrattan A. Hamins. Numerical Modeling of Pool Fires Using LES and Finite Volume Method for Radiation. Fire Safety Science - Proceedings of the 7th International Symposium, IAFSS, 2002.

[22]   A. Kashef N. Benichou G. Lougheed C. McCartney, A Computational and Experimental Study of Fire Growth and Smoke Movement in Large Spaces. Technical Report NRCC-45201, NRCC, Canada 2002

[23]   H. Gerhardt. Design methods of smoke and heat exhaust systems in construction works. 5th International Conference – Fire Safety of Buildings, Warsaw, 2005

[24]   G. Rein A Bar-Ilan A.C. Fernandez-Pello N. Alvares, A Comparison of Three Models for the Simulation of Accidental Fires, Journal of Fire Protection Engineering, 16(3) 2003

[25]   Private communication with Prof. Goran Holmstedt of the Lund University

[26]   Private communication with Mr. Brian Hume of the Fire Statistics and Research Division, Department for Communities and Local Government (UK)

[27]   Private communication with Mr. Noel Putaansuu of MDE Engineering Inc.

[28]   Private communication with Mr. Keith D. Calder of Senez Reed Calder Fire & Forensic Engineering

[29]   S. Miles, The predictive capability of CDF for fully developed fires, Fire and Explosion Hazards – Proceedings of the 3rd International Seminar, April 2000

[30]   Z. Wang F. Jia E. Galea M. Patel J. Ewer. Simulating one of the CIB W14 Round Robin Test Cases using the SMARTFIRE fire field models, CMS Press, London, 2000

APPENDIX A   Properties of fuels used in the simulations

A.1   **Kerosene**[1] (Exp_2_CN, Exp_2_CW, Exp_2_SN, Exp_2_MM, Exp_2_FN)

Property	FDS variable	Symbol	Unit	Value[2]
Reaction (REAC)				
Chemical formula	-	-	-	$C_{14}H_{30}$
Molar mass	MW_FUEL	M	g/mol	198
Stoich. coefficient CO_2	NU_CO2	-	-	14
Stoich. coefficient H_2O	NU_H2O	-	-	15
Stoich. coefficient O_2	NU_O2	-	-	21.5
Energy per unit mass O_2	EPUMO2	ΔH_O	kJ/kg	
CO yield	CO_YIELD	y_{co}	kg/kg	0.012
Soot yield	SOOT_YIELD	y_{soot}	kg/kg	0.041

Notes:

1)   Kerosene was not used as a fuel in the actual experiments. Due to the similarity with diesel oil, reaction properties for burning of kerosene were used in the simulations where heat release rate was provided as an input.

2)   All properties assumed for kerosene are as per *database4.data* file

A.2 Diesel[3] (Exp_2_CN_BR)

Property	FDS variable	Symbol	Unit	Value[4]
Reaction (REAC)				
Chemical formula	-	-	-	$C_{16}H_{34}$
Molar mass	MW_FUEL	M	g/mol	226
Stoich. coefficient CO_2	NU_CO2	-	-	16
Stoich. coefficient H_2O	NU_H2O	-	-	17
Stoich. coefficient O_2	NU_O2	-	-	24.5
Energy per unit mass O_2	EPUMO2	ΔH_O	kJ/kg	12,700
CO yield	CO_YIELD	y_{co}	kg/kg	0.012
Soot yield	SOOT_YIELD	y_{soot}	kg/kg	0.05
Material (SURF)				
Density	DENSITY	ρ	kg/m^3	850
Heat of vaporization	HEAT_OF_VAPORIZATION	ΔH_V	kJ/kg	326
Heat of combustion	HEAT_OF_COMBUSTION	ΔH	kJ/kg	41,000
Specific heat	C_P	c_p	kJ/kg/K	1.9
Temp of ignition	TMPING	T_{ign}	^{o}C	210
Thermal conductivity	KS	k	W/m/K	0.109
Phase	PHASE	-		'LIQUID'

Notes:

3) Reaction and material properties of diesel oil were used in the simulations where the burning rate was predicted by FDS (indicated by suffix BR in the file name)

4) Material and reaction properties for diesel oil are difficult to find in the literature, due to the fact that diesel oil is in fact a mixture of hydrocarbons, with composition varying between different countries and fuel grades.
Some values shown in the table were obtained from the internet and their reliability can not be fully confirmed.

A.3 **Ethanol** (Exp_5_CN, Exp_5_CW, Exp_5_MM)

Property	FDS variable	Symbol	Unit	Value
Reaction (REAC)[5]				
Chemical formula	-	-	-	C_2H_5OH
Molar mass	MW_FUEL	M	g/mol	46
Stoich. coefficient CO_2	NU_CO2	-	-	2
Stoich. coefficient H_2O	NU_H20	-	-	3
Stoich. coefficient O_2	NU_02	-	-	3
Energy per unit mass O_2	EPUMO2	ΔH_O	kJ/kg	12,842
Radiative fraction	RADIATIVE_FRACTION	-	-	0.2
Soot yield	SOOT_YIELD	y_{soot}	kg/kg	0.008
Material (SURF)[6]				
Density	DENSITY	ρ	kg/m^3	780
Heat of vaporization	HEAT_OF_VAPORIZATION	ΔH_V	kJ/kg	837
Heat of combustion	HEAT_OF_COMBUSTION	ΔH	kJ/kg	26,800
Specific heat	C_P	c_p	kJ/kg/K	2.4
Temp of ignition	TMPING	T_{ign}	^{o}C	78
Thermal conductivity	KS	k	W/m/K	0.16
Phase	PHASE	-		'LIQUID'

Notes:

5) Reaction properties shown in this table were used for all simulations involving ethanol.
6) Material properties for ethanol were used only in simulations where the burning rate was predicted by FDS (indicated by suffix BR in the file name)

APPENDIX B   Example of FDS input file (Exp_2_CW.data)

&HEAD CHID='Exp_2_CW', TITLE='Experiment 2, Coarse Grid, Wide Domain' /

&GRID IBAR=72, JBAR=72, KBAR=64 /
&PDIM XBAR0=-2.52, XBAR=2.52, YBAR0=-2.38, YBAR=2.66, ZBAR=5.12 /

&MISC TMPA=14, TMPO=14, NFRAMES=450, REACTION='KEROSENE' /

&TIME TWFIN= 900 /

&SURF ID='fire', HRRPUA= 1480, RAMP_Q='HRR', RGB=1,0,0 /

&RAMP ID='HRR', T=0,   F=0.00/   Exp_2   HRR ramp-up
&RAMP ID='HRR', T=55, F=0.12/
&RAMP ID='HRR', T=110, F=0.12/
&RAMP ID='HRR', T=180, F=0.19/
&RAMP ID='HRR', T=295, F=0.21/
&RAMP ID='HRR', T=390, F=0.41/
&RAMP ID='HRR', T=485, F=1.00/
&RAMP ID='HRR', T=500, F=1.00/
&RAMP ID='HRR', T=570, F=0.04/
&RAMP ID='HRR', T=620, F=0.00/

&RAMP ID='VEL', T=   1, F=0.87/   Exp_2   Vel ramp-up
&RAMP ID='VEL', T= 540, F=0.87/
&RAMP ID='VEL', T= 545, F=1.00/
&RAMP ID='VEL', T= 900, F=1.00/

&SURF ID='fan', VEL= 8.56, RAMP_V='VEL' /   Exp_2

&REAC ID='KEROSENE'
    FYI='Kerosene, C_14 H_30, Tewarson, SFPE Handbook'
    MW_FUEL=198.0
    NU_O2=21.5
    NU_CO2=14.0
    NU_H2O=15.0
    EPUMO2=12700.
    CO_YIELD=0.012
    SOOT_YIELD=0.042 /

&SURF ID   = 'SHEET METAL'
    RGBx=0.5,0.5,0.5
    C_DELTA_RHO = 4.7
    DELTA   = 0.0013 /

&SURF ID   = 'BOARD'
    BACKING = 'EXPOSED'
    C_P   = 1.5
    DENSITY = 500.
    KS   = 0.15
    DELTA   = 0.02 /

```
&SURF ID     = 'DURABOARD'
    BACKING = 'EXPOSED'
    C_P    = 1.13
    DENSITY = 260.
    RAMP_KS = 'KS'
    DELTA   = 0.04 /
&RAMP ID = 'KS',  T = 20.,  F = 0.07  /
&RAMP ID = 'KS',  T =800.,  F = 0.17  /
```

OBSTRUCTIONS – ISO ROOM

```
&OBST XB= 0.56, 1.89,-0.49, 0.49, 0.16, 0.24 SURF_ID='DURABOARD' RGB=0.7,0.7,0.3/
&OBST XB= 0.56, 1.89,-0.49, 0.49, 1.04, 1.12 SURF_ID='DURABOARD' RGB=0.7,0.7,0.3/
&OBST XB= 0.56, 1.89,-0.49,-0.42, 0.24, 1.04 SURF_ID='DURABOARD' RGB=0.7,0.7,0.3/
&OBST XB= 0.56, 1.89, 0.42, 0.49, 0.24, 1.04 SURF_ID='DURABOARD' RGB=0.7,0.7,0.3/

&OBST XB= 0.56, 0.63,-0.42, 0.42, 0.24, 1.04 SURF_ID='DURABOARD' RGB=0.7,0.7,0.3/
&OBST XB= 1.82, 1.89,-0.42, 0.42, 0.24, 1.04 SURF_ID='DURABOARD' RGB=0.7,0.7,0.3/

&OBST XB= 0.56, 0.63,-0.28, 0.28, 1.12, 1.60 SURF_ID='DURABOARD' RGB=0.7,0.7,0.3/

&HOLE XB= 0.56, 0.63,-0.14, 0.14, 0.24, 0.80 /

&OBST XB= 0.56, 0.63,-0.49,-0.42, 0.00, 0.16 SURF_ID='DURABOARD' RGB=0.7,0.7,0.3/
&OBST XB= 0.56, 0.63, 0.42, 0.49, 0.00, 0.16 SURF_ID='DURABOARD' RGB=0.7,0.7,0.3/
&OBST XB= 1.82, 1.89,-0.49,-0.42, 0.00, 0.16 SURF_ID='DURABOARD' RGB=0.7,0.7,0.3/
&OBST XB= 1.82, 1.89, 0.42, 0.49, 0.00, 0.16 SURF_ID='DURABOARD' RGB=0.7,0.7,0.3/

&OBST XB= 0.98, 1.19,-0.14, 0.14, 0.24, 0.32 RGB=0.3,0.3,0.3/  FUEL TRAY  210x280 mm

&OBST XB= 0.21, 0.56,-0.49, 0.49, 0.96, 1.04 SURF_ID='BOARD' RGB=0.75,0.7,0.7/  BALCONY

&OBST XB= 0.42, 0.56,-0.49,-0.42, 0.00, 0.96 SURF_ID='BOARD' RGB=0.75,0.7,0.7/  SIDE
&OBST XB= 0.42, 0.56, 0.42, 0.49, 0.00, 0.96 SURF_ID='BOARD' RGB=0.75,0.7,0.7/  SIDE
```

HOOD

```
&OBST XB=-1.54, 1.54,-1.54, 1.54, 2.00, 3.04 SURF_ID='SHEET METAL'  SAWTOOTH=.TRUE./
&HOLE XB=-1.47, 1.47,-1.47, 1.47, 2.00, 3.04 /

&OBST XB=-1.54, 1.54,-1.54, 1.54, 3.04, 3.12 SURF_ID='SHEET METAL'  SAWTOOTH=.TRUE./
&HOLE XB=-1.40, 1.40,-1.40, 1.40, 3.04, 3.12 /

&OBST XB=-1.47, 1.47,-1.47, 1.47, 3.12, 3.20 SURF_ID='SHEET METAL'  SAWTOOTH=.TRUE
&HOLE XB=-1.33, 1.33,-1.33, 1.33, 3.12, 3.20 /

&OBST XB=-1.40, 1.40,-1.40, 1.40, 3.20, 3.28 SURF_ID='SHEET METAL'  SAWTOOTH=.TRUE./
&HOLE XB=-1.26, 1.26,-1.26, 1.26, 3.20, 3.28 /

&OBST XB=-1.33, 1.33,-1.33, 1.33, 3.28, 3.36 SURF_ID='SHEET METAL'  SAWTOOTH=.TRUE./
&HOLE XB=-1.19, 1.19,-1.19, 1.19, 3.28, 3.36 /

&OBST XB=-1.26, 1.26,-1.26, 1.26, 3.36, 3.44 SURF_ID='SHEET METAL'  SAWTOOTH=.TRUE./
&HOLE XB=-1.05, 1.05,-1.05, 1.05, 3.36, 3.44 /

&OBST XB=-1.12, 1.12,-1.12, 1.12, 3.44, 3.52 SURF_ID='SHEET METAL'  SAWTOOTH=.TRUE./
&HOLE XB=-0.98, 0.98,-0.98, 0.98, 3.44, 3.52 /
```

&OBST XB=-1.05, 1.05,-1.05, 1.05, 3.52, 3.60 SURF_ID='SHEET METAL' SAWTOOTH=.TRUE
&HOLE XB=-0.91, 0.91,-0.91, 0.91, 3.52, 3.60 /

&OBST XB=-0.98, 0.98,-0.98, 0.98, 3.60, 3.68 SURF_ID='SHEET METAL' SAWTOOTH=.TRUE./
&HOLE XB=-0.84, 0.84,-0.84, 0.84, 3.60, 3.68 /

&OBST XB=-0.91, 0.91,-0.91, 0.91, 3.68, 3.76 SURF_ID='SHEET METAL' SAWTOOTH=.TRUE./
&HOLE XB=-0.70, 0.70,-0.70, 0.70, 3.68, 3.76 /

&OBST XB=-0.77, 0.77,-0.77, 0.77, 3.76, 3.84 SURF_ID='SHEET METAL' SAWTOOTH=.TRUE./
&HOLE XB=-0.63, 0.63,-0.63, 0.63, 3.76, 3.84 /

&OBST XB=-0.70, 0.70,-0.70, 0.70, 3.84, 3.92 SURF_ID='SHEET METAL' SAWTOOTH=.TRUE./
&HOLE XB=-0.56, 0.56,-0.56, 0.56, 3.84, 3.92 /

&OBST XB=-0.63, 0.63,-0.63, 0.63, 3.92, 4.00 SURF_ID='SHEET METAL' SAWTOOTH=.TRUE./
&HOLE XB=-0.49,-0.07,-0.49, 0.49, 3.92, 4.00 /   BAFFLE 1

&OBST XB=-0.56, 0.56,-0.56, 0.56, 4.00, 4.96 SURF_ID='SHEET METAL' SAWTOOTH=.TRUE./
&HOLE XB=-0.49, 0.49,-0.49, 0.49, 4.00, 4.40 /
&HOLE XB=-0.07, 0.49,-0.49, 0.49, 4.40, 4.48 /   BAFFLE 2
&HOLE XB=-0.49, 0.49,-0.49, 0.49, 4.48, 4.88 /

&OBST XB=-2.52,-0.56,-0.28, 0.28, 4.40, 4.48 SURF_ID='SHEET METAL' SAWTOOTH=.TRUE./
&OBST XB=-2.52,-0.56,-0.28, 0.28, 4.80, 4.88 SURF_ID='SHEET METAL' SAWTOOTH=.TRUE./
&OBST XB=-2.52,-0.56,-0.28,-0.21, 4.48, 4.80 SURF_ID='SHEET METAL' SAWTOOTH=.TRUE./
&OBST XB=-2.52,-0.56, 0.21, 0.28, 4.48, 4.80 SURF_ID='SHEET METAL' SAWTOOTH=.TRUE./
&HOLE XB=-0.56,-0.49,-0.21, 0.21, 4.48, 4.80 /

EXPERIMENTAL STANDS

&OBST XB= 0.07, 0.49,-1.40,-1.68, 0.16, 1.12 RGB=0.3,0.30,0.6 / Exp Stand 1
&OBST XB= 0.07, 0.14,-1.40,-1.68, 0.00, 0.16 RGB=0.3,0.30,0.6 /
&OBST XB= 0.42, 0.49,-1.40,-1.68, 0.00, 0.16 RGB=0.3,0.30,0.6 /
&OBST XB= 0.28, 1.33,-1.68,-2.10, 0.16, 1.28 RGB=0.3,0.35,0.7 / Exp Stand 2
&OBST XB= 0.28, 0.35,-1.68,-2.10, 0.00, 0.16 RGB=0.3,0.35,0.7 /
&OBST XB= 1.26, 1.33,-1.68,-2.10, 0.00, 0.16 RGB=0.3,0.35,0.7 /

CHANELING SCREENS

&OBST XB= 0.28, 0.42,-0.49,-0.42, 0.82, 0.96 SURF_ID='SHEET METAL' RGB=0.6,0.6,0.6/
&OBST XB= 0.28, 0.42, 0.42, 0.49, 0.82, 0.96 SURF_ID='SHEET METAL' RGB=0.6,0.6,0.6/

BOUNDARY CONDITIONS

&VENT CB= XBAR,   SURF_ID='OPEN'/
&VENT CB= YBAR0, SURF_ID='OPEN'/
&VENT CB= ZBAR,   SURF_ID='OPEN'/

&VENT XB= 0.98, 1.19,-0.14, 0.14, 0.32, 0.32, SURF_ID='fire'/   210x280 mm

&VENT XB=-2.52,-2.52,-0.21, 0.21, 4.48, 4.80, SURF_ID='fan' /

&VENT XB=-2.52,-2.52,-2.38, 2.66, 0.00, 4.40, SURF_ID='OPEN'/

RESULTS

&THCP XYZ= 0.68,-0.39, 0.94, QUANTITY='TEMPERATURE' /   1 COMPARTMENT TEMP
&THCP XYZ= 0.68,-0.39, 0.83, QUANTITY='TEMPERATURE' /   2
&THCP XYZ= 0.68,-0.39, 0.71, QUANTITY='TEMPERATURE' /   3
&THCP XYZ= 0.68,-0.39, 0.60, QUANTITY='TEMPERATURE' /   4
&THCP XYZ= 0.68,-0.39, 0.48, QUANTITY='TEMPERATURE' /   5
&THCP XYZ= 0.68,-0.39, 0.36, QUANTITY='TEMPERATURE' /   6

&THCP XYZ=-0.01, 0.00, 0.89, QUANTITY='TEMPERATURE'/   7 SPILL PLUME - Exp 2-4
&THCP XYZ=-0.01, 0.00, 1.04, QUANTITY='TEMPERATURE'/   8
&THCP XYZ=-0.01, 0.00, 1.19, QUANTITY='TEMPERATURE'/   9
&THCP XYZ=-0.01, 0.00, 1.34, QUANTITY='TEMPERATURE'/ 10
&THCP XYZ=-0.01, 0.00, 1.49, QUANTITY='TEMPERATURE'/ 11

&THCP XYZ= 0.46, 0.00, 0.60, QUANTITY='TEMPERATURE' / 12 COMP OPENING
&THCP XYZ= 0.46, 0.00, 0.70, QUANTITY='TEMPERATURE' / 13
&THCP XYZ= 0.46, 0.00, 0.80, QUANTITY='TEMPERATURE' / 14

&THCP XYZ= 0.00, 0.00, 2.00, QUANTITY='TEMPERATURE' / 15 SPILL PLUME (TOP)
&THCP XYZ= 0.00,-0.30, 2.00, QUANTITY='TEMPERATURE' / 16
&THCP XYZ= 0.00,-0.60, 2.00, QUANTITY='TEMPERATURE' / 17

&THCP XYZ= 0.00, 0.00, 3.00, QUANTITY='TEMPERATURE' / 18 SMOKE RESERVOIR
&THCP XYZ= 0.40, 0.40, 3.00, QUANTITY='TEMPERATURE' / 19
&THCP XYZ= 0.40,-0.40, 3.00, QUANTITY='TEMPERATURE' / 20
&THCP XYZ=-0.40,-0.40, 3.00, QUANTITY='TEMPERATURE' / 21
&THCP XYZ=-0.40, 0.40, 3.00, QUANTITY='TEMPERATURE' / 22

&THCP XYZ=-2.00,-0.15, 4.64, QUANTITY='TEMPERATURE' / 23 EXTRACTED AIR TEMP
&THCP XYZ=-2.00, 0.00, 4.64, QUANTITY='TEMPERATURE' / 24
&THCP XYZ=-2.00, 0.15, 4.64, QUANTITY='TEMPERATURE' / 25

&THCP XYZ= 0.46, 0.00, 0.80, QUANTITY='U-VELOCITY'/ 26 BI-DIRECTIONAL PROBES
&THCP XYZ=-0.01, 0.00, 1.19, QUANTITY='W-VELOCITY'/ 27
&THCP XYZ=-0.01, 0.00, 1.49, QUANTITY='W-VELOCITY'/ 28

&THCP XB=-2.20,-2.20,-0.28, 0.28, 4.48, 4.80 QUANTITY='MASS FLOW' /

&SLCF PBY=0.00,QUANTITY='TEMPERATURE',VECTOR=.TRUE. /
&SLCF PBX=0.00,QUANTITY='TEMPERATURE',VECTOR=.TRUE. /

APPENDIX C   **Geometry of FDS model**

<u>LEGEND</u>

$\oplus 19$ thermocouple (with number)

$\nabla 24$ bi-directional probe (with number)

(180)   dimension in physical model
            (where different from FDS model)

<u>NOTES</u>

1)   The distance from the front of the compartment
         to the fuel tray (in the FDS model) was 420 mm
         for Exp_2 and 350 mm for Exp_5. In the physical
         model it was 400 mm and 350 mm respectively

2)   The balcony and the chanelling screens were
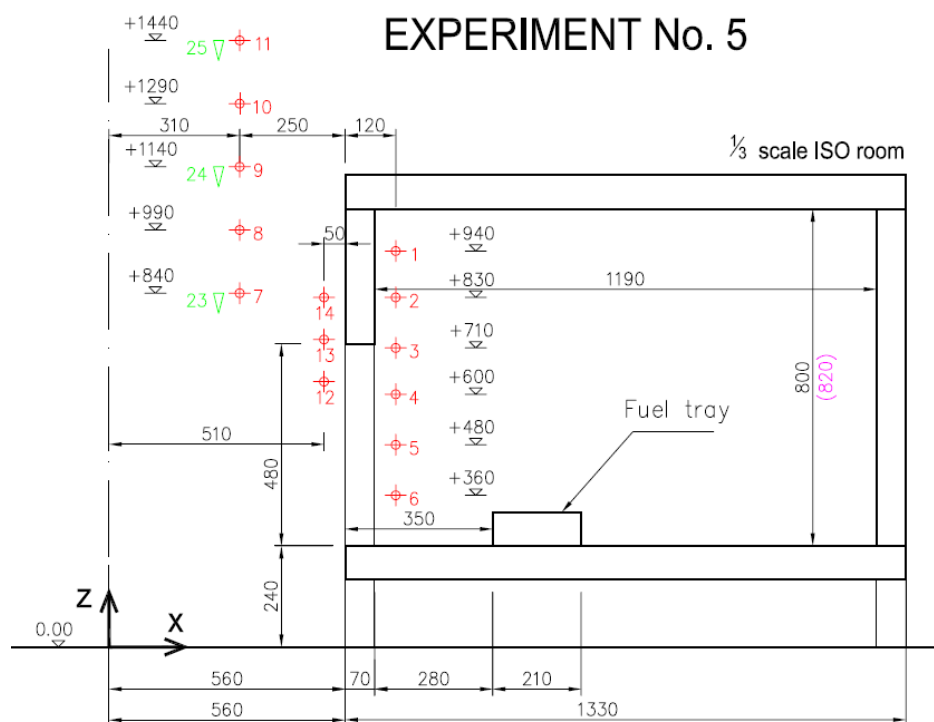   removed in experiment no. 5
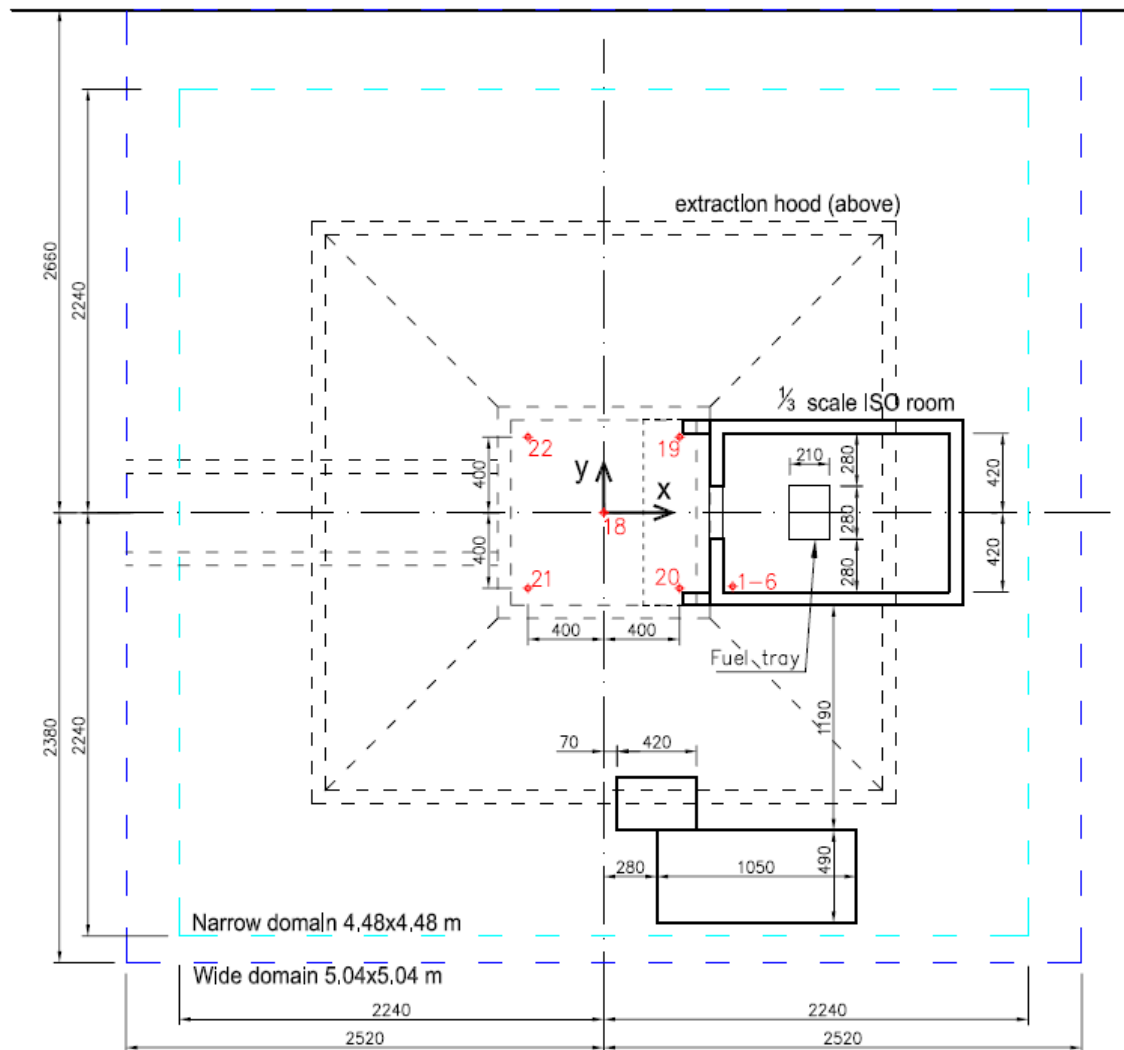
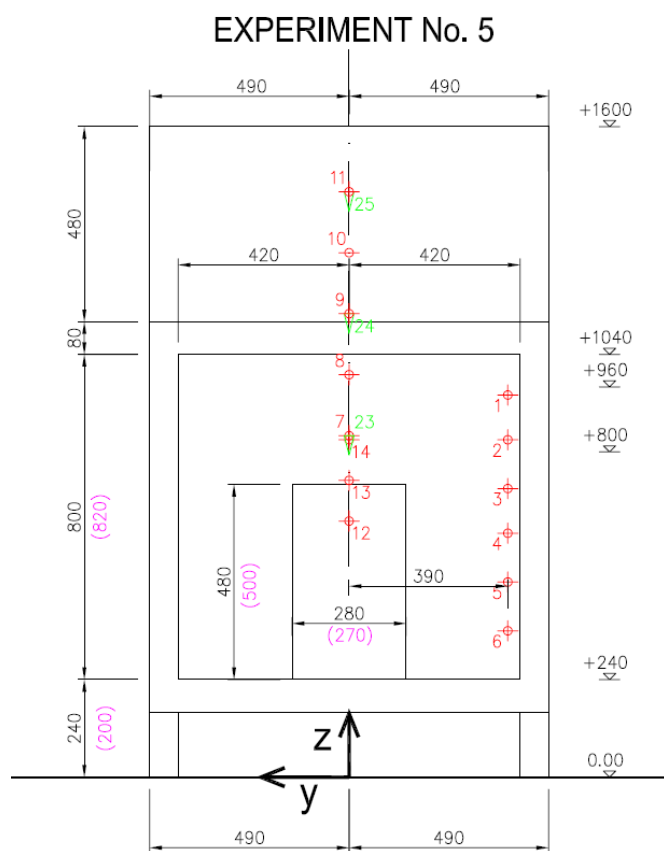**Fig. C.1 Model geometry (positions of selected thermocouples) – plan view**

Fig. C.2 Longitudinal section, Positions of thermocouples – Exp_2

Fig. C.3 Front view, Positions of thermocouples – Exp_2

Fig. C.4 Longitudinal section, Positions of thermocouples – Exp_5

Fig. C.5 Front view, Positions of thermocouples – Exp_5

101

APPENDIX D   **Experimental results**

APPENDIX E   FDS simulation results